

UNIVERSITY OF NAPLES FEDERICO II  
DEPARTMENT OF PHARMACY



**Ph. D. THESIS**  
**In Pharmaceutical Sciences**  
**XXVII Cycle**

**TRANSCRIPTION FACTORS AS TARGETS OF NEW  
MOLECULES WITH POTENTIAL ANTI-CANCER  
ACTIVITY.**

Ph. D.:  
Dott.ssa Paola De Cicco

Ph. D. Tutor:  
Ch.ma Prof.ssa Angela Ianaro

Programme in Pharmaceutical Sciences Coordinator:  
Ch.ma Prof.ssa M.Valeria D'Auria

# Table of contents

---

<b>Introduction</b>	<b>5</b>
1. Melanoma	5
1.1 <i>Etiology and Epidemiology</i>	5
1.2 <i>Stadiation</i>	9
1.3 <i>Molecular pathways activated in melanoma</i>	15
1.4 <i>Common genetic alteration in melanoma</i>	25
1.5 <i>Theraphy</i>	34
2. Hydrogen Sulphide	57
2.1 <i>Physical and Chemical Properties of H<sub>2</sub>S</i>	57
2.2 <i>Endogenous Production of H<sub>2</sub>S in mammalian cells</i>	61
2.3 <i>Molecular targets of H<sub>2</sub>S</i>	69
2.4 <i>Physio- pathological functions of H<sub>2</sub>S in mammals</i>	77
2.5 <i>H<sub>2</sub>S donors</i>	88
<b>Aim</b>	<b>105</b>
<b>Methods</b>	<b>107</b>
3.1 <i>Cell culture and reagents</i>	107
3.2 <i>Proliferation assays</i>	108
3.3 <i>Preparation of cellular extracts</i>	109
3.4 <i>Western blot analysis</i>	110
3.5 <i>Flow cytometry</i>	111
3.6 <i>Cell cycle</i>	112

3.7 Electrophoretic mobility shift assay (EMSA)	113
3.8 RNA purification and qPCR	113
3.9 Transfection	114
3.10 Generation of Vemurafenib-resistant human melanoma cells	115
3.11 Animals	116
3.12 Induction of subcutaneous B16 lesions	116
3.13 Induction of metastatic melanoma	117
3.14 Patients and specimens	117
3.15 Immunohistochemistry analysis	118
3.16 Statistical analysis	119
<b>Results</b>	<b>121</b>
4.1 Hydrogen sulfide donors inhibit human melanoma cell proliferation	121
4.2 Hydrogen sulfide donors cause cell cycle arrest and induces apoptosis of human melanoma cell lines	125
4.3 Hydrogen sulfide donors inhibit NF- $\kappa$ B activation and down-regulate NF- $\kappa$ B-dependent anti-apoptotic genes	128
4.4 Expression of CSE, CBS and of 3-MST in human melanoma cell lines	131
4.5 Overexpression of CSE in A375 cells modifies cell proliferation	133

<i>4.6 Hydrogen sulfide inhibits the growth of melanoma cutaneous in vivo in mice</i>	<i>136</i>
<i>4.7 Effect of hydrogen sulfide donors on MAPK/ERK and PI3/AKT pathways</i>	<i>141</i>
<i>4.8 Hydrogen sulfide inhibits A375rVem cell proliferation</i>	<i>143</i>
<i>4.9 Hydrogen sulfide inhibits metastatic melanoma in vivo in mice</i>	<i>145</i>
<i>4.10 CSE, CBS and 3-MST expression in human nevi</i>	<i>147</i>
<i>4.11 CSE, CBS and 3-MST expression in human primitive melanoma and metastases</i>	<i>147</i>
<b>Discussion</b>	<b>150</b>
<b>Reference</b>	<b>162</b>

# INTRODUCTION

---

## **1. Melanoma**

### **1.1 Etiology and Epidemiology**

Melanoma is the least common but the most aggressive form of skin cancer occurring when melanocytes, melanin-producing cells of the skin, eye, mucosal epithelia, and meninges undergo changes and become malignant. So, melanoma may occur in all parts of the body where are normally present melanocytes, as the skin of course, but also the mucous membranes, meninges and uvea. Has greater impact on the left side of the body<sup>1</sup>. Melanocytes are derived from neural crest progenitors, and their development is modulated by the receptor tyrosine kinase (RTK) c-KIT and microphthalmia-associated transcription factor (MITF). Melanocytes produce two main types of pigment: brown/black eumelanin, that protects from ultraviolet radiation (UVR) and red pheomelanin that contributes to melanomagenesis through a mechanism involving ROS<sup>2-3</sup>.

Genetic predisposition or an environmental stressor contributes to the genesis of melanoma. The strongest melanoma risk factors are a family history of melanoma, atypical moles or dysplastic nevi. Sun sensitivity, immunosuppression and exposure to ultraviolet radiation are additional risk factors<sup>4</sup>. In particular the exposure to

ultraviolet light causes variations in particular genes (polymorphisms) that affect both the defensive response of the skin to ultraviolet light and the risk of melanoma. Ultraviolet radiation has multiple effects on the skin: causes genetic changes, impairs cutaneous immune function, increases the local production of growth factors, and induces the formation of DNA-damaging reactive oxygen species that affect keratinocytes and melanocytes<sup>5</sup>. Clinically, variations in pigmentation and the protective response to ultraviolet light are associated with variations in susceptibility to melanoma. Also, specific phenotypic characteristics have been shown to correlate with increased risk of melanoma such as green/blue eye color, red/blond hair color, fair skin, the presence of freckles and inability to tan. Caucasians have a 20-fold increased risk of developing skin melanoma when compared to dark skin populations<sup>6</sup>.

According to the World Health Organization, in the last decades the incidence of cutaneous malignant melanoma is increasing faster than any other cancer in the world, about of 2-7% annually. This fact has led to the use of the term melanoma “epidemic”<sup>7</sup>. In 2014 the American Cancer Society and the National Cancer Institute estimated 76,100 new cases of patient with invasive melanoma and 9,710 deaths only in USA. Although melanoma represent less of 5% of cases of skin cancer it counts more of 75% of skin-related

deaths<sup>8</sup>. Melanoma is very common in young adults aged 15-34 years. Melanoma incidence is also dependent on gender, in fact in the U.S. women have a higher risk of melanoma than men before age 40, but they have a better prognosis in terms of survival. In men, the predominant anatomical location for melanoma lesions is the trunk and in women lesions are mainly found in the lower limbs<sup>9</sup>. This impressive increase in incidence may be due to several factors, including behavioural changes, better early detection by screening instruments, changes in diagnostic criteria in histopathology, and perhaps also the change in the medico-legal climate<sup>10</sup>.

A simple procedure to diagnose melanoma is founded on its pigmentation. The American Cancer Society has devised a simple **A-B-C-D-E** acronym to guide in the identification of pigmented lesions that should be evaluated with biopsy (Figure 1).

**A = asymmetry**, when one half the lesion is looking different from the other half; the common nevi are round and symmetrical whereas the most melanomas is asymmetric.

**B = border irregularity**, the common nevi have smooth edges whereas margins of melanomas in the initial phase are often irregular and jagged.

**C = color variegation**, the common nevi have the same shade of brown whereas the lesion is not one uniform color

but rather a combination of black, brown, blue, or even white.

**D = diameter**, lesions with a diameter greater than 5-6 mm is exposed to a higher risk of turning into melanoma.

**E = evolution or enlargement**, any change or evolution of a previously present pigmented lesion should raise suspicion for the lesion being melanoma and trigger a biopsy.

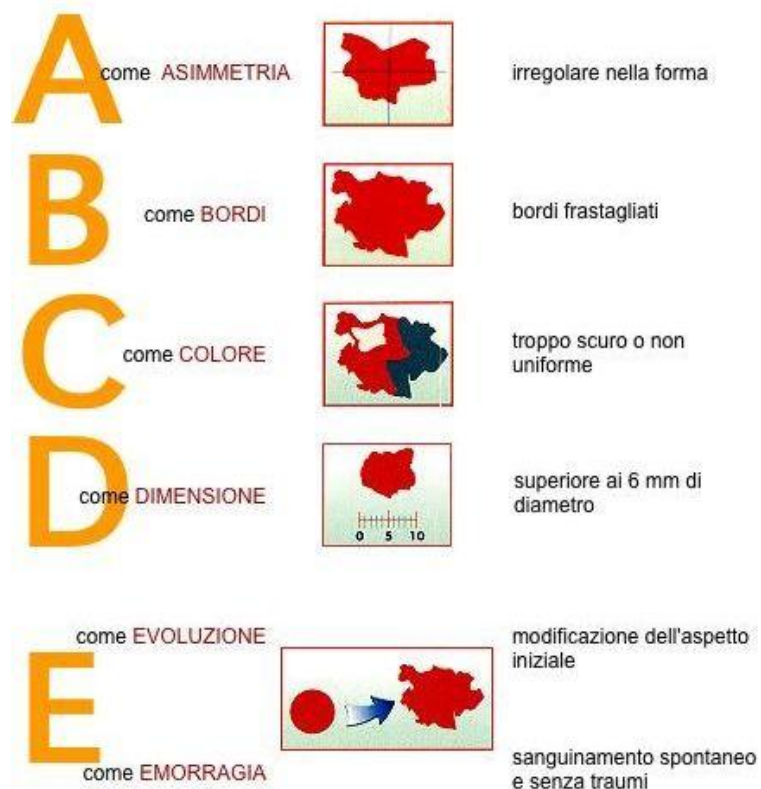


**Figure 1.** The ABCs of Melanoma Diagnosis

## **1.2 Stadiation**

The **Clark model** describes the histopathological changes that occur in the progression of melanoma, from normal melanocytes to malignant. In the Clark model, the first phenotypic change in melanocytes is the development of benign nevi, which are composed of neval melanocytes (Figure 2). Normal melanocytes progressively develop a malignant phenotype through the acquisition of various phenotypic features. The particular histologic features characterizing each step of progression are the visible manifestations of underlying genetic changes. When the growth of a nevus is controlled, probably by the oncogene-induced cell senescence, they rarely progresses to cancer. Instead, abnormal activation of the mitogen-activated protein kinase (MAPK) signaling pathway due to somatic mutations of N-RAS or BRAF stimulates growth in melanoma cells. These mutations occur at a similar frequency in benign nevi and in primary and metastatic melanomas. So most nevi stop proliferation and remain static for decades, other may acquire additional molecular lesions and become malignant.

The second step in the progression of melanoma is the trasformation of some benign nevi in dysplastic nevi, which are not really invasive malignancies, but rather just moles that have some architectural disorder. The third step is the radial growth phase melanoma in which there is

growth through the epidermis but not deeply into the dermis. In the fourth step, namely vertical-growth phase, appear the invasive characteristics of the melanoma cells. They acquire a potential to spread, grow intradermally and gains the capacity to invade the vascular and lymphatic systems.

Finally, a metastatic melanoma develops when tumor cells dissociate from the primary lesion, migrate through the surrounding stroma, and invade blood vessels and lymphatics to form a tumor at a distant site, whether it be in an organ, or a skin, or lymph node through vascular or lymphatic invasion<sup>11</sup>.

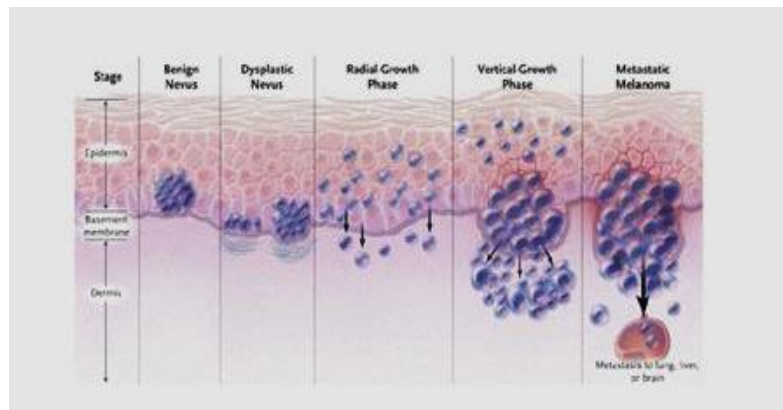


**Figure 2.** Biologic Progression of Melanoma  
(Miller et al., *N Engl J Med* 2006)

The **Breslow model** measures the melanoma thickness (in millimetres) as the distance between the upper layer of the epidermis and the deepest point of tumor penetration. Tumor depth is most accurately measured by evaluating the entire tumor via an excisional biopsy. Clinically, the Breslow index is considered one of the most significant factors in predicting the progression of the disease and primary criterion in melanoma staging<sup>12</sup> (Fig. 3).

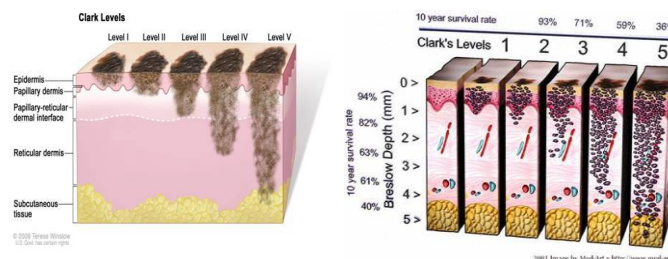


**Figure 3.** Clark and Breslow's model  
(Miller et al., *N Engl J Med* 2006)

The current melanoma staging refers at the seventh edition (2209) of the American Joint Committee on Cancer (AJCC) Cancer Staging Manual that was made on the basis of a multivariate analysis of 30,946 patients with stages I, II, and III melanoma and 7,972 patients with stage IV

melanoma. In this system histological features as tumor thickness, mitotic rate, and ulceration, are important hallmarks of melanoma prognosis and staging.

According to AJCC the melanoma stages are classified as reported:

**STAGE 0:** In situ (non-invasive) melanoma remains confined to the epidermis.

**STAGE I and II:** Localized Melanoma. These stages are divided each other in: Stage IA-IB and IIA-IIB-IIC on the base of tumor thickness "T" (thresholds of 1.0, 2.0, and 4.0 mm) and the presence of microscopic ulceration. The presence of at least one mitosis (cancer cell division) per millimeter squared (mm<sup>2</sup>) can upgrade a thin melanoma to a later stage at higher risk for metastasis.

**STAGE III:** Regional Metastatic Melanoma. These stages are divided each other in: Stage IIIA-IIIB-IIIC on the base of number of nodal metastases "N" (thresholds of 1, 2-3 and 4+ nodes, depends on factors such as whether the metastases are in-transit or have reached the nodes, the number of metastatic nodes, the number of cancer cells found in them) and micrometastases. This can be determined by examining a biopsy of the node nearest the tumor, known as the sentinel node.

**STAGE IV:** Distant Metastatic Melanoma, defined on the evaluated of the site(s) of the distant metastases "M"

(nonvisceral, lung, or any other visceral metastatic sites) and elevated serum lactate dehydrogenase (LDH) level (Table 1 e 2).

Table 1. TNM Staging Categories for Cutaneous Melanoma		
Classification	Thickness (mm)	Ulceration Status/Mitoses
<b>T</b>		
T <sub>is</sub>	NA	NA
T1	≤ 1.00	a: Without ulceration and mitoses < 1/mm <sup>2</sup> b: With ulceration or mitoses ≥ 1/mm <sup>2</sup>
T2	1.01-2.00	a: Without ulceration b: With ulceration
T3	2.01-4.00	a: Without ulceration b: With ulceration
T4	> 4.00	a: Without ulceration b: With ulceration
<b>N</b>		
	No. of Metastatic Nodes	Nodal Metastatic Burden
N0	0	NA
N1	1	a: Micrometastasis* b: Macrometastasis†
N2	2-3	a: Micrometastasis* b: Macrometastasis† c: In transit metastases/satellites without metastatic nodes
N3	4+ metastatic nodes, or matted nodes, or in transit metastases/satellites with metastatic nodes	
<b>M</b>		
	Site	Serum LDH
M0	No distant metastases	NA
M1a	Distant skin, subcutaneous, or nodal metastases	Normal
M1b	Lung metastases	Normal
M1c	All other visceral metastases	Normal
	Any distant metastasis	Elevated
Abbreviations: NA, not applicable; LDH, lactate dehydrogenase. *Micrometastases are diagnosed after sentinel lymph node biopsy. †Macrometastases are defined as clinically detectable nodal metastases confirmed pathologically.		

**Table 1.** TNM Staging Categories for Cutaneous Melanoma (Balch et al., *J Clin Oncol.* 2009)

	Clinical Staging*			Pathologic Staging†			
	T	N	M	T	N	M	
0	T <sub>0a</sub>	N0	M0	0	T <sub>0a</sub>	N0	M0
IA	T <sub>1a</sub>	N0	M0	IA	T <sub>1a</sub>	N0	M0
IB	T <sub>1b</sub>	N0	M0	IB	T <sub>1b</sub>	N0	M0
	T <sub>2a</sub>	N0	M0		T <sub>2a</sub>	N0	M0
IIA	T <sub>2b</sub>	N0	M0	IIA	T <sub>2b</sub>	N0	M0
	T <sub>3a</sub>	N0	M0		T <sub>3a</sub>	N0	M0
IIB	T <sub>3b</sub>	N0	M0	IIB	T <sub>3b</sub>	N0	M0
	T <sub>4a</sub>	N0	M0		T <sub>4a</sub>	N0	M0
IIIC	T <sub>4b</sub>	N0	M0	IIIC	T <sub>4b</sub>	N0	M0
III	Any T	N > N0	M0	IIIA	T <sub>1-4a</sub>	N <sub>1a</sub>	M0
					T <sub>1-4a</sub>	N <sub>2a</sub>	M0
				IIB	T <sub>1-4b</sub>	N <sub>1a</sub>	M0
					T <sub>1-4b</sub>	N <sub>2a</sub>	M0
					T <sub>1-4a</sub>	N <sub>1b</sub>	M0
					T <sub>1-4a</sub>	N <sub>2b</sub>	M0
					T <sub>1-4a</sub>	N <sub>2c</sub>	M0
				IIIC	T <sub>1-4b</sub>	N <sub>1b</sub>	M0
					T <sub>1-4b</sub>	N <sub>2b</sub>	M0
					T <sub>1-4b</sub>	N <sub>2c</sub>	M0
	Any T	N3	M0				
IV	Any T	Any N	M1	IV	Any T	Any N	M1

\*Clinical staging includes macrostaging of the primary melanoma and clinical/radiologic evaluation for metastases. By convention, it should be used after complete excision of the primary melanoma with clinical assessment for regional and distant metastases.

†Pathologic staging includes macrostaging of the primary melanoma and pathologic information about the regional lymph nodes after partial (ie, sentinel node biopsy) or complete lymphadenectomy. Pathologic stage 0 or stage IA patients are the exception; they do not require pathologic evaluation of their lymph nodes.

**Table 2. Anatomic Stage Groupings for Cutaneous Melanoma (Balch et al., J Clin Oncol. 2009)**

As with nearly all malignancies, the outcome of melanoma initially depends on the stage at presentation. An estimated 82% to 85% of patients present with localized disease, 10% to 13% with regional disease, and 2% to 5% with distant metastatic disease. In general, the prognosis is excellent for patients who present with localized disease and primary tumours 1.0 mm or less in thickness, with 5-years survival achieved in more than 90% of patients. For patients

with localized melanomas more than 1.0 mm in thickness, survival rates range from 50% to 90%. The likelihood of regional nodal involvement increases with increasing tumour thickness. When regional nodes are involved, survival rates are roughly halved. However, within stage III, 5-year survival rates range from 20% to 70%, depending primarily on the nodal tumour burden. Long-term survival in patients with distant metastatic melanoma, taken as a whole, is less than 10%. However, even within stage IV, some patients have a more indolent clinical course that is biologically distinct from that of most patients with advanced disease<sup>13</sup>.

### ***1.3 Molecular pathways activated in melanoma***

Cell signaling pathways regulate cell growth and death, cell metabolism migration and angiogenesis. In cancer progression there is a loss of control of these signalling that result hyperactivated and/or silenced irreversibly allowing to cancer cells to acquire specific phenotypes, such as the ability to resist to apoptosis, abnormal proliferation, angiogenesis, and invasion.

#### **RAS/RAF/MEK/ERK pathway**

The mitogen-activated protein kinase (MAPK) pathway plays an important role in cellular proliferation and

differentiation. Under normal physiological conditions growth factors bound their tyrosine kinases receptors and activate a small GTP binding protein RAS (existing in three isoform: ARAF, BRAF and CRAF in humans) on cell membranes, which triggers intracellular signaling. This is followed by the sequential stimulation of several cytoplasmic protein kinases. The first of the cascade is RAF, a serine/threonine kinase protein that leads to phosphorylation of MEK (mitogen-activated protein/ERK kinase) proteins that activate in highly specific manner the downstream components: the extracellular signal-related kinase-1 and 2 (ERK-1 or p44<sup>MAPK</sup> and ERK-2 or p42<sup>MAPK</sup>). These isoforms can be activated in response to a wide variety of growth factors and mitogens such as stem cell factor (SCF), fibroblast growth factor (FGF), hepatocyte growth factor (HGF), and glial-cell-derived neurotrophic factor (GDNF) as a result of phosphorylation of threonine and tyrosine residues in a -TXY- motif and then translocate into the nucleus and stimulate pro-growth signals. In particular, the main substrates of ERKs are the transcription factors and other nuclear proteins like c-Fos ATF-2, c-Myc, c-Myb, Ets2, NF-1L6, TAL-1 and p53. In addition to transcription factors, another set of substrates for the ERKs are PHAS, tyrosine hydroxylase, phospholipase A2, phospholipase Cy, RNA polymerase II, CDC2 and also apoptosis regulator protein

as Bim, Bax, Bcl-2, Bad. Therefore, ERK activation promote cell-cycle progression and proliferation<sup>14</sup>.

Unregulated activation of the MAPK pathway can lead to malignancy. The MAPK pathway is one of the most frequently deregulated signaling pathways in the great majority of melanomas. ERK is hyperactivated in 90% of human melanomas by growth factors and by genetic alterations of upstream factors, RAS and RAF proteins as well as mutations at upstream membrane receptors (e.g., KIT)<sup>15</sup>. Mutations in BRAF appear to be the most common genetic alteration and major driver of this pathway, which occur in 50–70% of melanomas. Although BRAF is thought to exert its oncogenic effects almost entirely through MEK, CRAF can lead to MEK-independent pro-survival effects, in part through its interaction with nuclear factor-kappa B (NF- $\kappa$ B), as well as through inhibitory effects of critical regulators of apoptosis, such as ASK-1 and MST-2<sup>16-17</sup>. These mutations can be identified in benign melanocytic proliferation and all stages of invasive and metastatic melanoma promoting proliferation, survival, invasion, and angiogenesis of melanoma. Specifically, the presence of a BRAF mutation has been associated with a more aggressive disease course and poorer prognosis compared with patients without BRAF mutations<sup>18</sup>.

In melanoma, NRAS gene also is mutated in 15-30% of tumor samples leading to its permanent activation and serial activation both the downstream components of the RAS effector pathways and the non-MAPK pathways, such as the phosphatidylinositol-3 kinases (PI3K) pathway resulting in increased v-akt murine thymoma viral oncogene homolog (AKT) activity<sup>19-20</sup>.

### **PI3K/AKT/mTOR pathway**

The PI3K/AKT/mTOR is an intracellular signaling pathway promoting cell survival and proliferation, and is hyperactivated in most malignancies, including melanoma<sup>21-22</sup>. Stimulation of the PI3K pathway arises via GTP binding of RAS proteins and stimulation of receptor tyrosine kinases (RTKs). PI3Ks, constitute a lipid kinase family characterized by their ability to phosphorylate inositol ring 3'-OH group in membrane phospholipids generating phosphatidylinositol-3,4-bisphosphate (PIP<sub>2</sub>) and phosphatidylinositol-3,4,5-trisphosphate (PI-3,4,5-P<sub>3</sub>) which is a key propagator of intracellular signaling.

AKT is a family of serine/threonine protein kinase that comprise three highly homologous members known as AKT1, AKT2 and AKT3. All three AKT isoforms consist of a conserved domain structure including a specific PH domain, a central kinase domain and a carboxyl-terminal regulatory

domain that mediates the interaction between signaling molecules. AKT normally exist in the cytoplasm in inactive conformation. After the interaction with PIP3 by its PH domain it traslocates to the inner membrane where it is phosphorylated in two critical residues, Thr308 and Ser473. Thr308 is in the activation loop within the kinase domain of AKT and it is phosphorylated by PDK1 (phosphoinositide-dependent kinase 1). Ser473 is in the C-terminal regulatory domain of AKT and it is phosphorylated by mTORC2 complex. Phosphorylation of Thr308 partially activates AKT, while phosphorylation of both sites is required for full activation. The numerous substrates of AKT include cellular regulators of insulin signaling, proliferation, and survival<sup>23-24</sup>. AKT is inactivated by phosphatases (PP2A, PHLPP1, and PHLPP2) that remove the phospho-group from these residues. The activity of the PI3K/AKT pathway overall is regulated by the tumour suppressor phosphatase and tensin homolog (PTEN).

PTEN dephosphorylates the 3' position of PIP2 and PIP3 antagonizing PI3K activity. Activated AKT phosphorylates a broad range of proteins involved in the control of apoptosis (the FOXO family of transcription factors, BAD or NF- $\kappa$ B), cell cycle regulation (GSK3 $\beta$ , p27kip1), and growth (TSC2)<sup>25</sup>, thereby facilitating the proliferation and survival of cells.

mTOR (mammalian target of rapamycin), a serine/threonine protein kinase, is a downstream effector of PI3K and AKT. mTOR carries out several functions via two different complexes, mTOR complex 1 (mTORC1) and mTOR complex 2 (mTORC2). mTORC1 includes mTOR regulatory-associated protein of mTOR (Raptor), mLST8, and proline-rich AKT substrate 40 (PRAS40)<sup>26</sup> and is allosterically inhibited by the macrolide antibiotic rapamycin<sup>27</sup>. It is an important effector of cell growth and proliferation and regulates protein synthesis acting on several components of the translation machinery as eukaryotic translation initiation factor (eIF4E) and p70S6 kinase<sup>28</sup>. mTORC2 includes rapamycin-insensitive companion of mTOR (Rictor), mLST8, and stress-activated MAPK-interacting protein 1 (Sin1)<sup>29</sup>. It plays important roles in signal transduction as well as activates directly AKT<sup>30</sup>.

The major mechanisms of PI3K pathway activation in melanoma are loss of PTEN and NRAS mutations. Lack of PTEN antagonism (observed in 12% of melanomas through mutation or methylation) causes increased levels of PIP3 and active (phosphorylated) AKT<sup>31</sup>. Mutated AKT may also independently activate the PI3K/AKT/mTOR signalling pathway. Elevated AKT phosphorylation and/or activated mTOR functioning arises in 70% of malignant melanomas<sup>32-33</sup>. In particular, increased levels of the active form of AKT

were found in the radial-growth phase of melanoma and was found correlate with poor prognosis in melanoma patients<sup>34-35</sup>. Activation of AKT in cancer cells induces cell survival, proliferation, metastasis, invasion, and angiogenesis. AKT, in fact, inhibits apoptosis through the inactivation of BCL-2 antagonist of cell death (BAD) protein and of caspase-9, and promotes cell proliferation by increasing CCND1 expression. Moreover, affects many other cell-survival and cell cycle genes through the activation of transcription factor as NF- $\kappa$ B<sup>36-37</sup>.

### **NF- $\kappa$ B pathway**

Nuclear Factor-kappa B (NF $\kappa$ B) is an inducible transcription factor that regulates the expression of many genes involved in the immune response.

The NF- $\kappa$ B proteins constitute a family of proteins with homology to the chicken oncogene, *rel*. There are five known mammalian NF- $\kappa$ B subunits, each characterized by ankyrin repeat elements: p65 (RelA), RelB, Rel (c-Rel), p50/p105, and p52/p100 which form homo- and hetero-dimers. These proteins share an approximately 300 amino acid N-terminal domain called the Rel homology (RH) domain containing important sequences for binding DNA or inhibitor of NF- $\kappa$ B (I $\kappa$ B) as well as sites of dimerization. However, they differ in their C-terminal domain in that RelA, RelB and c-Rel exhibit

transactivating functions, while p100 and p105 contain inhibitory domains. In fact, NF- $\kappa$ B1/p105 and NF- $\kappa$ B2/p100 are the inactive precursors of the p50 and p52 proteins, respectively. The most common Rel/NF- $\kappa$ B dimer in mammals contains p50-p65. In unstimulated cells, NF- $\kappa$ B is retained in the cytoplasm through interaction with inhibitory proteins called I $\kappa$ B $\alpha$  (nuclear factor of kappa light polypeptide gene enhancer in B-cells inhibitor,  $\alpha$ ). NF- $\kappa$ B activation is rapidly induced by primarily inflammatory stimuli, as well as proinflammatory cytokines (IL-1 and TNF- $\alpha$ ), endotoxins, viruses and UV, that lead to activation of the I $\kappa$ B kinase (IKK) complex. IKK activated phosphorylates I $\kappa$ B proteins that are recognized by the ubiquitin ligase machinery, leading to their polyubiquitination and subsequent degradation by the proteasome 26S. During this process, also p65 is phosphorylated and p100 and p105 are cleaved into active forms p52 and p50 respectively. These events generate active NF- $\kappa$ B complexes that is free to translocate into the nucleus where they bind to specific sequence in the promoters of target genes, inducing transcription<sup>38</sup>. These genes include: immunoregulatory and inflammatory genes (cytokines and chemokines, acute phase proteins, cell adhesion proteins, inducible nitric oxide synthase (iNOS), immunoglobulins, and viral genes; anti-apoptotic genes as tumor necrosis factor receptor-associated

factor 1 and 2 (TRAF1 and TRAF2) inhibitor-of-apoptosis protein 1 and 2 (c-IAP1 and c-IAP2), caspase8/FADD, c-FLIP, members of BCL2 family; genes that positively regulate cell cycle progression (cyclin D1, c-myc, MMP9); and genes that encode negative regulators of NF- $\kappa$ B<sup>39-40</sup>.

The earliest indication for its role in tumorigenesis was emerged following RelA/p65 cloning and sequencing, which revealed its homology to c-Rel and its viral oncogenic derivative v-Rel that leads to carcinogenesis in avian lymphoid cells<sup>41</sup>. Recently, NF- $\kappa$ B activity has been shown to be upregulated in many cancers, including melanoma. It was demonstrated that some components of NF- $\kappa$ B family, such as p50 and p65 are overexpressed in the nuclei of dysplastic nevi and lesions of human melanoma<sup>42</sup>. The activation of NF- $\kappa$ B promotes the multiple steps in melanoma progression such as transformation, initiation, promotion, angiogenesis, invasion and enhanced metastatic potential of malignant melanoma cells<sup>43</sup>. Moreover, NF- $\kappa$ B activated would be responsible of resistance of cancer cells to chemotherapeutic agents<sup>44</sup>. NF- $\kappa$ B activation in melanoma may be the result of either exposure to proinflammatory stimuli in the tumor microenvironment or mutational activation of IKK resulting in enhanced transactivating capacity of the NF- $\kappa$ B complex and an increased survival of melanoma cells<sup>45</sup>.

Data indicate that the enhanced activation of NF- $\kappa$ B may be due to deregulations in upstream signaling pathways such as Ras/Raf and PI3K/AKT<sup>46</sup>. It has recently been suggested that AKT phosphorylates IKK $\alpha$  at the consensus sequence RXXXS/T, leading to the p65 phosphorylation and also may facilitate directly the phosphorylation of p65 on serines 529 and 536<sup>47</sup>. Mutational activation of BRAF, common in human melanomas, has been also associated with an enhanced IKK activity and the activation of NF- $\kappa$ B transcriptional activity resulting in increased survival of melanoma cells<sup>48</sup>. Infact, constitutively active ERK may indirectly activate NF- $\kappa$ B through the upregulation of inflammatory cytokines such as TNF- $\alpha$  and IL-1 $\alpha/\beta$ , as well as chemokines, that activate NF- $\kappa$ B<sup>49-50</sup>.

Therefore, NF- $\kappa$ B is a downstream target of both RAF and AKT and the PI3K/AKT pathway can activate by oncogenic RAS<sup>51-52</sup>. The extensive interaction of these signaling pathways in malignant melanomas provides a possible mechanism for compensatory signaling to make resistance to molecular-targeted therapy (Figure 4).

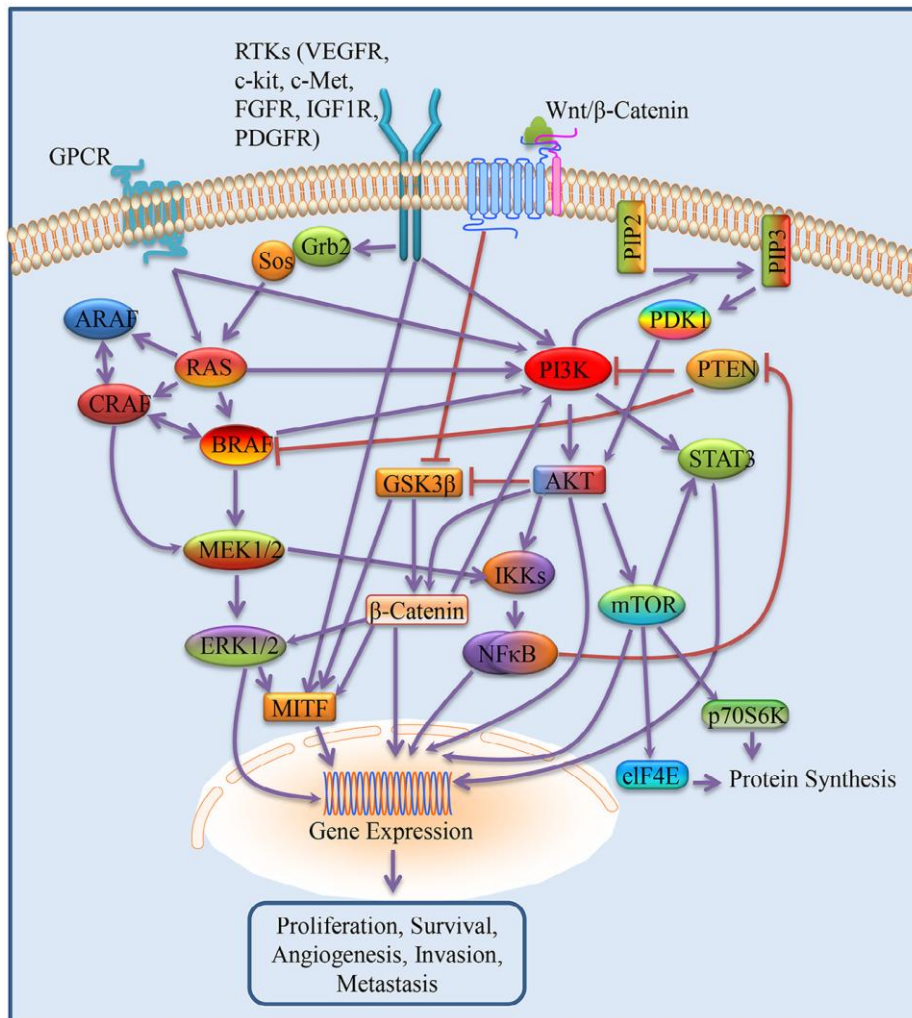


**Figure 4.** Signaling pathways activated in melanoma (Strickland et al., Cancer letters, 2015)

#### 1.4 Common genetic alteration in melanoma

The development and progression of malignant melanoma is related to gene mutations. In recent years, next-generation sequencing of melanoma has revealed the enormous genetic complexity of melanoma, with thousands

of mutations, deletions, amplifications, translocations, and DNA methylation changes being present in the genomes of individual tumors. The mutation rate of melanoma is higher than those reported for other aggressive tumors (Table 3). This may be due to the mutagenic effect of ultraviolet (UV) radiation involved in the melanoma pathogenesis<sup>53</sup>. In fact, a recent analysis of whole-exome sequences revealed that 46% of melanoma driver mutations can be attributed to the cytosine to thymine (C-to-T) transition, characteristic alteration due to UVR; a 9% of melanoma driver mutations, instead, showed the guanine to thymine (G-to-T) transversion, characteristic of UVA-associated oxidative damage. Most of these occur in tumor suppressor genes, including CDKN2A, PTEN, and TP53. However, although UVR causes many mutations, other mutagenic mechanisms are likely important in melanoma development<sup>54</sup>. Melanoma mutations must be differentiated into which mutations are causative in the disease “driver mutations” (confer a fitness advantage to the tumor cell) and which are only bystander mutations “passenger mutations” (that never conferred a fitness advantage)<sup>55</sup>.

One of the best-studied oncogenic events in melanoma is mutation of **BRAF** (v-Raf murine sarcoma viral oncogene homolog), a key protein kinase acting in the RAS–RAF–MEK–ERK mitogen-activated protein kinase (MAPK)

signal transduction pathway which regulates cell growth and proliferation. The RAF isoforms include ARAF, BRAF, and CRAF/RAF-1<sup>56</sup>. BRAF mutations are found in about 60% of all melanomas and in most of the benign nevi, which implies that the mutation by itself is not responsible for malignancy in melanocytic proliferations. BRAF mutations are more frequent in melanomas that develop in intermittently sun-exposed skin and less so in acral and mucosal melanomas. BRAF mutations are not found in uveal melanomas<sup>57</sup>. The most common mutation of BRAF are found in exon 15, at codon 600. In about 75% of all mutations in that area a valine is substituted by glutamic acid at codon (V600E). Less common mutations include valine by lysine (V600K) (about 20%), valine by aspartic acid (V600D) and valine by arginine (V600R) contribute another 5–6%. All this BRAF mutation cause the permanent activation of the protein and consequently induce MEK activation<sup>58</sup>. BRAF mutation, and in part also the special type of substitution, correlates with age, localization of the primary tumor, sun damage, and, in part, geographic region. A small number of BRAF mutants other than V600 were identified in human melanoma, as G469E, D594G, G466A, and N581S. These mutants have low kinase activity but shown to still activate ERK via a mechanism involving their ability to strongly activate CRAF<sup>59</sup>. Melanomas with wild type BRAF usually carry

oncogenic mutations in upstream components of the MAPK pathway.

**NRAS** (neuro-blastoma RAS viral oncogene homolog), a GTPase is mutated in approximately 20% of melanomas<sup>60</sup>.

**KIT** (v-Kit Hardy-Zuckerman 4 feline sarcoma viral oncogene homolog) is a receptor tyrosine kinase activated by binding of the cytokine stem cell factor (SCF); in melanoma KIT mutation and amplification are quite rare, they are found in particular subsets of melanoma, acral melanoma, mucosal melanoma, and lentigo maligna melanoma<sup>61</sup>. Approximately 70% of KIT mutations identified in melanoma are found in exon 11, most commonly L576P, and in the kinase domain in exon 13, most often K642E<sup>62</sup>. KIT mutations activate signal-transduction pathways (MAPK and PI3K) and increased melanocyte proliferation and melanoma survival<sup>63</sup>.

**GNAQ** (guanine nucleotide-binding protein, q polypeptide) and **GNA11** (guanine nucleotide-binding protein, a11), encoding members of the  $G\alpha$  (q) family of G protein  $\alpha$  subunits, are driver oncogenes in uveal melanoma. Mutations in GNAQ and GNA11 activate the MAPK pathway<sup>64-65</sup>.

Genetic alterations in components of the p16INK4A-cyclin D/CDK4-RB cell cycle checkpoint are found in virtually all melanoma cell lines in a mutually exclusive

fashion, underlining the importance of this checkpoint in preventing melanoma development<sup>66-67</sup>. **CDKN2A** is a well-known melanoma tumor suppressor gene that encodes for two tumor suppressor proteins through alternative splicing: p16INK4A, a key negative regulator of the cell cycle that activates retinoblastoma protein (RB) through negative regulation of CDK4, and p14ARF which activates p53 through inhibition of its major negative regulator, MDM2<sup>68</sup>. CDKN2A locus is mutated in about 25% of melanoma families and inactivated by mutation, deletion, or promoter hypermethylation in 50–80% of sporadic melanoma cases<sup>69</sup>. Loss of CDKN2A and CCND1 correlate with poor responses to dabrafenib<sup>70</sup>. Moreover, expression of oncogenic BRAFV600E in melanocytes induces expression of p16INK4A<sup>71</sup>. p53 mutations was found in 19% of melanoma tumors<sup>72</sup>, but several alterations in other genes affecting p53 activity inhibiting its function. Other known genetic alterations are: mutation of p14ARF<sup>73</sup>; overexpression of MDM2 or amplification of MDM4, the major negative regulators of p53 that promote its degradation and inactivation<sup>74-75</sup>; overexpression of p63, an antiapoptotic protein related to p53 that in melanoma cell lines prevents translocation of p53 to the nucleus<sup>76</sup>; increased expression of iASPP, a conserved ankyrin repeat protein that shuttles between nuclear and cytoplasmic compartments and

inhibits the pro-apoptotic function of p53<sup>77</sup>. **CDK4**, a cell cycle G1/S kinase, and cyclin D1 (**CCND1**), were shown to be amplified in melanoma<sup>78</sup>. CDK4 mutations are associated with familial melanoma<sup>79</sup>. Significantly, CDK4 pathway is deregulated in most melanomas as a consequence of increased activity of ERK or deletion of CDK4 inhibitor p16INK4A.

A cooperating event in BRAF-initiated melanomagenesis is constitutive activation of the PI3K/AKT/mTOR signaling pathway. BRAFV600E mutation are often associated with the PTEN aberrations inducing hyperactive-mTOR signaling in melanomas.

**PTEN** is a negative regulator of the PI3K/AKT pathway and it is mutated in 25% to 30% of melanoma, most commonly via allelic loss and focal deletions<sup>80</sup>. PTEN (or rather lack of PTEN) was shown to play a key role in the predisposition to melanoma in individuals carrying certain variants of melanocortin-1 receptor (MC1R). The mechanisms through which MC1R variants associated with red hair and fair skin predispose to melanoma were not understood until recently, when it was shown that wild-type but not variant MC1R protein associates with PTEN and protects it from degradation after UVB exposure. Disrupted MC1R-PTEN association was shown to be responsible for the

oncogenic transformation promoted by MC1R variants in presence of BRAFV600E<sup>81</sup>.

By contrast, activating mutations in PIK3CA, which encodes the catalytic subunit of PI3K, or in AKT1, AKT2, and AKT3, are rare in melanoma<sup>82</sup>. Only **AKT3** is deregulated in 25% of melanoma tumours promoting development of malignant melanoma<sup>83</sup>. Mutations in other PI3K pathways genes mTOR, IRS4, PIK3R1, PIK3R4, and PIK3R5 were detected in 17% of BRAFV600 and in 9% of NRAS-mutant tumors<sup>84</sup>.

Phosphoinositide-dependent kinase-1 (**PDK1**) is a serine/threonine protein kinase that phosphorylates and activates kinases of the AGC family, including AKT. Increased expression of PDK1 was observed in a large cohort of melanoma samples compared to nevi, and deletion of PDK1 in a GEMM of melanoma BRAFV600E/PTEN-/- significantly delayed development of tumours and metastases<sup>85</sup>.

**MAP2K1** and **MAP2K2** (MEK1 and MEK2, respectively) was found mutated in several melanoma cell lines with a frequency of 8%, resulting in constitutive ERK phosphorylation and higher resistance to MEK inhibitors<sup>86</sup>.

Microphthalmia-associated transcription factor (**MITF**) is a survival oncogene, amplified in 20% of melanoma cases. MITF acts both as a transcription activator to promote expression of genes involved in cell cycle, but

also as a transcriptional repressor of genes involved in invasion<sup>87</sup>; MITF amplification/alteration resulting in dysregulation of anti-apoptotic proteins. MITF is a melanoma-predisposition gene because is mutated in some familial melanomas<sup>88</sup>. The most significant mutation in MITF that occurs with higher frequency in patients affected with melanoma is a missense substitution (Mi-E318K). Codon 318 is located in a small-ubiquitin-like modifier (SUMO) consensus site ( $\Psi$ KXE) and Mi-E318K severely abolishes a SUMOylation of MITF inhibiting its transcriptional activity<sup>89</sup>.

PRIMARY SUBTYPES	PATHWAY	ABERRATION	FOUND IN TUMORS WITH...	FREQUENCY	POSSIBLE THERAPIES
BRAF	MAPK	Point mutation Gene fusions	NRAS wild type	50-60% rare	BRAF <sup>i</sup> + MEK <sup>i</sup> BRAF <sup>i</sup> + EGFR <sup>i</sup> + AKT <sup>i</sup>
NRAS	MAPK, PI3K, RALGDS		BRAF wild type	20-25%	MEK <sup>i</sup> + CDK <sup>i</sup>
KIT	MAPK, PI3K	Point mutation, amplification	NRAS BRAF wild type mostly	1% overall; 10% in mucosal; 10% in acral	Imatinib, nilotinib, imatinib
GNAQ/GNA11	Gα(q) family of G protein α subunits; MAPK activators	Point mutation	NRAS BRAF wild type	1%; 40-50% each in uveal	MEK <sup>i</sup> + PI3K <sup>i</sup> , everastaurin
MITF*	Transcription, lineage, cell cycle	Amplification	ALL	20%	HDAC <sup>i</sup>
NF1*	MAPK, PI3K negative regulator of RAS	Mutations, loss of expression	BRAF, NRAS wild type and less often in mutated	4% overall; 25% of BRAF, NRAS wild type	MEK <sup>i</sup> + mTOR <sup>i</sup> or PI3K <sup>i</sup>
TERT*	Telomerase	Mutations in the promoter of catalytic subunit	ND	70-80% overall; 33% primary; 85% metastatic	TERT inhibitors in preclinical
ERBB4	PI3K, MAPK	Point mutation	All types	15-20%	Lapatinib (ERBB <sup>i</sup> ) + PI3K <sup>i</sup>
MET	PI3K, MAPK	Activation by stromal HGF	All types	ND	Cabozantinib?
AKT3	PI3K	Amplification	All types	25%	AKT <sup>i</sup> , PI3K <sup>i</sup> , mTOR <sup>i</sup>
PTEN	PI3K	Point mutation or deletions	BRAF mutated; BRAF and NRAS wild type	40-60%	PI3K <sup>i</sup>
MAGI	PI3K; stabilizes PTEN	—	All types	—	PI3K <sup>i</sup>
TACC	Possibly stimulates PI3K AURKA signaling	—	BRAF and NRAS mutated	5%	PI3K <sup>i</sup> , AURK <sup>i</sup>
PREX2	RHO/RAC/MAPK; Rac exchange factor	Point mutations	BRAF or NRAS mutated	14%	
RAC1	RHO/RAC/MAPK; Regulator of cell adhesion, invasion, migration	Point mutations	BRAF or NRAS mutated	9% of sun exposed	
MAP2K1, MAP2K2	MAPK (MEK1/2)	Mutations	BRAF mutated; BRAF, NRAS wild type	5%	ERK <sup>i</sup>
MAP3K5, MAP3K9	RHO/RAC/MAPK	Mutations, loss of heterozygosity	All types	85% and 67%	MEK <sup>i</sup> , ERK <sup>i</sup>
MYC	Transcription	Amplification	All types	20-40%	mTOR <sup>i</sup> ?
ETV1	Transcription	Amplification	All types	15%	
TP53	Cell cycle, apoptosis	Point mutation	All types	10-20%	
MDM4	Negative regulator of p53	Overexpression	All types	65%	p53-MDM4 <sup>i</sup>
CDKN2A (P16INK4a, p14ARF)*	Negative regulator of TP53 and RB	Point mutation, deletion	BRAF and NRAS mutated, KIT amplified	30-40%	CDK <sup>i</sup>
BCL2, BCL2A1	Suppression of apoptosis	Elevated expression, amplification (BCL2A1)	All types	ND 30% (BCL2A1)	BH3 mimetics
CCND1	Cell cycle, G1/S cyclin	Amplifications	More frequent in BRAF, NRAS wild type	11%	CDK <sup>i</sup>
CDK4*	Cell cycle, G1/S cyclin-dependent kinase	Amplifications	More frequent in BRAF, NRAS wild type	3%	selective CDK <sup>i</sup>

**Table 3.** Common genetic alteration in melanoma

## **1.5 Therapy**

### **SURGERY and ADIUVANT Therapy**

Currently there isn't a "gold therapy" for melanoma but surgical excision is considered the primary treatment for patient with cutaneous melanoma because renders "disease-free" with relatively limited associated morbidity. The management of early-stage disease, melanoma in situ (margin of 0.5 cm) and low-risk primary melanomas (margins greater than 0.5 cm), being treated with wide excision and then follow-up skin exams. For patients with intermediate- and high-risk melanomas measuring 1.01 to 2.0 mm in thickness wide excision is recommended. Sentinel lymph node mapping and biopsy is routinely offered for patients having 1 mm or greater deep melanomas. Also the patients with cutaneous melanoma metastases (Stage IIIb or IVa) are frequently treated with local excision followed by skin exams, imaging for metastases or enrollment in clinical trials. Cutaneous melanoma metastases can be subdivided in 3 types: **satellite** close the primary tumor (within 2 cm), **in transit** which are > 2 cm from the primary tumor but within the same region as the primary, and **distant metastases** far from the primary site<sup>90</sup>. In this patients the surgical approach increases their survival. It was reported a 5-year survival rate of 20% in 144 patients with non-regional melanoma metastases<sup>91</sup>; and overall 3-4-year survival rates

of 36% and 31%, respectively, in stage IV melanoma patients<sup>92</sup>. However surgery alone cannot identify and address the microscopic in-transit malignant cells present which often give rise to future tumors. For this purpose, in 1996 was approved high-dose interferon-alfa as adjuvant therapy for the stage III or IV disease. Treatment with IFN- $\alpha$  is associated with a statistically significant improvement in disease-free survival but not in overall survival. Moreover, IFN- $\alpha$  could cause significant toxic effects as: severe fatigue, depression, and hepatotoxicity<sup>93</sup>.

Radiation therapy (RT) is used in 1–6% of patients with melanoma in the US in the setting of inoperable disease, particularly for patients in who tumor occurred predominately in the head and neck region. It is commonly used as adjuvant therapy or as palliative therapy to improve local control or in patient with desmoplastic neurotropic melanoma (DNM) <sup>94</sup>.

In the last 30 years many drugs and combination of drugs have introduced in melanoma therapy to improve patient survival for longer time. (Figure 5).

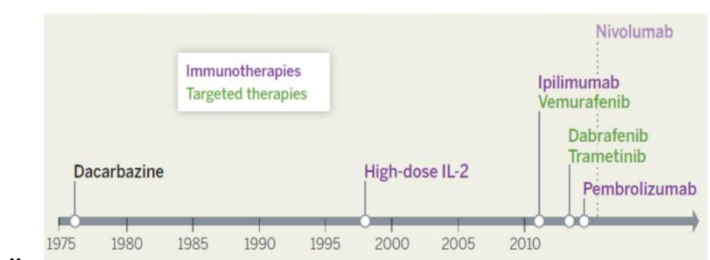


**Figure 5.** Timeline of FDA regulatory approval for metastatic melanoma. (Lo and Fisher. Science 2014)

## **CHEMOTHERAPY**

Cytotoxic chemotherapy was the main treatment strategy for metastatic melanoma. Common antineoplastic agents currently being used include dacarbazine, temozolomide, high-dose interleukin-2 and paclitaxel with or without cisplatin or carboplatin. These have shown modest response rates of less than 20% in first- and second-line settings.

**Dacarbazine** [5(3,3-dimethyl-1-triazeno)-imidazole-4-carboxamide] was the first chemotherapeutic agent approved by the U.S. Food and Drug Administration (FDA) in 1970 for treatment of metastatic melanoma and it was used for many years. Dacarbazine is a prodrug, one of the triazene derivatives, that is converted in the active metabolite, diazomethane, by cytochrome P450. Dacarbazine acts through DNA alkylation, forming crosslinks within and between helices that lead to local denaturation of the DNA strand, interfering with its form and function and killing the cancer cell. However, dacarbazine monotherapy is characterized with low overall response rates (approximately 10%-15%), and the drug doesn't offer survival benefit. To improve response rates several chemotherapeutic agents as Temozolomide (a DTIC analog), cisplatin, carmustine, fotemustine, vinblastine, and tamoxifen or cytokine as interleukin-2 (IL-2) and interferon-

alpha were added to DTIC in a variety of regimens but without a statistically significant survival benefit. Toxicities include nausea and vomiting, in over 90% of patients, myelosuppression (both leucopenia and thrombocytopenia) and flu-like illness, consisting of chills, fever, malaise, and myalgia<sup>95-97</sup>.

## **IMMUNOTHERAPY**

Immunological strategies in therapy of localized and metastatic melanoma have a long tradition. The importance of immune response in melanoma derived from observation of the correlation between higher melanoma incidence and immunosuppressed patient<sup>98</sup>. Several therapies was been proposed for disseminated disease modulating the immunologic response like the nonspecific immunostimulant *Bacillus Calmette-Guérin*, interferons, interleukins and others but they have failed to delivery major clinical benefits<sup>99-102</sup>. Also, melanoma vaccines has not shown significant clinical responses<sup>103</sup>.

### IL-2

The first immune-based therapy FDA-approved for advanced melanoma in 1998 was IL-2, an immune cytokine that activates citotoxic T cell activation and promotes their proliferation. It stimulates, also, the development of lymphokine-activated killer (LAK) cells, which have the

ability to lyse tumor cells<sup>104-105</sup>. The use of high-dose IL-2 showing long-term, durable complete responses in previously treated patients with metastatic melanoma<sup>106</sup>. However its use is limited by high toxicity due to anaphylactic shock and development of infectious granulomas at sites of injection and low response rates. To reduce systemic toxicity and increase local therapeutic effects, it was introduced intralesional interleukin-2 for treatment of cutaneous melanoma metastases, which showed a complete response in 78% of treated lesions<sup>107</sup>. Early studies showed that “tumor infiltrating lymphocytes” (TIL) present in tumors had potent anti-tumor activity<sup>108</sup>. So, adoptive cell therapies utilizing TILs in combination with IL-2 have been promising<sup>109</sup>. Lymphodepletion prior to TIL infusion improve effect on adoptive cell transfer therapy because reduce competition for growth factors and cytokines in vivo microenvironment. Although immunotherapy with adoptive transfer of TILs is a promising to treat patients with refractory metastatic melanomas there is a technically challenging to generate sufficient amount of tumor-specific lymphocytes that can maintain their tumor-killing activity in vivo. So, it will be difficult to implement these therapies into routine clinical practice<sup>110</sup>.

The most successful immunotherapy approach has been “immune checkpoints” inhibition. This therapy is based on the fact that T lymphocytes are critical to antitumor immunity. Two of the best-studied checkpoints involve cytotoxic T lymphocyte antigen-4 (CTLA-4) and programmed cell death-1 (PD-1), two coinhibitory T cell receptors that mediate immune tolerance<sup>111</sup>.

#### ANTI-CTLA4

CTLA-4 is a member of the immunoglobulin superfamily and it is a transmembrane inhibitory receptor that downregulates the immune system. CTLA4 is expressed on the surface of T cells CD4<sup>+</sup> and CD8<sup>+</sup>. CTLA4 is similar to the T-cell co-stimulatory protein, CD28, and both molecules bind to CD80 and CD86, also called B7-1 and B7-2 respectively, on antigen-presenting cells. CD28 transmits a stimulatory signal whereas CTLA4, as a control mechanism around 48 hours after the initial T-cell activation, transmits an inhibitory signal to T cells. Intracellular CTLA4 is also found in regulatory T cells and may be important to their function<sup>112</sup>. CTLA-4 blockade with anti-CTLA-4 monoclonal antibodies allows appropriate T-cell activation through re-establishment of the costimulatory binding of CD28 to B7. This interaction increases T-cell proliferation and amplifies T-cell-mediated immunity, thus, promoting the antitumor immune response in patients<sup>113</sup>. The first anti-CTLA-4 agent

to be investigated in patients with metastatic melanoma was **Tremelimumab**, a human monoclonal IgG2 anti-CTLA-4 antibody. Although in phase I/II clinical trials, it demonstrated antitumor activity in patients with stage III/IV melanoma, a phase III study failed because tremelimumab shows any benefit over chemotherapy<sup>114-115</sup>. More successes has had **Ipilimumab**, a human monoclonal IgG1 anti-CTLA-4 antibody that was approved by the FDA in 2011 for the treatment of patients with metastatic melanoma. In multiple phase III clinical trials in patients with stage III and IV melanoma ipilimumab monotherapy at a dose of 3 mg/kg bodyweight significantly improved overall survival (10.1 months) compared to gp100 peptide vaccine monotherapy (6.1 months) <sup>116</sup>. Also the treatment with ipilimumab at a dose of 10 mg/kg bodyweight plus dacarbazine compares with dacarbazine alone revealed a higher overall survival rate (11.2 months versus 9.1 months, respectively) with a 28% reduction in the risk of death<sup>117</sup>. The response to Ipilimumab as an immunologic reaction appears slowly but may be long lasting. Significant immune toxicities were reported in this trials. Common side effects that may result from autoimmune reactions associated with the use of ipilimumab include gastrointestinal immune-related events (diarrhea; colitis) and other autoimmune inflammations (hypophysitis; thyroiditis; hepatitis) <sup>118</sup>.

### ANTI PD-1/PDL-1

PD-1, like CTLA-4, is an inhibitory receptor expressed on T and B cells and some myeloid cells. The PD-1 ligands PD-L1 and PD-L2 have different expression patterns. PD-L1 acts as a negative regulator of T cells. It is located on multiple normal and tumor cells like melanoma, where, once bound by PD-1, attenuates immune responses inducing peripheral tolerance to “self” antigens and, in cancer, promotes downregulation/termination of the immune response against the tumor<sup>119</sup>. PD-L2 is expressed on antigen-presenting cells (APC), providing tolerance to orally administered antigens. Humanized antibodies against both PDL1 and PD-1 have been developed to inhibit their interaction increasing antitumor activity. In clinical trials for many cancers, including melanoma, they have shown more powerful, with higher response rates and fewer autoimmune toxicities<sup>120-122</sup>. The human antibody **nivolumab** (BMS-936558) is directed against PD-1, which in a phase I trial showed a response in 28% of the melanoma patients, with long-term responses longer than 1 year in 50% of responding patients. The best response was observed with a dosage of 3 mg/kg bodyweight with a low rate of grade 3 or 4 toxicity observed in only 6% of patients. Nivolumab was well tolerated in fact were observed common side effects as diarrhea, rash, and pruritus<sup>123</sup>. The better safety profile of

PD-1 antibody versus CTLA-4 antibody is most likely due to the fact that it acts at tumor sites, preventing interaction with PD-L1 on tumor cells. A second anti-PD-1 agent, **pembrolizumab** (MK-3475, formerly known as **lambrolizumab**) is a humanized IgG4 antibody approved by FDA on September 2014 following phase I trial with 135 advanced melanoma patients. It showed a response rate of 38% in patients receiving a larger dose (10 mg/kg of bodyweight intravenously every 2 or 3 weeks). Most of the responses became evident after 12 weeks and were long lasting (in 81%, lasting more than 11 months). Adverse drug reactions, reported in 79% of patients, included fever, chills, fatigue, rash and pruritus<sup>124</sup>. An anti-PD-L1 human IgG4 antibody (BMS- 936559) is being tested in phase I trial in 55 patients with melanoma. Preliminary results showed significant tumor long-term response of 29% with the dose 3 mg/kg bodyweight and a comparable rate of grade 3 or 4 adverse effects<sup>125</sup>. Other two anti-PD-L1 antibodies, MPDL3280A (Genentech) and MEDI4736 (MedImmune), are being tested in solid tumors under early phase clinical trials. Recent preliminary results of MDPL3280A trial showed an overall response rate of 29% in 44 patients with melanomas of different origins<sup>126</sup>. Combination therapies utilizing multiple immune modulating agents that block of both immune checkpoints (PD-1 and CTLA4) are showing great

promise. Anti-PD-1/nivolumab/MK-3475 and anti-CTLA-4/Yervoy antibodies are being combined in clinical trials (NCT01024231). This treatment produced an objective response rate of 40% in 52 patients at a variety of dose levels and in several patients tumors disappeared completely<sup>127</sup>.

### **TARGET THERAPY**

Concurrent advances in targeted molecular therapy have also improved the treatment and prognosis of a subset of advanced melanoma patients. Approval of single substances directed against mutated proteins has dramatically changed the options available in melanoma therapy.

#### BRAF inhibitors

BRAF-targeted therapies represent the first major breakthrough in systemic therapy for metastatic melanoma. The earlier BRAF inhibitor is nonselective multikinase inhibitor **sorafenib** (BAY 43-9006). It acts as a pan-inhibitor of RAF, which targets not only BRAF but also CRAF as well as the vascular endothelial growth factor (VEGF) and platelet-derived growth factor (PDGF) receptor tyrosine kinases (RTKs) <sup>128</sup>. However, sorafenib did not show great benefit, in clinical trials neither as monotherapy or in combination with

other anticancer compounds, such as dacarbazine, carboplatin and paclitaxel in patients with metastatic melanoma<sup>129</sup>. The latest generation of highly specific and potent BRAF inhibitors offers a significant improvement over sorafenib against mutant BRAF. These drugs show a greater selectivity for mutant BRAF and have fewer off-target effects. The first selective BRAF inhibitor targeting the mutant V600E form is PLX4720 (**vemurafenib**).

Vemurafenib is a potent ATP-competitive RAF inhibitor that co-crystallizes with a protein construct containing the kinase domain of BRAF V600E to enable preferential binding to the ATP-binding domain of mutant BRAF<sup>130</sup>. Pre-clinical studies showed that vemurafenib inhibits the kinase activity of BRAF harboring the V600E mutation with an half maximal inhibitory concentration (IC<sub>50</sub>) of 13 nM, resulting in selectively blocked the RAF/MEK/ERK pathway and consequent cell-cycle arrest and the induction of apoptosis in melanoma cells<sup>131</sup>. In 2011 vemurafenib/Zelboraf (960 mg twice daily) received FDA approval for treatment of metastatic or unresectable melanoma harbouring the BRAF mutation V600E following the results of a phase III trial, BRIM-3. The 675 enrolled patients, previously untreated, with BRAF V600E mutation-positive metastatic melanoma were randomized to receive vemurafenib at 960 mg orally twice daily, or dacarbazine

chemotherapy of 1,000 mg/m<sup>2</sup> intravenously every three weeks. The six-month overall survival was 84% in the vemurafenib arm and 64% in the dacarbazine arm. Many patients treated with vemurafenib had a rapid tumor response with resultant decreased tumor weight as indicated by the high overall response rate that was 48% for vemurafenib compared to 5.5% for dacarbazine<sup>132</sup>. Vemurafenib is not truly selective for BRAF mutant melanoma cells and can paradoxically activate the MAPK pathway in wild-type BRAF cells<sup>133</sup> which resulting in several toxicities, concerning frequency and intensity during treatment, as the development of a rash, in some associated with a severe photosensitivity (UVA), arthralgia, keratinocytic neoplasia and squamous cell carcinoma<sup>134</sup>.

The second BRAF inhibitor that has been approved for the treatment of BRAF V600 mutated metastatic melanoma by the FDA on May 30th 2013 is **dabrafenib**. Dabrafenib/Tafinlar is a specific inhibitors of BRAF V600E/K. In a phase III clinical trial (BREAK-3), dabrafenib (150 mg twice daily) was compared with dacarbazine in previously untreated patients with advanced melanoma with mutated BRAF. As vemurafenib dabrafenib showed significant high response rates and reduced of 70% in risk for disease progression versus standard therapy<sup>135</sup>. Toxic side-effects included skin lesions, pyrexia, frequent fatigue,

nausea and pain. The development of photosensitivity and epithelial tumors were less frequent than vemurafenib.

Other BRAF inhibitors that are currently being evaluated in clinical trials are LGX818, BMS-908662, XL281 ARQ736, and RAF265 (clinicaltrials.gov). In particular, **LGX818** is in a phase I trial and has shown the similar response rates (58%) but lower toxicity than vemurafenib and dabrafenib<sup>136</sup>. New inhibitors are in development to eliminate the side effects associated with the paradoxical activation by vemurafenib of the ERK1/2 pathway in wild-type BRAF cells. **PLX7904**, a new “paradox-breaking” BRAF inhibitor, that inhibits MAPK signaling in BRAF-mutant cells without activating BRAF in BRAF wild-type cells<sup>137</sup>.

A major problem with the use of these inhibitors and the further advancement of melanoma therapies is *de novo* or acquired drug resistance. Infact, unfortunately, some patients with BRAF-mutated melanoma do not respond to therapy or show tumours progress or grow again with a median time to progression of approximately 6-8 months<sup>138</sup>. Primary or *de novo* resistance may be due to pre-existing mutations (intrinsic) or interactions between tumor cells and microenvironments (extrinsic). Further additional mutations in the MAPK pathway (eg. MEK2) and in the PIK3 pathway (eg. PIK3 and AKT1), or loss of NF1 function (which regulates RAS) have been shown to escape the effects of

BRAF (and MEK) inhibitors activating bypass survival pathways, in particular, PI3K/AKT pathway<sup>139-141</sup>. Secondary or acquired resistance to BRAF inhibitors, when melanomas begin to grow again following an initial successful treatment, occurs inevitably in most of the patients treated. The secondary resistance to BRAF inhibitor was mainly associated to several MAPK pathway -dependent or -independent mechanisms. Acquisition of new mutations in NRAS or the downstream kinase MEK1, BRAF amplification or splicing, overexpression of cancer osaka thyroid (COT), and activation of RTKs cause rapid regrowth of existing metastases or the emergence of new<sup>142-145</sup>. Although the resistance mechanisms identified so far are diverse, most appear correlate to reactivation of MEK/ERK signaling and increased of the PI3K/AKT/mTOR pathway. Moreover, cell growth and proliferation are controlled by a network of pathways consisting of various key proteins which might be mutated, so the block of a single checkpoint will not be successful in the long-term. Correspondingly, to overcome the impact of resistance to BRAF inhibitors, the designed drug combination may provide a more durable response rate and may prolong progression-free survival (PFS) in patients with BRAF mutant melanoma, compared with either agent alone. The most promising combination strategy is the simultaneous inhibition of BRAF, MEK and PI3K pathway<sup>146-</sup>

<sup>147</sup>. Another interesting strategy being investigated in clinical trials that may help overcome BRAF inhibition resistance is the use of intermittent dosing of vemurafenib after the maximum response to therapy to prolong the response duration<sup>148</sup>. A better understanding of the molecular biology of melanoma has helped the development of new therapies.

### MEK inhibitors

There are two major classes of MEK inhibitors, ATP non-competitive and ATP competitive inhibitors. Currently, most MEK inhibitors are non-competitive, indicating that they do not compete for the ATP binding site and instead bind to an adjacent allosteric site, which explains their high specificity<sup>149</sup>. MEK is a downstream kinase of BRAF so its inhibition leads to decreased cell signalling and proliferation in cancer cells inducing apoptosis<sup>150</sup>. **Trametinib/Mekinist** (GSK1120212) is a non-competitive MEK1/2 inhibitor and it was FDA-approved in 2013 for the treatment of adult patients with the BRAF V600E/K mutation and unresectable or metastatic melanoma at the dose of 2 mg orally once daily<sup>151</sup>. Inhibition of MEK has been explored in clinical trials for melanoma patients with mutant BRAF. In a phase III randomized trial trametinib compared to chemotherapy (dacarbazine or paclitaxel) showed a marked improvement in both progression free and overall survival (respectively 4.8

months and 81% vs 1.5 months and 67%)<sup>152</sup>. The adverse effects is mild, including rash, cardiac dysfunction, ocular toxicities, diarrhea, peripheral edema, and hypertension which could be managed with dose reduction or interruption. Currently, several MEK inhibitors have showed efficacy in the treatment of melanoma as **selumetinib** and **MEK162**, while other are in clinical development as PD-0325901, refametinib, RO-4987655, TAK-733, and XL518. Recently, MEK162 monotherapy revealed a response rate of 21% in NRAS-mutated melanoma<sup>153-154</sup>. Patients who did not respond to vemurafenib or who have develop resistance to BRAF inhibitor usually will not benefit from MEK inhibitor monotherapy because the mechanisms involved in development of resistance to mutant BRAF confer resistance to MEK inhibition.

#### MEK and BRAF combined therapy

Numerous preclinical and clinical studies have shown that the combination of BRAF and MEK inhibitors is a successful strategy for the treatment of metastatic melanoma. Preclinical studies have demonstrate that this co-inhibition reduces tumor growth, increases apoptosis and delays the onset of resistance when compared with monotherapy<sup>155</sup>. The first combination to be tested in clinical trials was the BRAF inhibitor dabrafenib with the MEK inhibitor trametinib. In a phase II trial, in 54 MAPK

inhibitor-naïve patients with BRAFV600E/K mutation, the CombiDT (dabrafenib 150 mg twice daily and trametinib 2 mg daily) showed promising activity in patients with stages III or IV melanoma and fewer side effects compared with vemurafenib. They induce a significantly higher response of 76% vs 54% for dabrafenib alone and an evident improvement in PFS (9.4 months in the combination group vs 5.8 months in the monotherapy group). No patient recorded progressive disease as their best response<sup>146; 156</sup>.

The CombiDT showed, also, less toxicities than dabrafenib alone. In fact, the addition of trametinib reduced the appearance of cutaneous squamous cell carcinomas<sup>146</sup>. The most common toxicity was pyrexia, which occurred in 71% of patients (5% had grade 3 or 4 reactions). On the basis of these results FDA has granted accelerated approval of the combination of dabrafenib and trametinib for the treatment of patients with metastatic melanomas that carry the BRAFV600E or BRAFV600K mutation in January 2014. A phase III clinical trial comparing the combination of dabrafenib and trametinib with dabrafenib alone (NCT01584648) and dabrafenib and trametinib with vemurafenib monotherapy (NCT01597908) is also in progress. Other BRAF and MEK inhibitor combinations have also shown promise and are in phase III trials as vemurafenib and cobimetinib (CombiVC)

(NCT01689519)<sup>157</sup>; and LGX818 and MEK162 (NCT01909453)<sup>158</sup>. Unfortunately, it has been shown that the response to Combi therapy after disease progression with BRAF inhibitors has little efficacy. Moreover, a dual BRAF/MEK inhibitor, RO5126766, has recently shown activity in patients with metastatic melanoma, suggesting that combined inhibition of BRAF and MEK will be of the greatest benefit for metastatic melanoma patients<sup>159</sup>. However, about 50% of individual metastases have a complete response but most patients still relapse within a year although rarely resistance emerges in the lesions that had a complete response<sup>146</sup>. Other early-phase combination trials with approved BRAF inhibitors explore addition of inhibitors of PI3K, AKT, CDK, HSP90, RTKs and other targets, as well as immunotherapy, to improve durability of responses.

#### ERK inhibitors

ERK1/2 are the kinases below MEK in the MAPK cascade, they are the primary effector of this pathway, and regulates the activity and expression of transcription factors and proteins that result in cell growth, proliferation, and cell cycle progression. Most BRAF inhibitor resistance (and combination BRAF and MEK inhibitor resistance so far) results in reactivation of ERK signalling. Thus, inhibition of ERK might represent an emerging therapeutic strategy for

the treatment of BRAF inhibitor-resistant melanoma. Preclinical evidence suggests that ERK inhibition is effective in BRAF inhibitor-resistant melanoma with common MAPK-reactivating resistance drivers (RAS, MEK1 mutations, BRAF splice variants, and BRAF amplification). Several candidate drugs are in phase I trials, as MK-8353 (NCT01358331)<sup>160-161</sup>.

### KIT inhibitors

C-KIT is a receptor tyrosine kinase that when binding to its ligand activates the MAPK, PI3K/AKT and Janus Kinase/Signal Transducer and Activator of Transcription (JAK/STAT) signaling pathways, resulting in proliferative and survival effects<sup>162</sup>. Selective inhibitors of KIT (**imatinib; sunitinib; nilotinib; dasatinib**) which were developed and used for the treatment of other types of cancer (such as gastrointestinal stroma tumor [GIST] or chronic myeloid leukemia) became interesting also for melanoma treatment<sup>163</sup>. In a phase II trial using imatinib (400 mg orally once-daily), in selected melanomas (acral; mucosal; sun-damaged skin), the best overall response rate was 77% in cases with KIT mutation compared to only 18% in cases with KIT amplification<sup>164</sup>. Imatinib was well tolerated and didn't show very serious adverse effects at utilized dose. On the basis of these data, imatinib has shown promising results as a therapeutic agent in patients with metastatic melanoma

and mutations in the KIT gene. Other tyrosine kinase inhibitors (sunitinib, dasatinib, and nilotinib) are underway a phase III trials. The major limitation of this study has been the rarity of mutations in this gene, which occur in less than 5% of patients with melanoma<sup>165</sup>.

### NRAS inhibitors

Neuroblastoma RAS viral oncogene homolog (NRAS) is mutated in approximately 15% to 20% of melanoma and seems to correlate with a worse prognosis compared to NRAS/BRAF wild-type patients<sup>166</sup>. Developing drugs targeting mutated NRAS is challenging because multiply pathways are unregulated due to this mutation. Infact, current drug development focuses on targeting the downstream effectors of NRAS, the MAPK and PI3K pathways. MEK162 is the most promising MEK inhibitor, showing response in 20% of the patients with NRAS-mutated melanoma<sup>167</sup>. It is most likely that such patients will benefit much more from the combination therapies and a trial (NCT01781572) that combining MEK162 and LEE011, a cyclin-dependent kinase (CDK) 4/6 inhibitor, in patients with NRAS-mutated melanoma is ongoing.

### PI3K/AKT inhibitors

The PI3K/AKT pathway regulates several cellular processes including proliferation, survival, motility, metabolism, and angiogenesis. This pathway is activated by receptor tyrosine kinases and RAS proteins and is inhibited by PTEN. Alterations in the PI3K pathway have also been reported in 60% of the melanomas<sup>168-169</sup>. Several classes of PI3K pathway inhibitors exist including PI3K inhibitors, AKT inhibitors, mTOR inhibitor, dual PI3K\mTOR inhibitor and dual mTOR1\2 inhibitor that down-regulate the activation of this survival pathway. The first generation of inhibitors of PI3K signaling in melanoma was rapamycin and the second-generation agents were everolimus (RAD001) and temsirolimus (CCI-779), they allosterically inhibit the mTORC1 complex<sup>170-171</sup>. These agents have long been used as immunosuppressor in patients with organ transplants and have demonstrated anti-proliferative effects against many human cancers<sup>172</sup>. However, clinical trials in melanoma have shown a lack of objective responses to mTORC1 inhibitors as single agents or in combination with BRAF inhibitors<sup>173-174</sup>. The reason for this seems to be interruption of negative feedback loops mediated by mTORC1, causing activation of PI3K, AKT and ERK<sup>175</sup>.

mTOR complex-1 inhibitors are now in use in a multitude of cancer types. Dermatologic side effects are

common and include stomatitis, eruptions, and nail changes, including paronychia. Few data are available about the pharmacodynamics effects of PI3K and AKT inhibitors in patient. Most of them are now under clinical trials in melanoma (both wild-type and BRAF mutant), often in combination with MAPK inhibitors (clinicaltrials.gov; NCT01820364; NCT01616199; NCT01337765; NCT01941927; NCT01166126; NCT01014351; NCT00022464).

#### CDK4 and CDK6 inhibitors

The CDK4-CDK6 pathway sits below the MAPK pathway and involves p16, cyclin D, CDK4 and CDK6, and the RB1 protein. This pathway is aberrantly activated in most melanomas resulting in increased cell cycle progression, reduced induction of apoptosis, and cell senescence<sup>176-177</sup>. Inhibitors of CDK4, such as palbociclib (PD0332991; NCT01037790), SCH 727965 (dinaciclib), LY2835219, BAY1000394, LEE011), and the combination of LGX818 with LEE011 (NCT01777776), are currently in clinical trials for various advanced cancers including melanoma.

#### Other targets

Several other targets exist in BRAF-mutant melanoma, ranging from growth factors in the tumour microenvironment (eg, HGF and VEGF), receptor tyrosine

kinases at the cell surface (eg, MET, FGFR, and VEGFR), epigenetic regulators (eg, histone deacetylase), and apoptosis regulators (eg, MDM2). Lapatinib, an Epidermal Growth Factor Receptor/Human Epidermal growth factor Receptor 2 (EGFR/HER2) inhibitor, showed activity in cell lines harboring ERBB4 mutations and not in ERBB4 wild-type cells. Mutations in ERBB4 observed in 19% of patients with melanoma can cause an overactivation of the ERK and AKT pathways. Currently, a phase II trial testing lapatinib in patients with advanced melanoma with ERBB4 mutations is ongoing (clinicaltrials.gov; NCT012 64081)<sup>178</sup>.

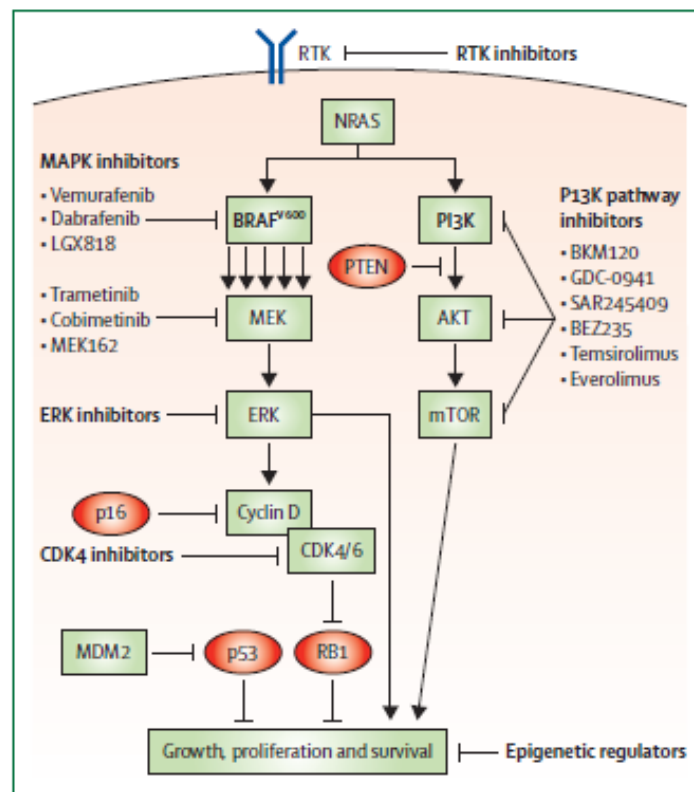


**Figure 6.** Cell signalling pathways and drug targets (Menzies and Long, *Lancet Oncol.* 2014)

## **2. *Hydrogen Sulphide***

### **2.1 *Physical and Chemical Properties of H<sub>2</sub>S***

Over millions of years hydrogen sulphide (H<sub>2</sub>S) caused life destructions and extinctions on the earth. It is believed that in Permian period H<sub>2</sub>S provoked a mass extinctions on earth, than the emissions from massive volcanic eruptions in Siberia caused a chain reaction of environmental events that resulted in oxygen depletion in the world's oceans and, therefore, the died of many species that lived there. Otherwise, some non-oxygen (anaerobic) breathing organisms called green sulfur bacteria (Chlorobium) continued to grow and reproduce at high rates. These green sulfur bacteria used sulfate dissolved in water for respiration instead of oxygen, and subsequently produced H<sub>2</sub>S. According to this theoretical perspective the large amounts of H<sub>2</sub>S produced by these organisms created so much lethal gas in the ocean that it then diffused into the air and land destroyed the plant and animal life as well. By the end of the Permian period, 95% of marine species and 70% of terrestrial ones had vanished<sup>179</sup>. Actually a great diversity of microorganisms, bacteria, fungi as well as plants, are able to produce H<sub>2</sub>S<sup>180-181</sup>. Interestingly, plants are the primary producers of organic sulfur compounds and are able to couple photosynthesis to the reduction of sulfate,

assimilation into cysteine, and further metabolism into methionine, glutathione, and many other compounds. Animals, instead, have a dietary requirement for sulfur amino acids. Cysteine is the central intermediate from which most sulfur compounds are synthesized<sup>182</sup>.

H<sub>2</sub>S, along with nitric oxide (NO) and carbon monoxide (CO), forms part of a group of biologically active gases that are termed gasotransmitters or gasomediators. H<sub>2</sub>S is a colorless, water-soluble and flammable gas with an unpleasant smell of rotten eggs. H<sub>2</sub>S is the predominant sulphur contaminant of natural gas and ranges in concentration from <1 to >90%.

H<sub>2</sub>S has a molecular weight of 34.08 and its chemical structure is analogue to that of water molecule with an atom of sulfur being less electronegative than the first and much less polar (Figure 7). Infact, H<sub>2</sub>S has a vapor density (d) of 1.19, heavier than air (d=1.0), boiling point (-60.7 °C) and melting point (-82.3°C) is much lower than they are in water and freezing point is -86°C.

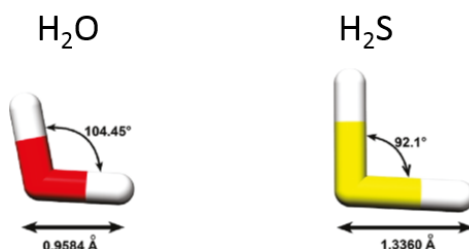
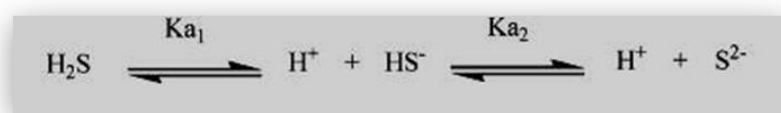


**Figure 7.** Similarity in molecular structure between water (H<sub>2</sub>O) and hydrogen sulfide (H<sub>2</sub>S).

H<sub>2</sub>S is a weakly acidic, dissociating in aqueous solution into hydrogen cation (H<sup>+</sup>) and hydrosulfide anion (HS<sup>-</sup>) (K<sub>a1</sub>= 1.3\*10<sup>-7</sup> M), which subsequently may decompose to H<sup>+</sup> and sulfide anion (S<sup>2-</sup>) (K<sub>a2</sub>= 1\*10<sup>-19</sup> M) in the following reaction<sup>183-185</sup>:



#### Hydrogen Sulfide Dissociation

Under physiological conditions, at 37°C and pH 7.4, equal amounts of H<sub>2</sub>S and HS<sup>-</sup> are within the cell, and approximately a 20% H<sub>2</sub>S/80% HS<sup>-</sup> ratio in extracellular fluid and plasma. Conversely, the chemical form S<sup>2-</sup> is not present in appreciable amounts, since the dissociation of HS<sup>-</sup> occurs only at high pH values.

H<sub>2</sub>S present in the air comes from organic and inorganic sources. Organic sources include bacteria and decomposition of matters such as released from septic tanks, sewers, or water treatment plants, while inorganic sources are natural gas, petroleum refinery, rayon manufacturing, paper and pulp mill industry, sulfur deposits, volcanic gases, and sulphur springs. The half-life of H<sub>2</sub>S in air varies from 12 to 37 h. The temperature would change the half-life and the solubility of H<sub>2</sub>S. H<sub>2</sub>S is a highly lipophilic molecule, such as it can easily penetrates lipid bilayer of cell membranes.

The toxic effects of this small molecule were known long before its physiological properties. Back to World War One, H<sub>2</sub>S was used by the British as a chemical agent. It has been postulated that H<sub>2</sub>S exerts dose-dependent toxicity with millimolar concentrations. Accumulation of H<sub>2</sub>S gas in confined or closed spaces, including septic tanks and cesspools, animal processing plants, pump mills, and sludge plants has been the cause of numerous cases of human deaths. Sudden release of H<sub>2</sub>S gas in a huge amount from oil wells or refineries leads to infamous “knock-down” phenomenon of oilers and other petrochemical workers, an instant loss of consciousness often associated with respiratory failure<sup>186-188</sup>. Most organ system are susceptible to the effects of H<sub>2</sub>S and each system exhibits a different response according as a concentration, time or rate of exposure. The lethal concentration for 50% of humans for 5 min exposure (LC50) is 800 ppm, and concentrations over 1,000 ppm cause immediate collapse with loss of breathing, with only a single inhalation needed. Tissues most susceptible to H<sub>2</sub>S toxicity are those with exposed mucous membranes and those with high oxygen demands<sup>189</sup>. This gas is considered a broad-spectrum poison to humans in the nervous system, respiratory system, and cardiovascular system; infact, at concentrations <1000ppm, can have toxic effects that occur with eye irritation, sore throat, dizziness, nausea, difficulty breathing and chest stiffness; at concentrations >1000ppm, it can cause serious adverse effects

resulting in respiratory paralysis, pulmonary edema, cardiac arrhythmias, stroke and death.

The molecular mechanisms underlying the toxicological effects of H<sub>2</sub>S are mostly attributed to its ability to induce K (+)-channel-mediated hyperpolarization of neurons and potentiation of other inhibitory mechanisms, or to inhibit cytochrome c oxidase in mitochondria, at micromolar concentrations, reducing ATP production<sup>190</sup>. However, over the last decade it has become clear that it is not only detectable in significant amounts in mammals, including humans, where it appeared in blood from nanomolar to micromolar concentration range, but that it is also produced endogenously and may play a significant role in both normal physiology and the pathophysiology of disease.

## ***2.2 Endogenous Production of H<sub>2</sub>S in mammalian cells***

### **Enzymatic Production of H<sub>2</sub>S**

In mammals, H<sub>2</sub>S is endogenously produced by enzymatic reactions and by nonenzymatic pathways. The key precursors for endogenous H<sub>2</sub>S synthesis are sulfur-containing amino acids as L-cysteine, that derives from alimentary sources, or synthesizes from L-methionine, through the so-called “trans-sulfuration pathway” with homocysteine (Hcy) as an intermediate, or liberates from endogenous protein. H<sub>2</sub>S is generated by four separate

enzymes that are cystathionine gamma-lyase (CSE, EC 4.4.1.1), cystathionine beta-synthase (CBS, EC4.2.1.22), cysteine aminotransferase (CAT, EC 2.6.1.3) and 3-mercaptopyruvate sulfurtransferase (3-MST EC 2.8.1.2)<sup>191</sup> (Figure 8).

Interestingly, these enzymes are evolutionarily conserved and occur in many lower species as well as in mammals and their expression is tissue-specific<sup>192</sup>. CBS is the predominant enzyme responsible for H<sub>2</sub>S generation in the brain and the nervous system, and is also highly expressed in the liver and kidney<sup>193</sup>. CSE is expressed abundantly in mammalian cardiovascular system and respiratory system. It also appears to be the main H<sub>2</sub>S-forming enzyme in the liver, kidney, uterus, placenta, smooth muscle as well as pancreatic islets<sup>194-195</sup>. 3-MST can be found in proximal tubular epithelium in the kidney, pericentral hepatocytes in the liver, cardiac cells in the heart and neuroglial cells in the brain<sup>196</sup>. Both CSE and CBS are expressed in the human colon in the myenteric plexus neurons, and evidence indicates that human colonic mucosa metabolizes L-cysteine to H<sub>2</sub>S<sup>197</sup>. Importantly, while CBS and CSE are hemeproteins primarily located in the cytosol, 3-MST is a zinc-dependent protein found in both the mitochondria and cytosol. CBS and CSE are pyridoxal 5'-phosphate (PLP) dependent enzymes and they

are responsible for the majority of the endogenous production of H<sub>2</sub>S in mammalian tissues.

CBS is a cystathionine-forming enzyme and it catalyzes  $\beta$ -replacement reactions between L-serine, L-cysteine, cysteine thioethers, or some other  $\beta$ -substituted  $\alpha$ -L-amino acids, and a variety of mercaptans. Homocysteine is the physiological substrate for CBS and in presence of cysteine their condensation generate, as final products, cystathionine and H<sub>2</sub>S<sup>198</sup>. In addition to H<sub>2</sub>S production, CBS has a prominent role in maintaining homocysteine levels *in vivo*. Patients with homocysteinaemia exhibit impaired CBS activity, due to mutations of the regulatory domain of CBS, and display markedly increased levels of homocysteine and low H<sub>2</sub>S levels that contribute to the cardiovascular disease<sup>199-200</sup>. Human CBS is a homotetramer consisting of 63 kDa subunits which bind two cofactors, PLP and heme. Each CBS subunit of 551 amino acid residues binds two substrates (homocysteine and serine). The NH<sub>2</sub> terminal of CBS contains the binding sites for both PLP and heme (protoporphyrin IX). Although, there is no clear a role of heme in the catalytic activity of CBS, seems to be redox sensor because its deletion renders CBS insensitive to oxidative stress<sup>201</sup>. The PLP binding domain is the catalytic domain, and it is deep in the heme domain, linked by a Schiff base. The COOH terminal of CBS contains a regulatory

domain of 140 residues, playing an autoinhibitory role for the activity of full-length CBS. Binding of the allosteric activator, S-adenosyl-L-methionine (AdoMet or SAM), to this domain will cause a conformational change so that CBS is instantly activated. Deletion of the regulatory domain constitutively activates CBS<sup>202</sup>. The activity of CBS is, also, regulated at the transcriptional level by glucocorticoids and cyclic AMP. The activity of CBS can be directly inhibited by nitric oxide (NO) and carbon monoxide (CO)<sup>203</sup>.

CSE has been described as an exclusively beta-replacing lyase with a strict specificity for the primary substrate L-cysteine and for several sulfur-containing cosubstrates. It catalyses a  $\beta$ -disulphide elimination reaction that results in the production of thiocysteine, pyruvate, and  $\text{NH}_4^+$  from cystathionine. Thiocysteine may react with cysteine or other thiols to form  $\text{H}_2\text{S}$ . CSE is able to convert, also, directly L-cysteine in pyruvate,  $\text{NH}_3$  and  $\text{H}_2\text{S}$  and L-homoserine in  $\text{H}_2\text{O}$ ,  $\text{NH}_3$ , and 2-oxobutanoate (or  $\alpha$ -ketobutyrate)<sup>204</sup>. Rat CSE (but not human CSE) may also use cystine, the disulfide form of Cys, as a substrate to generate  $\text{H}_2\text{S}$  in the presence of a reductant<sup>205</sup>. The concentration of cystine in the reducing environment of cells is extremely low, so it is unlikely that cystine contributes to  $\text{H}_2\text{S}$  biogenesis under normal conditions. CSE seems to be the dominant enzyme for the formation of  $\text{H}_2\text{S}$  in mammalian tissues as demonstrates by

CSE-KO mice that exhibit a profound depletion of H<sub>2</sub>S in peripheral tissues<sup>206</sup>. Human deficiency of CSE may lead to cystathioninuria, a metabolic disorder characterized by an excess of cystathionine in the urine that is inherited in an autosomal recessive manner. Other diseases related to CSE mutation include hypercystathioninemia and increase the risk of developing atherosclerosis and bladder cancer<sup>207</sup>. CSE is a protein of 405aa and is a tetramer formed by two homodimers, both contributing to the active site pocket. There are two isoforms of human CSE as the consequence of alternative splicing<sup>208</sup>. Activity of CSE is regulated at transcriptional level by myeloid zinc finger 1 (MZF1) and specificity protein 1 (SP1; also known as Sp1 transcription factor), and the enzyme can be upregulated by bacterial endotoxin<sup>209</sup>. A recent study has reported the crystal structures of human CSE (hCSE), in apo form (apo-hCSE), complexed with PLP (hCSE·PLP) and with the inhibitor DL-propargylglycine (PAG) (hCSE·PLP·PAG). The structure of hCSE·PLP·PAG complex highlights the particular importance of Tyr114 in hCSE and the mechanism of PAG-dependent inhibition of hCSE<sup>210</sup>.

In mitochondria 3-MST produces H<sub>2</sub>S through a reaction involving the generation of pyruvate from 3-mercaptopyruvate (3-MP). It also catalyse the transsulfuration of a thiol to a persulfide, which can

subsequently join a second thiol to form a disulfide and release H<sub>2</sub>S. 3-MP is provided through the reaction of cysteine and  $\alpha$ -ketoacid (e.g.  $\alpha$ -ketoglutarato) by CAT. In the cytosol, the thiocysteine formed by cystathionase can act as an acceptor of the sulfur transferred from 3-mercaptopyruvate by MST<sup>211</sup>.

### **Non-enzymatic Production of H<sub>2</sub>S**

Non-enzymatic production of H<sub>2</sub>S occurs through glucose, glutathione, inorganic and organic polysulfides and elemental sulfur. H<sub>2</sub>S can be generated from glucose via glycolysis or from phosphogluconate via NADPH oxidase. Glucose reacts with methionine, homocysteine or cysteine to produce gaseous sulfur compounds. H<sub>2</sub>S is also produced through direct reduction of glutathione and elemental sulphur that is mediated by NADH or NADPH. Increased oxidative stress and hyperglycemia will promote H<sub>2</sub>S production from this path<sup>212</sup>. The enterobacterial flora is an important source of H<sub>2</sub>S. The intestinal epithelium expresses specialized enzyme namely sulfate-reducing bacteria (SRB) that efficiently degrade sulphide to thiosulphate and sulphate to protect itself against high local concentrations of sulphide and to prevent an excessive entry of H<sub>2</sub>S into the systemic circulation<sup>213</sup>. H<sub>2</sub>S can also be released from thiosulfate and persulfides. Garlic and garlic-derived organic polysulfides induce H<sub>2</sub>S production in a thiol-dependent



the persulfides to sulfite ( $\text{H}_2\text{SO}_3$ ). Sulfur from the second persulfide is transferred from the SQR to sulfite by sulfur transferase (ST) producing thiosulfate ( $\text{H}_2\text{S}_2\text{O}_3$ ). Thiosulfate is, subsequently, converted in sulfite ( $\text{SO}_3^{2-}$ ) and sulphate ( $\text{SO}_4^{2-}$ ), by thiosulfate reductase and sulfite oxidase or is conjugated with cyanide ions ( $\text{CN}^-$ ) to generate thiocyanic acid by rhodanase enzyme (RHOD; also known as thiosulfate cyanide sulfurtransferase, TST). Also, sulfite originating through this reaction is quickly oxidized to sulfate, the major end-product of  $\text{H}_2\text{S}$  metabolism under physiological conditions<sup>214</sup>. For every mole of  $\text{H}_2\text{S}$  oxidized 1.5 mole of oxygen is consumed along the electron transport chain. Metabolism of  $\text{H}_2\text{S}$  through SQR appears ubiquitous in all tissues except the brain<sup>215</sup>. This process maintains very low intracellular  $\text{H}_2\text{S}$  concentrations. In cytosol and in the gastrointestinal tract,  $\text{H}_2\text{S}$  is catalyzed mainly by thiol-S-methyltransferase (TSMT) that converts sulfide to methanethiol ( $\text{CH}_3\text{SH}$ ), which is less toxic to colonocytes than sulphides, by methylation. These enzymes are presumed to have a protective function, preventing excessively high local concentrations of sulfide and  $\text{H}_2\text{S}$  entry into the systemic circulation<sup>216-217</sup>.

Methemoglobin, considered a “common sink” for endogenous gases including CO and NO, also binds  $\text{H}_2\text{S}$  to form sulfhemoglobin. Therefore, the half-life of free  $\text{H}_2\text{S}$  in

blood may also be short<sup>218</sup>. It was demonstrated that pretreating wild-type HEK-293 cells with methemoglobin for 1 h prior to adding 100 $\mu$ M H<sub>2</sub>S significantly abolished the antiproliferative effect of H<sub>2</sub>S<sup>219</sup>. H<sub>2</sub>S can also be scavenged by metallo- or disulfide-containing molecules such as horseradish peroxidase, catalase, and oxidized glutathione<sup>220</sup>.

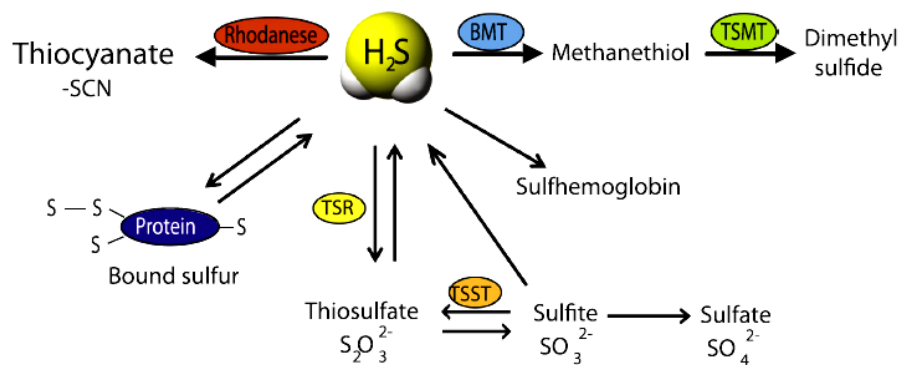


**Figure 9.** Catabolism of H<sub>2</sub>S (Kolluru et al., *Nitric Oxide*, 2013)

### 2.3 Molecular targets of H<sub>2</sub>S

Once produced in mammalian cells, H<sub>2</sub>S can directly exert its biological effects via interaction with different signalling molecules or can store as sulfur and released later in response to a physiological signal (Figure 10). Acid-labile sulfur and sulfane sulphur are the two main forms of sulfur stores in mammalian cells<sup>221</sup>.

In the cells  $\text{H}_2\text{S}$  exists in equilibrium with its anionic form  $\text{HS}^-$ , (ratio 1:4). As a gas transmitter,  $\text{H}_2\text{S}$  does not use a specific transporter, and its lipophilic nature allows it to rapidly travel through cell membranes<sup>222</sup>, whereas  $\text{HS}^-$  anions cannot cross cell membranes and therefore might only target intracellular proteins. Recently was identified a channel permeable to  $\text{HS}^-$  anions in the bacterium *Clostridium difficile*<sup>223</sup>. The best mode of  $\text{H}_2\text{S}$  signalling is through protein sulfhydrylation, which occurs at reactive Cys residues of target proteins. In this process, the sulfhydryl group of a reactive Cys is modified to a -SSH group, resulting in increased reactivity of the Cys residue. The regulation machineries for S-sulfhydrylation depend by ATP level, pH value, ionic strength, and oxygen partial pressure<sup>224</sup>. The first reported molecular target for  $\text{H}_2\text{S}$  was the ATP-sensitive potassium channels ( $\text{K}_{\text{ATP}}$ ) which activation accounts in numerous distinct pharmacological effect of  $\text{H}_2\text{S}$ <sup>194</sup>. The stimulatory effect of  $\text{H}_2\text{S}$  on  $\text{K}_{\text{ATP}}$  channel complex relied on a direct interaction between  $\text{H}_2\text{S}$  molecule and the disulphide bond on the extracellular loop of the SUR1 subunit of  $\text{K}_{\text{ATP}}$  channels<sup>225</sup>. A direct confirmation of the effect of this gas on the  $\text{K}_{\text{ATP}}$  channel has come from electrophysiological studies in which NaHS increased the  $\text{K}_{\text{ATP}}$  current in rat aortic and mesenteric smooth muscle cells.  $\text{H}_2\text{S}$  is also known to act on a number of other ion channels.  $\text{H}_2\text{S}$  inhibits BKCa (big conductance  $\text{Ca}^{2+}$ -sensitive  $\text{K}^+$ ) channels in stably

transfected HEK-293 cells<sup>226</sup>, whereas the opposite effect was noted in rat pituitary tumor cells<sup>227</sup>; inhibits L-type Ca<sup>2+</sup> channels in cardiomyocytes<sup>228</sup>; T-type Ca<sup>2+</sup> channels mediating visceral pain in the mouse<sup>229</sup> and intracellular chloride Cl<sup>-</sup> channels in rat heart lysosomal vesicles<sup>230</sup>; it activates transient receptor potential vanilloid (TRPV) channels in both urinary tract<sup>231</sup> and airway smooth muscle<sup>232</sup>. Important targets of H<sub>2</sub>S are the intracellular transcription factors. The first evidence was done by Oh and colleagues that demonstrated NaHS reduce LPS-induced NF-κB activation in cultured RAW 264.7 macrophages inhibiting IκB-α degradation and NF-κB nuclear translocation<sup>233</sup>. As NaHS, many H<sub>2</sub>S donors, like GYY4137, S-diclofenac, garlic compounds such as diallyl sulfide (DAS), can also downregulate NF-κB activation<sup>234-236</sup>. The functional consequence of reduced NF-κB activation in inflammatory cells is downregulation of a number of proinflammatory genes, including those that encode for inducible nitric oxide synthase (iNOS) and cyclooxygenase-2 (COX-2), as well as downregulation of inflammatory cytokines/chemokines and adhesion molecules.

However, under some experimental circumstances, NaHS can be proinflammatory and can augment (not inhibit) IκB-α degradation and thence increase (not reduce) NF-κB activation<sup>237</sup>. Moreover, recently, was established that H<sub>2</sub>S

synthesized by CSE, than TNF- $\alpha$  stimulation, is able to sulfhydrylate the p65 subunit of NF- $\kappa$ B at cysteine-38, enhancing its binding to the co-activator RPS3, thereby augmenting the transcription of several anti-apoptotic genes<sup>238</sup>. Clearly, there is considerable variation in the way that the NF- $\kappa$ B system responds to H<sub>2</sub>S that depends on the cell type and/or culture conditions used during the studies and, also, on the precise stage of the inflammatory response. Infact NF- $\kappa$ B has a proinflammatory role in the early stages of inflammation and anti-inflammatory role in the resolution phase. Additional transcription factors are also targets for H<sub>2</sub>S. The signal transducer and activator of transcription 3 (STAT3), that regulate the expression of many genes that mediate cell survival (e.g., survivin), proliferation (e.g., c-fos), and angiogenesis (e.g., vascular endothelial growth factor), results activated by H<sub>2</sub>S<sup>239</sup>. NaHS also induces the nuclear localization of the transcription factor NF-E2-related factor 2 (Nrf-2) that regulates gene expression of a number of cellular cardioprotective enzymes, including heme oxygenase-1 (HO-1) and thioredoxin-1 (Trx-1)<sup>240</sup>. Finally, H<sub>2</sub>S increases hypoxia-inducible factor-1 (Hif-1) activity in the nematode, *Caenorhabditis elegans* whereas in mammalian has not seen yet<sup>241</sup>.

The effect of H<sub>2</sub>S on MAPK signalling is not clear due to the cell type and concentrations used. The MAPK

superfamily is composed of three main members, stress-activated protein kinase/c-JunNH<sub>2</sub>-terminal kinase (SAPK/JNK), p38-MAPK, and ERK. MAPK regulate cell proliferation, apoptosis, differentiation, inflammation, and cycle progression. The activation of different MAPK members by H<sub>2</sub>S in different types of cells results in inducing apoptosis. Infact, H<sub>2</sub>S induces apoptosis of human aortic SMCs via activating ERK<sup>242</sup>, of insulin-secreting beta cells (INS-1E) by the activation of p38 MAPK<sup>243</sup> and of human derived dopaminergic neuroblastoma cell line (SHSY5Y) by downregulation of JNK<sup>244</sup>. The activation of the same MAPK member by H<sub>2</sub>S in different cells may be responsible for the opposite functional consequences. For instance, H<sub>2</sub>S increase endothelial cell proliferation (but also rat vascular smooth muscle cells and human colon cancer cells<sup>245-246</sup>) via stimulating a sustained phosphorylation\activation of ERK<sup>247</sup> and increase the proliferation of nontransformed intestinal epithelial cells (IEC-18) cells by upregulation of JNK expression<sup>248</sup>. Instead, the activation of p38 by H<sub>2</sub>S is responsible of survival of human polymorphonuclear cells, anti-inflammation of microglial cells and SH-SY5Y cells<sup>244; 249-250</sup>.

Additional kinases are also targets of H<sub>2</sub>S. In isolated hearts subjected to ischemic preconditioning, a brief infusion of NaHS stimulates both cardiac AKT and protein

kinase C (PKC) activity; this effect has been associated with improved cardiac mechanical performance and reduced injury<sup>251</sup>.

Cell cycle is realized by the progression from G1 phase to S phase, G2 phase, and M phase (mitosis). Once this progression is stopped at any checking point, the cells enter G0 phase or the so-called quiescence status. The fate of cells going through this cycle is determined at three checkpoints. H<sub>2</sub>S can affect cell proliferation or death by altering the fate of the cell going through cell cycle. On epithelial-like cells H<sub>2</sub>S induced cell cycle arrest downregulating cyclin D1 and upregulating p21Cip/WAF-1, involved in the control of cyclin-cdk activity<sup>252-253</sup>. In nontransformed intestinal IEC-18 cell NaHS (1 mM) promotes the proliferation facilitating the cell cycle entry<sup>254</sup>.

It has been reported that H<sub>2</sub>S increase [Ca<sup>2+</sup>]<sub>i</sub> by the activation of cAMP pathway in primary cultures of brain cells, neuronal and glial cell lines, and *Xenopus* oocytes selectively enhance N-methyl-d-aspartate (NMDA)-receptor mediated responses and facilitate the induction of hippocampal long-term potentiation in the CNS<sup>255</sup>. Another signaling pathway activated by cAMP/PKA in the CNS is the PI3K/AKT/p70 ribosomal S6 kinase (p70S6K). NaHS has been shown to increase cAMP concentration and expression of PI3K, AKT, and p70S6K in isolated rat hippocampal

neurons<sup>256</sup>. In the kidney NaHS reduce renovascular hypertension in hypertensive rats lowering level of cAMP, and, consequently, of angiotensin II<sup>257</sup>. Differential effects of H<sub>2</sub>S on cAMP/PKA pathway have been related to the expression of different isoforms of AC and/or PDE in different types of cells. As regard the effect of H<sub>2</sub>S on cGMP/PKG pathway it was demonstrated that NaHS increased the level of cGMP in cultured rat aortic smooth muscle cells inhibiting phosphodiesterase (PDE), isoenzymes responsible for the hydrolysis of both cGMP and cAMP, without to modify the activity of guanylyl cyclase<sup>258</sup>.

H<sub>2</sub>S is a strong reducing agent and may scavenges of reactive oxygen species and nitrogen species. H<sub>2</sub>S significantly inhibites ONOO<sup>-</sup> with a potency like to that of glutathione (GSH), a major intracellular antioxidant<sup>259</sup>. The antioxidant property of H<sub>2</sub>S may also be indirectly realized due to its capability in increasing the level of GSH. This could partially result from the stimulatory effect of H<sub>2</sub>S on  $\gamma$ -glutamylcysteine synthetase and cysteine transport in neurons<sup>255</sup>.

The antioxidant effects of H<sub>2</sub>S can affect the remodelling or proliferative process of the blood vessels but doesn't affect the vascular contractility<sup>260</sup>. H<sub>2</sub>S reduces, also, H<sub>2</sub>O<sub>2</sub>, ONOO<sup>-</sup>, and O<sub>2</sub>, homocysteine-induced, in cultured vascular smooth muscle cells<sup>261</sup> and hydrogen peroxide and

oxLDL-induced cytotoxicity of cultured HUVECs<sup>262</sup>. H<sub>2</sub>S also can bind to haem proteins as an axial ligand for the prosthetic group enhancing the activities of haem-containing enzymes in vitro, such as haemoglobin, neuroglobin and cytochrome c oxidase, which contributes to some of its (patho) physiological effects. H<sub>2</sub>S reacts with hemeproteins in distinct ways: (i) by incorporation of H<sub>2</sub>S into one of the pyrrole rings of the heme, (ii) generating the sulfheme derivative, (iii) binding to alternate sites of hemeproteins such as cysteine, copper, and zinc ions; or to the ferric iron with subsequent reduction of the heme, and (iv) through coordination with the ferric heme iron without inducing reduction or sulfheme production<sup>263</sup>.

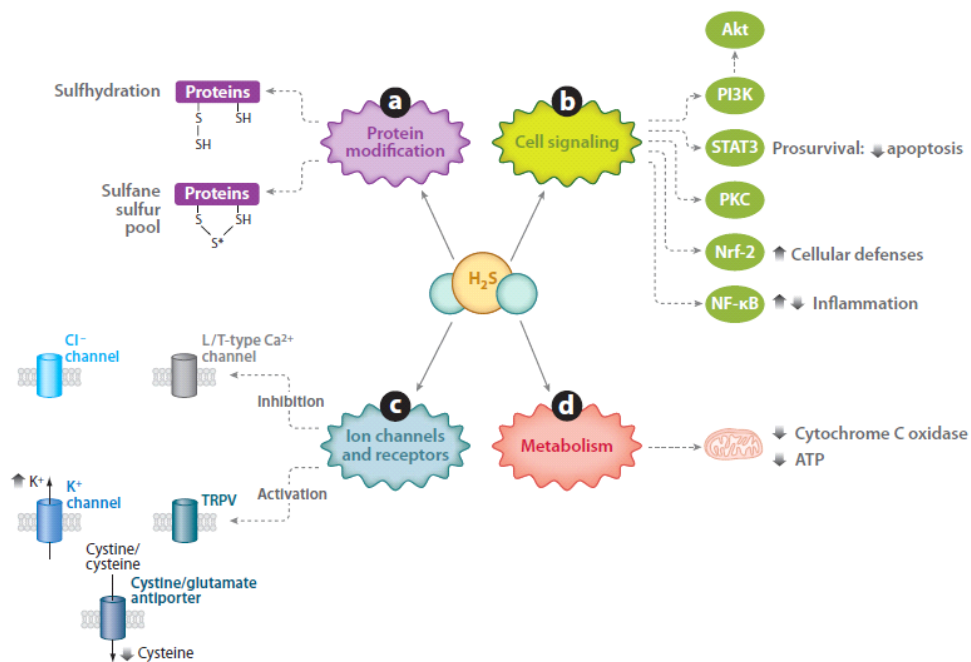


**Figure 10.** Molecular targets of H<sub>2</sub>S (Li et al., 2011. *Annu. Rev. Pharmacol. Toxicol.*)

## **2.4 Physio- pathological functions of H<sub>2</sub>S in mammals**

H<sub>2</sub>S is involved in numerous physiological and pathophysiological functions. H<sub>2</sub>S exerts its biological effects at low concentrations and toxic effects at high concentrations acting on various biological targets without a specific receptors for intracellular signaling<sup>264</sup>. At micromolar (physiological) concentrations, multiple studies have demonstrated the cytoprotective (antinecrotic or antiapoptotic) effects of H<sub>2</sub>S which may be related to its antioxidant activities. H<sub>2</sub>S is able to neutralize a variety of reactive species including oxyradicals, peroxynitrite, hypochlorous acid, and homocysteine<sup>261; 265-266</sup>. Moreover, low levels of H<sub>2</sub>S exerts cytoprotective effect increasing activity of endogenous antioxidant cellular systems as glutathione, by the activation/expression of  $\gamma$ -glutamylcysteine synthetase, N-acetylcysteine and superoxide dismutase as demonstrated in primary cortical neurons exposed to the excitotoxin NMDA<sup>255</sup>. Higher (millimolar) H<sub>2</sub>S concentrations are cytotoxic to the cells; this is due to free radical and oxidant generation, calcium mobilization, glutathione depletion, intracellular iron release, as well as induction of mitochondrial cell death pathways.

## **H<sub>2</sub>S and the Cardiovascular System**

In the cardiovascular system H<sub>2</sub>S induces dilation of blood vessels by stimulating K<sub>ATP</sub> channels in vascular smooth muscle cells (SMCs)<sup>194</sup>. H<sub>2</sub>S shows, also, cardioprotection effect during ischemia/reperfusion injury in isolated hearts inducing negative inotropic effect and reducing central venous pressure by the opened of K<sub>ATP</sub> channels in the myocardium<sup>267</sup>. All these effects can be prevented by pretreatment with glibenclamide a classical K<sub>ATP</sub>-channel inhibitors, to demonstrate the specificity of H<sub>2</sub>S cardiac effects<sup>268</sup>. H<sub>2</sub>S possesses many common features of an endothelium-derived hyperpolarizing factor (EDHF). The absence of endothelium shifted the H<sub>2</sub>S concentration-response curve to the right with the IC<sub>50</sub> changed from 136 to 273 μM. The endothelium-dependent vasorelaxing effect of H<sub>2</sub>S becomes even more significant in small resistance arteries. The vasorelaxant effect of H<sub>2</sub>S is due to the activation of both K<sub>ATP</sub> channels on vascular SMCs and charybdotoxin/apamin-sensitive K<sub>Ca</sub> channels in vascular endothelial cells<sup>194; 269</sup>.

H<sub>2</sub>S reduces atherogenesis by interfering with vascular inflammation<sup>250</sup>, by inhibiting leukocyte infiltration and adhesion<sup>270</sup> and by reducing calcification<sup>271</sup>. Deficiency of CSE significantly enhances atherosclerosis development in ApoE knockout mice involving disruption of vascular redox

status, increased intimal proliferation and inflammatory adhesion molecule expression<sup>272</sup>, and whereas treatment with NaHS of the same mice resulted in reduced atherosclerotic plaque thanks to reduction of ICAM-1 level in circulation and its expression in aortic endothelial cells<sup>273</sup>. H<sub>2</sub>S can also inhibit calcification and osteoblast differentiation of vascular smooth muscle cells that can contribute to atherogenesis<sup>274</sup>.

H<sub>2</sub>S play an important role in regulating platelet function and thrombosis. It inhibits cyclooxygenase activity and collagene-induced platelet aggregation reducing, moreover, thromboxane formation<sup>275-276</sup>. It was demonstrate that chronic intake of garlic powder and garlic oil also inhibits platelet aggregation in humans<sup>277</sup>. Several reports indicate a potential synergistic effect between NO and H<sub>2</sub>S in controlling various biological responses of vascular function. Several study reveale that inhibition of NO production by blocking eNOS attenuates H<sub>2</sub>S mediated angiogenic activity and reduces H<sub>2</sub>S-dependent vasorelaxation highlighting the importance of NO in vascular H<sub>2</sub>S signalling, and *viceversa*<sup>278</sup>.

### **H<sub>2</sub>S and the Nervous System**

H<sub>2</sub>S exerts important effects in central nervous system (CNS) through regulation of neurotransmission and

neuromodulation. The potential physiological functions of H<sub>2</sub>S in the brain may include calcium homeostasis, potentiation of hippocampal long-term potentiation (LTP), suppression of oxidative stress and regulates survival/death of neurons. Most of these effects are mediated by activation of N-methyl-D-aspartate (NMDA) receptors, normal receptor for glutamate, express in both central and peripheral nervous systems. H<sub>2</sub>S selectively enhance NMDA-receptor-mediated currents by stimulating the production of cAMP in primary cultures of brain cells, neuronal and glial cell lines, and *Xenopus* oocytes, which then activates protein kinase A (PKA). PKA activated, consequently, phosphorylates the NMDA receptor and induces also LTP<sup>279</sup>.

Moreover, H<sub>2</sub>S is able to increase directly glutamate secretion<sup>280</sup>. The interaction of H<sub>2</sub>S and NMDA receptors affects other neuronal activities, such as epilepsy, neuropathic pain, stroke, and Alzheimer's and Parkinson's diseases. In fact, prolonged activation of NMDA receptors by H<sub>2</sub>S causes calcium overload in cells and leads to their death<sup>281-284</sup>. Thus, inhibition of its production has been suggested to be a potential treatment approach in stroke therapy. Neuromodulator effects of H<sub>2</sub>S is, also, due increasing release of GABA, a major inhibitory neurotransmitter in CNS, that induces upregulation of GABA<sub>B</sub> receptors located at pre- and postsynaptic sites<sup>285</sup>.

The increased GABAergic inhibition by H<sub>2</sub>S may find its application in several situations where the excitation/inhibition balance in CNS is disturbed, such as seizures and epilepsy, stimuli leading to pain, and cerebral ischemia<sup>282; 286</sup>. In addition, H<sub>2</sub>S regulates synaptic activity inducing Ca<sup>2+</sup> wave from neurons<sup>287</sup> and increases norepinephrine and epinephrine levels in the hippocampus, striatum, and brain stem by inhibiting monoamine oxidase<sup>288</sup>.

### **H<sub>2</sub>S and Inflammation**

Another area attracting considerable attention is the role of H<sub>2</sub>S in inflammation. H<sub>2</sub>S has been reported to exert both pro-inflammatory and anti-inflammatory effects.

Among anti-inflammatory effects of H<sub>2</sub>S there are inhibition of proliferation of T lymphocytes<sup>289</sup>, induction of apoptosis in polymorphonuclear cells<sup>290</sup>, increases phagocytosis of bacteria by macrophages and promotes a shift of phenotype of macrophages to the “M2”, pro-resolution state<sup>291</sup>. Several studies in recent years showed that, in some inflammation model as carrageenan-induced paw edema and air pouch, injection of rats with NaHS inhibited leukocyte infiltration and their adherence to vascular endothelium and edema formation. The mechanism underlying anti-inflammatory role seems due to activation of

K<sub>ATP</sub> channels on endothelial cells and leukocytes because they are attenuated by pretreatment with glibenclamide<sup>270</sup>. H<sub>2</sub>S donors can also down-regulate inflammatory process by reducing the expression of a number of proinflammatory cytokines, e.g. tumour necrosis factor (TNF)- $\alpha$ , interleukin (IL)-1 $\beta$ , IL-8, IL-1 $\alpha$ , interferon (IFN)- $\gamma$  or proteins, such as heme oxygenase (HO) and increasing the anti-inflammatory cytokine IL-10. These effects are most likely due to suppression of NF $\kappa$ B activity by H<sub>2</sub>S<sup>234; 292-294</sup>. In model of neuroinflammation H<sub>2</sub>S also attenuates LPS-induced production and release of NO and TNF- $\alpha$ <sup>250</sup>. Moreover, H<sub>2</sub>S reduces the gastrointestinal mucosal damage caused by nonsteroidal anti-inflammatory drugs. There are a number of mechanisms of action underlay this beneficial effects. For example, H<sub>2</sub>S stimulates secretion of bicarbonate in the stomach and duodenum, inhibits gastric acid secretion and reduces gastric mucosal blood flow and prevents the adherence of leukocytes to the vascular endothelium in the early stages of gastric injury. Therefore, it has been synthesized a new class of NSAID derivatives that release H<sub>2</sub>S. These drugs results the same efficacy in terms of retaining anti-inflammatory activity with reduced GI toxicity<sup>295-297</sup>.

Experimental evidence has showed pro-inflammatory role for H<sub>2</sub>S in various animal models, as hindpaw edema<sup>298</sup>,

acute pancreatitis<sup>299</sup>, LPS-induced endotoxemia<sup>300</sup> and cecal ligation and puncture-induced sepsis<sup>301</sup>. Abnormal synthesis or activity of H<sub>2</sub>S may play a part in septic or endotoxic shock because its capacity to open K<sub>ATP</sub> channels. Intriguingly, plasma H<sub>2</sub>S concentrations were also markedly increased in patients with septic shock<sup>302</sup>. Therefore, inhibiting the activity of H<sub>2</sub>S generating enzymes would be beneficiary. Infact, in cecal ligation and puncture induced sepsis, PPG treatment attenuated inflammatory response by reducing neutrophil infiltration and reducing animal mortality, whereas NaHS treatment significantly aggravated septic inflammatory damages<sup>301; 303</sup>. H<sub>2</sub>S has also been reported to stimulate the generation of pro-inflammatory cytokines from human monocytes<sup>237</sup>. The mechanisms for these pro-inflammatory effects of H<sub>2</sub>S would be the releasing endogenous tachykinins such as substance P (SP), calcitonin gene-related peptide (CGRP), and neurokinin A, and activation of TRPV-1 that mediate neurogenic inflammation. A number of factors are involved in determining whether H<sub>2</sub>S is anti-inflammatory or pro-inflammatory. The first is the dose–response relationships. At low, physiological concentrations H<sub>2</sub>S is predominantly anti-inflammatory, whereas at high concentrations H<sub>2</sub>S promotes inflammation, Administration routes (intravenous infusion or bolus) may also cause opposite effects. Another

important factor is the releasing rate: the slow releasing of H<sub>2</sub>S inhibited inflammation whereas the fast release of H<sub>2</sub>S increased the synthesis of proinflammatory factors<sup>304</sup>. Finally, animal species (rats vs. mice and others), inflammation models (regional vs. systemic inflammation), and the organ origin of H<sub>2</sub>S (brain vs. pancreas, etc.) also influence the role of H<sub>2</sub>S in inflammation.

### **H<sub>2</sub>S and cell proliferation**

H<sub>2</sub>S is involved in modulating cell proliferation and apoptosis in a variety of cells<sup>195</sup>. H<sub>2</sub>S promotes a number of cellular signals that regulates metabolism, cardiac function and cell survival. Overexpression of CSE in human aortic SMCs or treatment with NaHS and other endogenously produced H<sub>2</sub>S inhibited cell growth and induced cell apoptosis. The antiproliferative and/or proapoptotic effect of H<sub>2</sub>S treatment may be related to activation of MAPK/ERK pathway and its downstream factor caspase-3<sup>195</sup>. H<sub>2</sub>S also induces stabilization of p53 coupled with the induction of downstream proteins such as p21, p53AIP1, induces translocation of proapoptotic protein Bax from cytoplasm to mitochondria and release of cytochrome c from the mitochondria without altering the antiapoptotic protein Bcl-2<sup>243; 305</sup>. In addition, H<sub>2</sub>S act as a cyclin dependent kinase (cdk) inhibitor in cell cycle progression in the rat smooth

muscle cells<sup>305</sup>, human lung fibroblast<sup>306-307</sup> and oral epithelial<sup>252</sup> cells by the up-regulation of key cell cycle proteins such as cyclin-E and CDC-6 (cell division cycle- 6) and by decrease cyclin D1 and p27 involved in cell growth. However, H<sub>2</sub>S inhibit cell proliferation at G1 phase only at the early time points (12 and 24 h) such cells might be eliminated by the process of apoptosis as indicated by a higher incidence of DNA content in the sub-G1 phase, whereas at later time point (48 h)<sup>306</sup> follows a partial recovery in cell survival. The anti-proliferative and/or pro-apoptotic effect of H<sub>2</sub>S may be of importance for the prevention of cell proliferation in disorders such as atherosclerosis, vascular graft occlusion, and neointimal hyperplasia leading to restenosis after angioplasty<sup>308</sup>. In neuroblastoma cell line (SH-SY5Y) NaHS, at concentrations lower than 300 μM, suppress rotenone-induced apoptosis by inhibition of p38- and c-Jun NH<sub>2</sub>-terminal kinase (JNK), phosphorylation of MAPK, normalization of Bcl-2/Bax levels, and reduction of cytochrome c release, caspase-9/3 activation and poly(ADP-ribose) polymerase cleavage<sup>309</sup>. The same anti-apoptotic effect of NaHS has also been observed on rat pheochromocytoma cells (PC12)<sup>310</sup>. The opposite effects of H<sub>2</sub>S on apoptosis are cell type-specific and also depends H<sub>2</sub>S concentration used.

## **H<sub>2</sub>S and cancer**

Given the complexity of DNA damage and repair, controversy exists on the role of H<sub>2</sub>S in cancer cell proliferation. In colon epithelial cancer cell line NaHS (50–200 μM) treatment killed the cancer cells stimulating the phosphorylation of ERK and p38 MAPK and butyrate also induces apoptosis stimulating CBS and CSE expression and H<sub>2</sub>S production<sup>311</sup>. In another colon cancer cell line, HCT 116 cells, indeed NaHS (20 μM) promoted their proliferation increasing AKT and ERK phosphorylation and reducing activity of cyclin dependent kinase inhibitor p21 (Waf1/Cip1)<sup>312</sup>. H<sub>2</sub>S-releasing NSAIDs have also showed to be effective and safe in chemoprevention in colon cancer and other types of cancers. The mechanism of action of these drugs may include inactivation of Nrf2 via sulhydration of Keap1, induction of glycolysis within cancer cells and induction of apoptosis of cancer cells associated with inhibition of COX-2 activity<sup>313</sup>. Recently, CBS has emerged as a potential therapeutic target in both colon cancer and ovarian cancer<sup>314-315</sup>. In contrast a latest study demonstrates that H<sub>2</sub>S increases nicotinamide phosphoribosyltransferase (Nampt) and ATP levels in cancer cells (HepG2, MDA-MB-231, MDA-MB-435S) inducing intensified glycolysis and rapid proliferation. In this way H<sub>2</sub>S-Nampt pathway protects

cells from drug induced damage and it may responsible for resistance to therapy<sup>316</sup>.

### **Other biological effects**

The opening of the  $K_{ATP}$  channel also underpins the relaxant effect of  $H_2S$  in colonic<sup>317</sup> and eye<sup>318</sup>, but not bronchial smooth muscle<sup>319</sup>. Because of the crucial role of  $K_{ATP}$  channels in the regulation of pancreatic insulin secretion, multiple studies have examined the effect of  $H_2S$  on  $\beta$ -cells, where  $H_2S$  opens the  $K_{ATP}$  channels and inhibites insulin secretion promoting hyperglycemia<sup>320</sup>.

$H_2S$  is produced also in the lung and airway tissues, via the actions of CSE and CBS express in SMCs, vascular SMCs, and vascular endothelial cells<sup>321-323</sup>, where it participates in the regulation of contractility of airway smooth muscles and lung circulaiton. It has been suggested that decreased CSE expression and  $H_2S$  levels in pulmonary tissues are related to the pathogenesis of asthma. Infact, in an animal model of asthma administration of NaHS reduces airway inflammation, the number of eosinophils and neutrophils in bronchoalveolar lavage fluid airway (BALF), the expression of inflammatory genes, and also increased peak expiratory flow (PEF) indicating alleviation of airway obstruction<sup>324</sup>.

## 2.5 *H<sub>2</sub>S* donors

With the myriad of purported biological actions of H<sub>2</sub>S there is growing interest in more precise delivery of this volatile gas to target tissues in the form of H<sub>2</sub>S “donating” compounds. Pharmacologically useful donors should be soluble in aqueous media, should not be toxic, should not metabolize quickly and should release H<sub>2</sub>S in vivo slowly over a period of time.

H<sub>2</sub>S donating compounds can be divided into three general classes:

- Sulphide salts;
- Natural compounds (mainly in foods);
- Synthetic compounds.

### **Sulfide salts**

Sodium hydrosulfide (NaHS), sodium sulfide (Na<sub>2</sub>S) and calcium sulphide (CaS) are fast delivering compounds. They form HS<sup>-</sup> and H<sub>2</sub>S immediately upon solvation in physiological buffers. These have the advantage of the ready availability of high pure H<sub>2</sub>S concentration, but because H<sub>2</sub>S is rapidly lost from solution by volatilization in laboratory conditions their effective residence time in tissues is relatively short. Therefore it's difficult to achieve the desired final concentration of H<sub>2</sub>S and maintain that at constant level over a relatively long period. H<sub>2</sub>S can be released from the

solution in a temperature- and concentration-dependent manner. At 37°C or below, the concentration of H<sub>2</sub>S of the bath solution was relatively stable. At concentration below 1 mM, within 30 min H<sub>2</sub>S amounts decreases of 15% in the solution<sup>325</sup>. Also *in vivo*, the bolus injection of the animals with NaHS/Na<sub>2</sub>S stock solution creates, immediately, a great surge of H<sub>2</sub>S level, but thereafter, a much lower and declining level of H<sub>2</sub>S is encountered and declining. These properties limits their therapeutic potential.

NaHS is the most used H<sub>2</sub>S donor for its convenient preparation. In solution (water or ethanol) NaHS dissociates into Na<sup>+</sup> and HS<sup>-</sup> that in presence of H<sup>+</sup> forms H<sub>2</sub>S. In physiological condition (pH 7.4 and temperature of 37°C) NaHS solution will yield about one-third of the undissociated H<sub>2</sub>S and the other two-third remains as HS<sup>-</sup><sup>326</sup>. Some effects of NaHS cannot be fully explained by H<sub>2</sub>S. Also the altered Na<sup>+</sup> concentration or ionic strength as well as the redox potential may be associated with NaSH effect, especially at high end of the concentrations used.

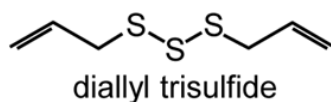
Na<sub>2</sub>S (or IK-1001) is a salt water soluble. In solution, it dissociates and generates H<sub>2</sub>S. Administration of Na<sub>2</sub>S increased blood sulfide and thiosulfate levels and that exhaled H<sub>2</sub>S could be detected<sup>327</sup>.

## **Natural compounds**

In our daily life, many dietary elements directly and indirectly supply H<sub>2</sub>S to our body so that the advantage of this gasotransmitter can be realized, in many cases, without conscious thought.

### Garlic: Polysulfides and S-allyl-L-Cysteine

Garlic (*Allium sativum*) has antioxidant, anti-inflammatory and anticarcinogenic functions. In particular, garlic consumption has been correlated with the reduction in multiple risk factors associated with cardiovascular diseases such as increased reactive oxygen species, high blood pressure, high cholesterol and platelet aggregation<sup>328</sup>. Garlic is also effective against bacterial, viral, fungal, and parasitic infections and stimulates the immune system<sup>329</sup>. The National Cancer Institute (NCI) set garlic on the top of a vegetable pyramid, representing potency in cancer prevention<sup>330</sup>. The benefic pharmacological effects of garlic derive from H<sub>2</sub>S production by the numerous organosulfur compounds present such as allicin, allyl sulfides, ajoene, polysulfides, as diallyl disulfide (DADS) and diallyl trisulfide (DATS); S-alk(en)yl-L-cysteine sulfoxides and S-allyl cysteine (SAC)<sup>331</sup>.



Organic polysulfides can interact with either exofacial membrane protein thiols or intracellular thiols, such as GSH, to form H<sub>2</sub>S. Benavides et al. demonstrate the capacity of garlic extract (DADS and DATS) to produce H<sub>2</sub>S measuring H<sub>2</sub>S production in real time with a polarographic sensor. In particular the release of H<sub>2</sub>S from DATS is 3 times that from DADS<sup>236</sup>. One of the nonenzymatic mechanisms have been proposed to explain the chemical conversion of garlic-derived organic polysulfides to H<sub>2</sub>S is the conversion of S-allyl-glutathione and allyl perthiol to allyl-GSSG and to H<sub>2</sub>S through a sequence of reactions. Another mechanism is the direct thiol/disulphide exchange during the interaction of polysulfides and GSH<sup>332-333</sup>. Additional evidences of the H<sub>2</sub>S production from garlic derive by *in vivo* studies. For example, infusion of diallyl disulfide 1.8 mg/kg/min in rats increases exhaled H<sub>2</sub>S<sup>334</sup>. Moreover, in an acute myocardial infarction (AMI) rat model, pretreatment of the animals with S-allylcysteine protected partially the heart from ischemia damage and saved the animals from mortality by about 11% and these effects were antagonized by PPG inhibition of CSE<sup>335</sup>. Direct administration of allicin (8 mg/kg) to rats also led to lowered systolic blood pressure and triglycerides.

Other examples of the therapeutic potential of garlic compounds are the reduction of  $\beta$ -amyloid fibril formation in Alzheimer's disease transgenic model<sup>337</sup>; inhibition of angiotensin converting enzyme<sup>338</sup>, prevention of vascular remodeling<sup>339</sup> and suppression of L-NAME-induced hypertension<sup>340</sup>.

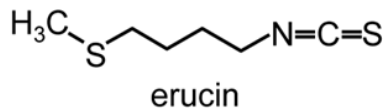
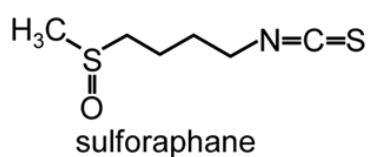
### Broccoli and Sulforaphane

Broccoli (*Brassica oleracea*) as well as other cruciferous vegetables tends to release strong smell of H<sub>2</sub>S when cooked or became rotten. Previous studies have reported the health beneficial effects of broccoli on the prevention and treatment of hypertension and atherosclerotic changes in the SHR stroke-prone rats<sup>341</sup>. These effects of broccoli are largely ascribed to the action of sulforaphane, an isothiocyanate compound that exhibits anticancer properties. It is rapidly absorbed by humans, reaching peak concentrations at 1 h and declining thereafter with a half-life of 1.8 hours<sup>342</sup>. Sulforaphane protects vascular smooth muscle cells and endothelial cells from oxidative and inflammatory stress and suppresses angiogenesis<sup>343-344</sup>. In addition, it has neuroprotective and anti-inflammatory actions mediated in part through activation of heme oxygenase-1 and it provides some protection against ischemia reperfusion injury, hemorrhage

and serotonin-induced toxicity<sup>345</sup>. Sulforaphane induces death of PC-3 cells (a human prostate cancer cell line) in a dose-dependent manner by the activation of p38 MAPK and JNK, and this effect is reversed scavenging of free H<sub>2</sub>S with methemoglobin or oxidized glutathione<sup>346</sup>.

Another proof of the release of H<sub>2</sub>S is that sulforaphane in human breast cancer MCF-7 cells induces upregulation of thioredoxin reductase 1 (EC 1.8.1.9) that reduces thioredoxin that is fundamental for H<sub>2</sub>S synthesis from 3-MST.

A related isothiocyanate compound, erucin, is found in high levels in rocket salad species (*Eruca sativa*).



#### Other H<sub>2</sub>S-food

Durian (*Durio zibethinus* Murray) is a notably flavorful or pungent fruit, of the Southeast Asia. Durian is rich in sulfur compounds, mostly dialkyl polysulfides<sup>347</sup> that are responsible for its health benefits<sup>348</sup>. Thousand-Year Egg is a Chinese delicacy made from duck, quail, or chicken eggs preserved in a mixture of clay, ash, lime, salt, and rice straw that is a source of H<sub>2</sub>S<sup>349</sup>.

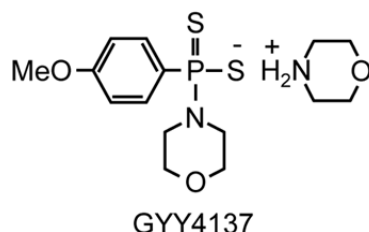
Red meat, cheese, milk, fish, soybeans, preserved bean curd (stinky tofu), breads, beers, sausages and dried fruit are all high-protein foods rich in sulfur amino acids generating H<sub>2</sub>S in the colon following fermentation by colonic bacteria or by sulfate-reducing bacteria<sup>350</sup>.

### Synthetic compounds

In the last years have been developed several H<sub>2</sub>S slow-releasing compounds to allow a long-term sustained therapeutic supply of H<sub>2</sub>S.

#### GY4137

GY4137 (morpholin-4-ium 4 methoxyphenyl (morpholino) phosphinodithioate) is a water-soluble molecule that releases H<sub>2</sub>S slowly and steadily, either in aqueous solution or administered to the animal (intraperitoneal or intravenous).



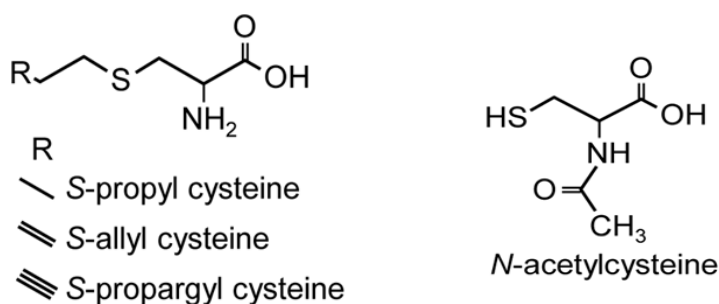
One mmol/l of GY4137 releases ~40 μmoles of H<sub>2</sub>S in the first 10 min and then releases approximately 40 μmoles of H<sub>2</sub>S for hour for the ensuing 80 min when

dissolved in acidic (pH 3.0) phosphate buffer whereas in buffer at pH 7.4 or 8.5 releases minus of 3  $\mu\text{moles}$  of  $\text{H}_2\text{S}$  in the same period. Injection of 133  $\mu\text{mol/kg}$  either intraperitoneally (ip) or intravenously (iv) into rats, increases plasma  $\text{H}_2\text{S}$  levels from  $\sim 32 \mu\text{mol/l}$  to  $\sim 80 \mu\text{mol/l}$  in 30 min and this remains elevated ( $50 \mu\text{mol/l}$ ) for 3 hours.  $\text{H}_2\text{S}$  concentrations quickly increases in the liver and heart for the enduring 20 min, which is even longer in the kidney. The slow-releasing property of GYY4137 results in slow vasorelaxation without affecting heart rate or myocardial contraction of rats. This effect is in part mediated by  $\text{K}_{\text{ATP}}$  channels. Furthermore, GYY4137 exhibits antihypertensive activity in a NG-nitro-L-arginine methyl ester (L-NAME)-evoked rat hypertension model<sup>235</sup>. GYY4137, administered 1 or 2 hours after LPS stimulation, significantly decreases secretion of many of the markers of LPS-induced inflammation in cultured RAW 264.7 cells including nitrate/nitrite, PGE<sub>2</sub>, TNF- $\alpha$ , IL-1 $\beta$ , IL-6, NF- $\kappa$ B, expression of inducible nitric oxide synthase (iNOS), myeloperoxidase activity and COX-2<sup>351</sup>. Anti-cancer effects of GYY4137 have been observed in vitro and in vivo. Five-day treatment with GYY4137 ( $400 \mu\text{mol/l}$ ) significantly reduced proliferation of breast adenocarcinoma (MCF-7), acute promyelocytic leukemia (MV4-11) and myelomonocytic leukemia (HL-60) cells; and at  $800 \mu\text{mol/l}$  GYY4137 kills also human cervical

carcinoma (HeLa), colorectal carcinoma (HCT-116), hepatocellular carcinoma (Hep-G2), osteosarcoma (U2OS), without affect survival of non-cancer human diploid lung fibroblasts (IMR90 and WI-38). This antiproliferative effect of GYY4137 is due to induction of apoptosis and cell-cycle arrest in the G2/M. Daily i.p. injection of GYY4137 also decreased the growth of HL-60 and MV4-11 tumors subcutaneously transplanted in immunodeficient mice<sup>352-353</sup>.

### Cysteine analogs

The cysteine analogs act as potential substrates for endogenous cysteine-metabolizing enzymes increasing H<sub>2</sub>S production at least two-fold. They are: S-propyl cysteine (SPC), S-allyl cysteine (SAC, also a derivative of garlic), S-propargyl cysteine (SPRC) and N-acetyl cysteine (NAC)<sup>354</sup>.



SAC (50 mg/kg/day for 7days) has been shown to low mortality and to reduce infarct size in an acute myocardial infarction rat model. Inhibition of CSE with PPG eliminated

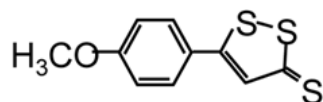
the beneficial effects of SAC, increased infarct size, and significantly elevated blood pressure<sup>355</sup>. Moreover, daily i.p. injection of cysteine analogs significantly protected the hearts from ischemia reperfusion injury and was associated with preserved superoxide dismutase (SOD), glutathione peroxidase activity, and tissue GSH levels, while reducing lipid peroxidation products<sup>354</sup>. SPRC attenuated LPS-induced deficits in spatial learning and memory in rats and restored the LPS deficit in hippocampal H<sub>2</sub>S levels<sup>356</sup>. SPRC and SAC have also anti-cancer activity. SPRC (1 μM-30 mM) inhibited growth of cultured human gastric cancer cells (SGC-7901) in a dose dependent manner, stimulating apoptosis and inducing cell cycle arrest at the G1/S phase. In male nude mice with SGC-7901 tumors implanted in the flank, SPRC and SAC (50 and 100 mg/kg) increased plasma H<sub>2</sub>S concentration, reduced tumor volume, increased apoptotic tumor cell number and increased protein expression of Bax and p53 while decreased Bcl-2<sup>357</sup>. SPRC reduced LPS-induced inflammatory response of rat by inhibiting NF-κB activation and ERK1/2 phosphorylation and reducing intracellular ROS production<sup>358</sup>. SPRC effects were more pronounced than SAC but both act not only as a substrate for H<sub>2</sub>S by CSE but they also up-regulate the enzyme. SPRC and SAC have been conjugated with leonurine, an alkaloid in Chinese motherwort, which make them more effective to induce H<sub>2</sub>S

production. Leonurine-SPRC has a cardioprotective effect in hypoxic neonatal rat ventricular myocytes by increasing cell viability, decreasing LDH leakage, decreasing MDA and ROS<sup>359</sup>.

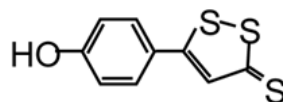
### **H<sub>2</sub>S-releasing hybrid compounds**

These molecules are created by combining a H<sub>2</sub>S-releasing moiety with another parent compound with known molecular structure and biological functions. The purpose to create such a new compound is to enhance the functionality and safety of both composing compounds and reduce potential side effects of each part.

Anethole dithiolethione (ADT) and its main metabolite (ADTOH; 5-(4-hydroxyphenyl)-3H-1,2-dithiole-3-thione) have been used extensively as a donor of H<sub>2</sub>S and its ease of esterification with other therapeutics has led to a considerable variety of H<sub>2</sub>S “donating” drugs.



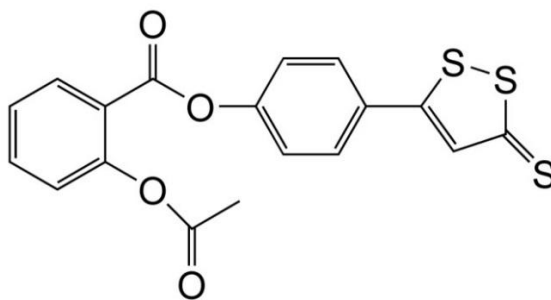
ADT



ADT-OH  
ACS 1

### ACS14 (S-ASPIRIN)

It is a hybrid between ADTOH and aspirin that conserves the cardioprotective efficacy with reduced gastric damage. Infact, ACS14 inhibited thromboxane synthesis, similar to aspirin, but caused much weaker gastric reactions than aspirin did<sup>360</sup>. This could be due to the antioxidant effect of H<sub>2</sub>S, released from the hybrid. Another related compound with S-aspirin is ACS21, S-salicylic acid. Both ACS14 and ACS21, limited the development of metabolic syndrome in rats induced by GSH depletion (including hypertension, endothelial dysfunction, and insulin resistance), and protected the heart from I/R damage limiting gastric lesion<sup>361-362</sup>.

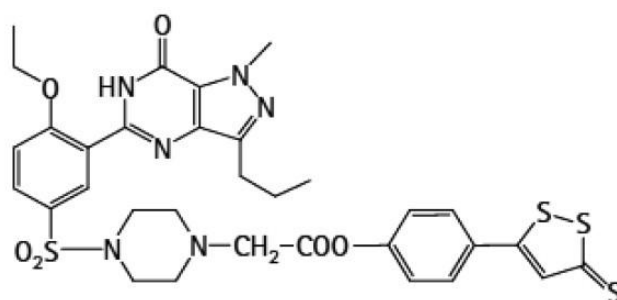


### ACS6 (S-SILDENAFIL)

It is a hybrid between ADTOH and sildenafil. ACS6 like sildenafil is an effective and selective inhibitor of type 5 phosphodiesterase (PDE5) and relaxe cavernosal smooth muscle, but it is more potent in inhibiting the formation of superoxide and expression of p47(phox) and PDE5 than

sildenafil<sup>363</sup>. Normally increased oxidative stress level and NOX expression compromise the efficiency of sildenafil in treating erectile dysfunction.

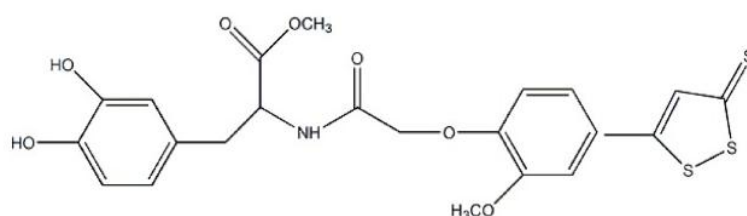
This hybrid will take the advantage of sildenafil-maintained cGMP activity and H<sub>2</sub>S-activated K<sub>ATP</sub> channels and suppressed oxidative stress in penile tissues, leading to an enhanced potency in relaxing penile cavernosal muscles. This hybrid may also find its application in the treatment of abnormalities in male reproductive system and urinary system.



#### ACS84 (S-DOPAS)

It is a hybrid between H<sub>2</sub>S-donating dithiolthione (ACS1) or allyldisulfide and L-DOPA methyl ester. L-DOPA (Levodopa) is extensively used for treatment of Parkinson's disease but it has the adverse effect to induce apoptosis of substantia nigra dopaminergic neurons. The presence of H<sub>2</sub>S moiety allows to protect neurons from apoptosis via its anti-oxidant and anti-inflammatory effects. Moreover, ACS84 reached the brain is metabolized as early as 1 h after

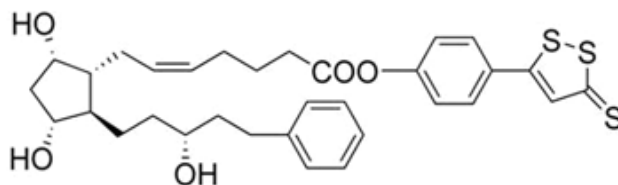
administration to rats intravenously, causing more than 2-fold increase in brain dopamine and 1.4-fold increase in GSH than L-DOPA did<sup>364</sup>. In fact, ACS84 has a better permeability to blood brain barrier than L-DOPA. With cultured human microglia, astrocytes, SH-SY5Y neuroblastoma cells, and human THP-1 U373 cell lines, ACS84 increased intracellular H<sub>2</sub>S levels.



#### ACS67 (S-LATANOPROST)

It is a hybrid between H<sub>2</sub>S-donating dithiolthione (ACS1) and latanoprost. Latanoprost is a synthetic derivative of the natural prostaglandin F<sub>2</sub> and it is used in the treatment of glaucoma because it reduces intraocular pressure (IOP) but latanoprost does not protect retina from ischemia damage and its tolerance by patients is low. ACS67, instead, attenuated the death of cultured retinal ganglion cells by increasing GSH levels and decreasing H<sub>2</sub>O<sub>2</sub> toxicity<sup>365</sup>. In glaucomatous (carbomer model) pigmented rabbits intravitreal injection of ACS67 achieved a greater

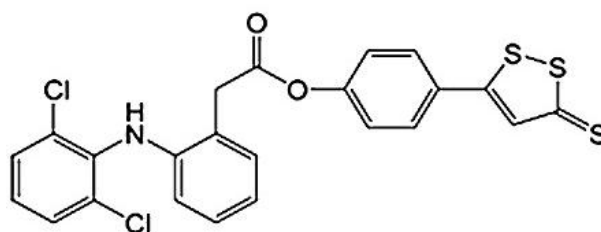
anti-IOP effect than latanoprost preventing, also, ischemia damage thanks to the neuronal protective effect of H<sub>2</sub>S<sup>366</sup>.



### H<sub>2</sub>S-NSAIDs

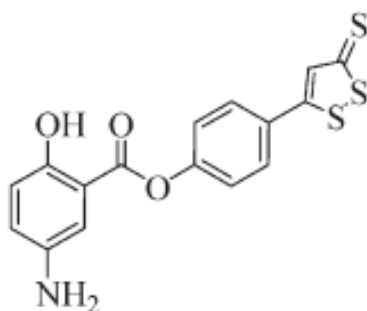
Another line of research that is producing new molecules and exploiting the H<sub>2</sub>S concept is aimed at reducing the toxicity of nonsteroidal anti-inflammatory drugs (NSAIDs). H<sub>2</sub>S donors were shown to reduce the severity of NSAID-induced damage in the rat stomach. Moreover, NSAIDs decreased endogenous H<sub>2</sub>S synthesis<sup>367-368</sup>. ACS15 (S-DICLOFENAC or ATB337) it is a hybrid between ADTOH and diclofenac. Diclofenac is one of the NSAIDs that inhibiting inflammation and eliciting analgesia but also may cause GI toxicity among other side effects. This undesired side effect of NSAIDs has been shown to be minimized by H<sub>2</sub>S donors in the rat stomach<sup>367</sup>. Therefore ACS15 is more potent than diclofenac for anti-inflammatory activity and reduces the common side effects of diclofenac, such as neutrophil infiltration, leukocyte adherence, and GI

lesion<sup>234; 369</sup>, as well as pancreatitis-related lung injury<sup>370</sup> and has no effect on haematocrit.



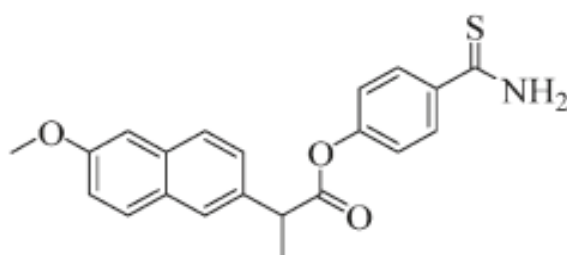
With the same principle and expectations, other H<sub>2</sub>S-NSAIDs have been made:

ATB-429 is a derivative of mesalamine a drug commonly used in the treatment of inflammatory bowel disease (IBD). ATB-429 has been shown to be significantly more effective than mesalamine in animal models of Crohn's disease (CD) and ulcerative colitis (UC). Moreover, there is also considerable preclinical evidence that it is significantly more effective in treating the visceral pain associated with IBD<sup>371-372</sup>.



ATB-346 is a derivative of naproxen, widely used in the control of pain in osteoarthritis. However, like other NSAIDs,

naproxen carries a significant risk of serious gastrointestinal bleeding and cardiovascular effects (e.g., heart attacks, elevated blood pressure). In preclinical studies, ATB-346 exhibited increased effectiveness over its parent drug and a remarkable reduction in the gastrointestinal and cardiovascular toxicity<sup>373</sup>. In addition, ATB-346 has been shown to have chemopreventive effect in colon cancer<sup>374</sup>.



Others are ATB-343 (derivative of indomethacin) and ATB-345. All these H<sub>2</sub>S -NSAIDs, they are metabolized by carboxylesterases in the body to slowly generate H<sub>2</sub>S.

# AIM

---

Melanoma is the deadliest form of skin cancer and it is rising in incidence. Although in the past 3 years have been made notable advances in the understanding the molecular pathogenesis of melanoma and its treatment, melanoma therapy is still a challenge. Therefore, it is critical to identify other important potential targets in melanoma development and progression that are amenable to pharmacological inhibition.

In the last few years, numerous physiological and pathophysiological effects have been proposed for the gasotransmitter hydrogen sulphide, even its role in cancer molecular mechanisms is still unclear. Recently, it has been shown that CSE enzyme is expressed in melanoma cell lines<sup>375</sup> and that CBS enzyme plays a key role in colon and ovarian cancer<sup>314-315</sup>.

Starting from these evidence, the aim of my PhD project was to investigate the role of the metabolic H<sub>2</sub>S pathway in human melanoma.

To address this issue we:

- (i) evaluated the role of H<sub>2</sub>S on human melanoma cell proliferation and explained its possible mechanism of action;

- (ii) evaluated the role of the endogenous pathway of H<sub>2</sub>S in melanoma development and progression;
- (iii) defined the clinical relevance of the H<sub>2</sub>S donors in order to propose them as new therapeutic agents.

# METHODS

---

## ***3.1 Cell culture and reagents***

NHEM was purchased from Lonza (Walkersville, MD, USA) and grown in melanocyte growth medium 2 (Lonza). The melanoma cell lines B16/F10, Sk-Mel-5 and Sk-Mel-28 were purchased from IRCCS AOU San Martino – IST (Genoa, Italy), A375 from Sigma–Aldrich (Milan, Italy). The cell lines were cultured in Dulbecco’s modified Eagle’s medium (DMEM) containing 10% fetal bovine serum, 2 mmol/l L-glutamine, 100 µmol/l nonessential amino acids, penicillin (100 U/ml), streptomycin (100 µg/ml) and 1 mmol/l sodium pyruvate (all from Sigma–Aldrich). Cells were grown at 37°C in a humidified incubator under 5% CO<sub>2</sub>. The cell line PES 43 was isolated from a lung metastases of a patient from the National Cancer Institute, G. Pascale Foundation (Scala et al., 2006), and cultured in Iscove’s modified Dulbecco’s medium (Cambrex Bioscience, Verviers, Belgium) supplemented with heat-inactivated 10% fetal bovine serum, penicillin and streptomycin (100 units/ml each).

DATS (LKT Laboratories) was diluted in DMSO to produce a stock solution of 10 mM for in vitro experiments; GYY4137 (Cayman Chemical, Ann Arbor, MI, USA) was solubilized in PBS; PAG, CHH, 3-MP and NaHS (Sigma–Aldrich) were solubilized in H<sub>2</sub>O; thioglycine and L-

thiovaline, a kind gift of Prof. Andreas Papapetropoulos, were solubilized in PBS. Vemurafenib (PLX4032) (Selleckchem) was solubilized in DMSO.

### ***3.2 Proliferation assays***

Cell proliferation was measured by the 3-[4,5-dimethylthiazol-2-yl]-2,5-diphenyl tetrazolium bromide (MTT) assay or by the 5-bromo-2'-deoxy-uridine assay following the manufacturer's instructions (Roche, Milan, Italy). Briefly, for the MTT assay the human melanoma cells (A375, Sk-Mel-5, Sk-Mel-28 and PES 43) and the NHEM cells were seeded onto 96-well plates ( $2 \times 10^3$  cells/well) a day earlier and successively treated with vehicle or various concentrations of different H<sub>2</sub>S-releasing compounds for 24, 48 and 72 h before adding 25  $\mu$ l MTT (Sigma-Aldrich; 5 mg/ml in saline). Cells were then incubated for an additional 3 h at 37°C. After this time interval, cells were lysed and dark blue crystals were solubilized with a solution containing 50% N,N-dimethyl formamide and 20% sodium dodecylsulfate with an adjusted pH of 4.5. The optical density of each well was measured with a microplate spectrophotometer (TitertekMultiskan MCC/340), equipped with a 620-nm filter. None of the compounds tested under the same experimental conditions had a cytotoxic effect on NHEM.

### ***3.3 Preparation of cellular extracts***

A375 cells ( $1 \times 10^6$ ) were seeded in 6-well plates and were treated with DATS 100  $\mu\text{M}$  for 1, 3 and 6 h or with GYY4137 1 mM for 3, 6 and 24 h. To obtain cytosolic or nuclear extracts the cell pellet was resuspended in 100  $\mu\text{L}$  of ice-cold hypotonic lysis buffer (10 mmol/L Hepes, 10 mmol/L KCl, 0.5 mmol/L phenylmethylsulfonyl fluoride, 1.5  $\mu\text{g}/\text{mL}$  soybean trypsin inhibitor, 7  $\mu\text{g}/\text{mL}$  pepstatin A, 5  $\mu\text{g}/\text{mL}$  leupeptin, 0.1 mmol/L benzamidine, 0.5 mmol/L dithiothreitol) and incubated on ice for 15 minutes. The cells were lysed by rapid passage through a syringe needle 5 times and centrifuged for 10 minutes at 13 000g. The supernatant containing the cytosolic fraction was removed and stored at  $-80^\circ\text{C}$ . The nuclear pellet was resuspended in 30  $\mu\text{L}$  of high-salt extraction buffer (20 mmol/L Hepes pH 7.9, 10 mmol/L NaCl, 0.2 mmol/L EDTA, 25% v/v glycerol, 0.5 mmol/L phenylmethylsulfonyl fluoride, 1.5  $\mu\text{g}/\text{mL}$  soybean trypsin inhibitor, 7  $\mu\text{g}/\text{mL}$  pepstatin A, 5  $\mu\text{g}/\text{mL}$  leupeptin, 0.1 mmol/L benzamidine, 0.5 mmol/L dithiothreitol) and incubated at  $4^\circ\text{C}$  for 30 minutes with constant agitation. The nuclear extract was then centrifuged for 10 minutes at 6000g, and the supernatant was aliquoted and stored at  $-80^\circ\text{C}$ .

Whole-cell extracts of A375 cells were prepared after lysis in extraction buffer (50 mM Tris [tris(hydroxymethyl)aminomethane]/HCl, pH 7.4, 150 mM NaCl, 0.1% Triton X-100, 5 mM EDTA [ethylenediaminetetraacetic acid], 1 mM Na<sub>3</sub>VO<sub>4</sub>, 1 mM phenylmethylsulfonyl fluoride, and complete protease inhibitor cocktail tablets, Roche). The protein concentration was measured by the Bradford method (Bio-Rad, Milan, Italy).

### ***3.4 Western blot analysis***

Equal amounts of protein (40 µg/sample) from whole or nuclear cell extracts were separated by sodium dodecylsulfate polyacrylamide gel electrophoresis (SDSPAGE) and blotted onto a nitrocellulose membranes (Trans-Blot Turbo Transfer Starter System, Bio-Rad). The membranes were blocked for 2 h in 5% low-fat milk in PBS with 0.1% Tween 20 (PBST) at room temperature. Then the filters were incubated with the following primary antibodies: IκBα (sc-1643 Santa Cruz Biotechnology, Santa Cruz, CA, USA; diluted 1:200); Bcl-2 (2876, Cell Signaling, Beverly, MA, USA; diluted 1:1000); caspase 3 (9662, Cell Signaling; diluted 1:1000); PARP (9542, Cell Signaling; diluted

1:1000); p44/42 MAPK (Erk1/2) (9102, Cell Signaling; diluted 1:1000); phospho-p44/42 Erk MAPK (Erk1/2, Thr202/Tyr204) XP (4370, Cell Signaling; diluted 1:2000); AKT (9272, Cell Signaling; diluted 1:1000); phospho-AKT (Ser473) XP (4060, Cell Signaling; diluted 1:2000); c-FLIP (06-864, Millipore; diluted 1 µg/ml); XIAP (R&D Systems, Minneapolis, MN, USA; 1 lg/ml); NF-κB p65 (F-6) (sc-8008 Santa Cruz Biotechnology; diluted 1:200); b-actin (Santa Cruz Biotechnology; diluted 1:1000) overnight at 4°C. The membranes were washed three times with PBST and then incubated with horseradish peroxidase-conjugated antibodies (Santa Cruz Biotechnology; diluted 1:2000) for 2 h at room temperature. The immune complexes were visualized by the ECL chemiluminescence method and acquired by the Image Quant 400 system (GE Healthcare).

### ***3.5 Flow cytometry***

Apoptosis was detected with an annexin V-FITC (BD Pharmingen, San Diego, CA, USA) according to manufacturer's instructions. A375 cells were seeded in 35-mm culture dishes and allowed to attach overnight. The cells were treated with DATS (100 µM) for 3, 6, 24 and 48 h, collected, and washed twice with PBS. Samples were then taken to determine baseline and drug-induced apoptosis by Annexin V-FITC/propidium iodide (PI) (Beckman Coulter,

Brea, CA, USA) double staining or PI staining and flow cytometry analysis using a FACSCanto II 6-color flow cytometer (Becton Biosciences, San Jose, CA, USA). To detect early and late apoptosis, both adherent and floating cells were harvested together and resuspended in annexin V binding buffer (10 mM HEPES/NaOH pH 7.4, 140 mM NaCl, 2.5 mM CaCl<sub>2</sub>) at a concentration of 10<sup>6</sup> cells/ml. Subsequently, 5 µl of FITC-conjugated Annexin V and 5 µl of PI were added to 100 µl of the cell suspension (10<sup>5</sup> cells). The cells were incubated for 15 min at room temperature in the dark. Finally, 400 µl of annexin V-binding buffer was added to each tube. A minimum of 50 000 events for each sample were collected and data were analyzed using FACSDIVA software (Becton Biosciences).

### ***3.6 Cell cycle***

Cells were plated in six-well plates at a density of 5x10<sup>5</sup> cells/well. Cells were then treated with DATS 100 µM for 3, 6 and 24 h. Cells were collected, washed twice with ice-cold PBS buffer (pH 7.2–7.4), fixed with 70% alcohol overnight and stained with PI (1 mg/ml) in the presence RNase A (1 mg/ml) for at least 30 min prior to analysis by flow cytometry. The flow-cytometric analysis was performed using a FACSCanto II and the cycle analysis was performed with the MODFIT LT software (Verity Software House).

### ***3.7 Electrophoretic mobility shift assay (EMSA)***

Aliquots of total extracts (12 µg protein/sample) in 0.1% Triton X-100 lysis buffer were incubated with <sup>32</sup>P-labeled κB DNA probes in binding buffer for 30 min. DNA-protein complexes were analyzed using non-denaturing 4% polyacrylamide gel electrophoresis. Quantitative evaluation of NF-κB-κB complex formation was done using a Typhoon-8600 imager (Molecular Dynamics Phosphor-Imager, MDP, Amersham Biosciences, Piscataway, NJ, USA) and IMAGEQUANT software (Amersham Biosciences) (MDP analysis). For control of equal loading, NF-κB values were normalized to the level of the nonspecific protein-DNA complex in the same lane.

### ***3.8 RNA purification and qPCR***

Total RNA was isolated from cells using the TRI-Reagent (Sigma-Aldrich, Milan, Italy) according to the manufacturer's instructions, followed by spectrophotometric quantization. Final preparation of RNA was considered DNA- and protein-free if the ratio between readings at 260/280 nm was  $\geq 1.7$ . Isolated mRNA was reversetranscribed by iScript Reverse Transcription Supermix for RT-qPCR (Bio-Rad, Milan, Italy). qPCR was carried out in CFX384 real-time PCR detection system (Bio-

Rad) with specific primers using SYBR Green master mix kit (Bio-Rad). Samples were amplified simultaneously in triplicate in a one-assay run with a non-template control blank for each primer pair to control for contamination or primer-dimers formation, and the ct value for each experimental group was determined. The housekeeping gene (ribosomal protein S16) was used as an internal control to normalize the ct values, using the  $2^{-\Delta Ct}$  formula.

### ***3.9 Transfection***

A375 cells were seeded onto 96-well plates ( $2 \times 10^3$  cell/well) and transfected the next day with the human CSE/pIRES-EGFP, the human CBS cDNA/pCMV-SPORT6 or the human 3-MST/pCI-HA using Lipofectamine 2000 (Life Technologies, Milan, Italy). Forty-eight hours after transfection, cell proliferation was evaluated by MTT assay (see Proliferation assays). Western blot analysis of CSE, CBS and 3-MST expression was carried out on whole cell extracts to confirm effective gene overexpression (anti-CSE, clone 2E12-1C10, mouse, 1:500, Novus Biologicals, Ltd; anti-CBS, clone H-300, rabbit, 1:500, Santa Cruz Biotechnology); anti-3-MST (clone NBP1-54734, rabbit 1:500, Novus Biologicals). For the silencing experiments, A375 cells were seeded onto 96-well plates ( $2 \times 10^3$  cell/well) and transfected the next day, according to the manufacturer's instructions, with CSE

Silencer® Select Pre-designed siRNA (Ambion, Carlsbad, CA, USA) (sense strand 5'-CUAUGUAUUCUGCAACAAtt-3', antisense strand, 5'-UUUGUUGCAGAAUACAUAAGaa-3'); human 3-MST siRNA SMART pool siGENOME (ThermoFisher Scientific, Hudson, NH, USA) (GGAGAAGAGCCCUGAGGAG, CCGCCUUCAUCAAGACCUA, CCACCCACGUCGUGAUCUA, AGAAAGUGGACCUGUCUAA); human CBS siRNA SMART pool siGENOME (GGAAGAAGUUCGGCCUGAA, GGACGGUGGUGGACAAGUG, CACCACCGCUGAUGAGAUC, AGACGGAGCAGACAACCUA). Forty-eight hours after transfection, cell proliferation was evaluated by MTT assay (see Proliferation assays).

### ***3.10 Generation of Vemurafenib-resistant human melanoma cells***

To generate Vemurafenib-resistant human melanoma subline, exponentially growing cell A375 were treated with increasing concentrations of vemurafenib<sup>145</sup>. After attaining confluence, the cells were repassaged and retreated with vemurafenib. Every three passages, the vemurafenib sensitivity was redetermined (see Proliferation assays), and the process was repeated with higher dose of vemurafenib until to obtain vemurafenib-resistant clone cells. Cells with the ability to grow in 1µM of vemurafenib were obtained ~6 months after the initial drug exposure. Resistant lines were

maintained in culture medium in presence of 1 $\mu$ M vemurafenib, supplemented every 72h. Then, A375 vemurafenib-resistant (A375rVem) cell were treated with DATS at different concentrations (10 $\mu$ M - 30 $\mu$ M - 100  $\mu$ M) for 24, 48 and 72 h and cell proliferation was evaluated by MTT assay (see Proliferation assays).

### ***3.11 Animals***

Animal care was in accordance with Italian and European regulations on the protection of animals used for experimental and other scientific purposes. Mice were observed daily and humanely euthanized by CO<sub>2</sub> inhalation if a solitary subcutaneous tumor exceeded 1.5 cm in diameter or mice showed signs referable to metastatic cancer. All efforts were made to minimize suffering. Female C57BL/6 mice (18-20 g) were from Charles River Laboratories, Inc. Mice were housed at the Animal Research Facility of the Department of Pharmacy of the University of Naples Federico II.

### ***3.12 Induction of subcutaneous B16 lesions***

Mice were subcutaneously (s.c.) injected in the right flank with B16-F10 cells (1x10<sup>5</sup>/0.1 ml). When tumors reached an average diameter of 2-4 mm, L-cysteine (300 or 600 mg/kg), DATS (50 mg/kg) or a combination of L-

cysteine (600 mg/kg), + PAG (10 mg/kg) or L-cysteine (600 mg/kg) + CHH (10 mg/kg) was given orally. Control mice received only vehicle. Tumor size was measured using a digital caliper, and tumor volume was calculated using the following equation: tumor volume =  $\Pi/6(D1 \times D2 \times D3)$  where D1 = length; D2 = width; D3 = height and expressed as cm<sup>3</sup>.

### ***3.13 Induction of metastatic melanoma***

Mice were intravenously (i.v.) injected with  $5 \times 10^5$  B16-F10 melanoma cells, in the caudal vein. Starting on the 1st day after tumor cell inoculation, DATS (50 mg/kg) or L-cysteine (600 mg/kg), was given orally every day for 14 days. Control mice received only vehicle. After 14 days the lungs were removed and was calculated the percentage of metastatic area using ImageJ software.

### ***3.14 Patients and specimens***

In all, 102 patients of the National Cancer Institute 'Giovanni Pascale' of Naples have been included in this study from 2004 to 2012. All patients were caucasians, and all gave their written informed consent according to the institutional regulations. This study was approved by the ethics committee of the National Cancer Institute 'G. Pascale'.

### ***3.15 Immunohistochemistry analysis***

Tissue samples were retrieved from the paraffin blocks of the National Cancer Institute of Naples archives. Hematoxylin & eosin staining of a 4- $\mu$ m section was used to verify all samples. Immunohistochemical analysis was performed on 4- $\mu$ m sections from formalin-fixed, paraffin-embedded tissues in order to evaluate the expression of CSE and CBS. Negative control slides without primary antibody were included for each staining. Paraffin slides were deparaffinized in xylene and rehydrated through graded alcohols. Antigen retrieval was performed with slides heated in 0.01 M citrate buffer (pH 6.0) for CSE antibody and 1 mM EDTA buffer, pH 8.0 for CBS and 3-MST antibodies, in a bath for 20 min at 97°C. After antigen retrieval, the slides were allowed to cool. The slides were rinsed with TBS and the endogenous peroxidase inactivated with 3% hydrogen peroxide. After protein block (BSA 5% in PBS 1X ), every slide was incubated with specific primary antibody: anti-CSE (clone 2E12-1C10, mouse, 1:1200, Novus Biologicals, Ltd, Cambridge, UK; anti CBS (clone H-300, rabbit, 1:500, Santa Cruz Biotechnology) anti 3-MST (clone NBP1-54734, rabbit 1:500, Novus Biologicals). The sections were rinsed in TBS and incubated for 20 min with Novocastra biotinylated secondary antibody (RE7103), a biotin-conjugated

secondary antibody formulation that recognizes mouse and rabbit immunoglobulins. Then the sections were rinsed in TBS and incubated for 20 min with Novocastra streptavidin-HRP (RE7104). Finally, peroxidase reactivity was visualized using 3,3'-diaminobenzidine (DAB) and the sections counterstained with hematoxylin and mounted. Results were interpreted using a light microscope. CSE, CBS and 3-MST expression was evaluated in stained tissue sections by two pathologists (G.B, A.A.) in a blinded manner. In each sample the number of positive cells was evaluated in 10 non-overlapping fields using 9400 magnification. Data are expressed as the percentage of positive cancer cells over the total number of cancer cells. The obtained median value was used as cut off for that specific marker (CSE, CBS, 3-MST). Therefore in order to be defined as negative, a sample has to be equal or below the median value.

### ***3.16 Statistical analysis***

Data from all in vivo experiments are reported as mean±SEM unless otherwise noted. Data were analyzed and presented using GRAPHPAD PRISM software (GraphPad). Significance was determined using Student's 2-tailed t-test. Results were considered significant at P values less than 0.05 and are labeled with a single asterisk. In addition, P

values less than 0.01 and 0.001 are designated with double and triple asterisks, respectively.

## **RESULTS**

---

#### ***4.1 Hydrogen sulfide donors inhibit human melanoma cell proliferation***

To explain the role of H<sub>2</sub>S in human melanoma, we assessed the effect of several H<sub>2</sub>S-donors on A375 melanoma cell proliferation. All the compounds, but sodium hydrosulfide monohydrate (NaHS), inhibited the growth of A375 cells in a concentration-dependent manner (Table 4). Among all the H<sub>2</sub>S donors tested, the most potent in inhibiting melanoma cell proliferation was DATS, with an IC<sub>50</sub> of 89 μM.

Similar results were obtained with all the other cell lines: Sk-Mel-5, Sk-Mel-28 and PES 43 whereas didn't affect NHEM proliferation (Table 5). To better confirm that the anti-proliferative effect elicited by the H<sub>2</sub>S-donors was not due to an artefact consequent to the hydrogen sulfide-induced reduction of mitochondrial respiration (MTT assay) we performed another proliferation assay, the 5-bromo-20-deoxy-uridine assay. Results obtained with this assay show a greater anti-proliferative effect of DATS (100 μM; -73% P < 0.001) and of GYY4137 (1 mM; -39%, P < 0.001; Figure 11). On the basis of the results obtained with both assays, DATS was selected for all subsequent experiments.

To further prove that the anti-proliferative effect of DATS was due to release of H<sub>2</sub>S we had used haemoglobin, an H<sub>2</sub>S

scavenger with whom it forms an inactive complex. Results obtained by MTT assay demonstrate a significantly reversion of anti-proliferative effect of DATS in the presence of haemoglobin (10  $\mu$ M) (Figure 12).

$\mu$ M	CTL	NaHS	DATS	GY4137	TIOGLYCINE	TIOVALIN
0	0.341 $\pm$ 0.02	-	-	-	-	-
3	-	0.350 $\pm$ 0.01	0.330 $\pm$ 0.01	-	-	-
10	-	0.357 $\pm$ 0.01	0.257 $\pm$ 0.01**	-	-	-
30	-	0.340 $\pm$ 0.005	0.240 $\pm$ 0.009***	-	-	-
100	-	0.365 $\pm$ 0.01	0.165 $\pm$ 0.02***	0.342 $\pm$ 0.002	0.343 $\pm$ 0.02	0.303 $\pm$ 0.02
300	-	0.351 $\pm$ 0.02	-	0.281 $\pm$ 0.003***	0.318 $\pm$ 0.02	0.250 $\pm$ 0.01*
1000	-	0.333 $\pm$ 0.01	-	0.244 $\pm$ 0.001***	0.210 $\pm$ 0.009**	0.200 $\pm$ 0.01***

**Table 4. Effect of H<sub>2</sub>S-donors on cellular proliferation.**

Growth inhibition was measured using the MTT assay and is expressed as OD values at 48h. All the compounds used, but NaHS, inhibited the growth of A375 cells. Experiments were run in triplicate (\*P<0.05; \*\*P<0.01; \*\*\*P<0.001 vs CTL).

(A) PES 43

$\mu\text{M}$	CTL	DATS	GY4137
0	0.481 $\pm$ 0.02	-	-
3	-	0.456 $\pm$ 0.006	-
10	-	0.437 $\pm$ 0.02	-
30	-	0.385 $\pm$ 0.009*	-
100	-	0.299 $\pm$ 0.01***	0.499 $\pm$ 0.01
300	-	-	0.455 $\pm$ 0.003
1000	-	-	0.344 $\pm$ 0.001**

(B) SkMel 5

$\mu\text{M}$	CTL	DATS	GY4137
0	0.251 $\pm$ 0.003	-	-
3	-	0.277 $\pm$ 0.006	-
10	-	0.261 $\pm$ 0.02	-
30	-	0.189 $\pm$ 0.01**	-
100	-	0.135 $\pm$ 0.004***	0.260 $\pm$ 0.008
300	-	-	0.245 $\pm$ 0.003
1000	-	-	0.178 $\pm$ 0.006**

(C) SkMel 28

$\mu\text{M}$	CTL	DATS	GY4137
0	0.315 $\pm$ 0.006	-	-
3	-	0.301 $\pm$ 0.007	-
10	-	0.284 $\pm$ 0.01	-
30	-	0.229 $\pm$ 0.009**	-
100	-	0.171 $\pm$ 0.002***	0.339 $\pm$ 0.01
300	-	-	0.301 $\pm$ 0.002
1000	-	-	0.214 $\pm$ 0.001**

**Table 5. Effect of H<sub>2</sub>S-donors on cellular proliferation.**

Growth inhibition was measured using the MTT assay and is expressed as OD values at 48h. Both DATS and GYY4137 inhibited the growth of PES 43 (A), SkMel 5 (B) and SkMel 28 (C) cells. Experiments were run in triplicate (\*P<0.05; \*\*P<0.01; \*\*\*P<0.001 vs CTL).

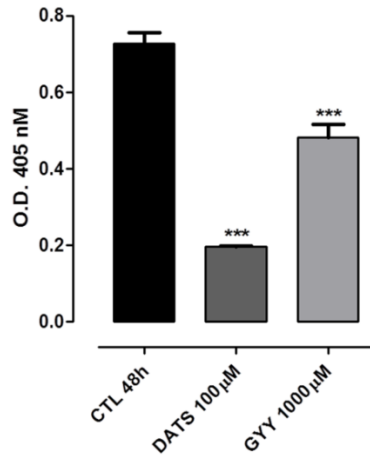


**Figure 11. Effect of hydrogen sulfide donors on A375 cell proliferation.**

Cell proliferation was measured by using the 5-bromo-2'deoxy uridine assay and it is expressed as OD values at 48h. Both DATS and GYY4137 inhibited the growth of A375 cells. Each experiment (n=3) were run in quadruplicate (\*\*P<0.001 vs CTL).

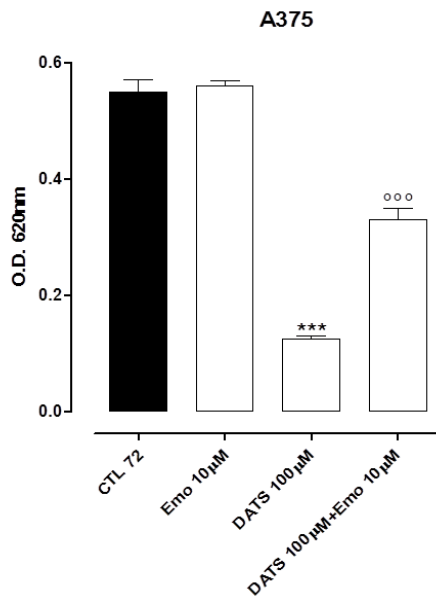


**Figure 12. Reversion of the anti-proliferative effect of DATS**

Growth inhibition was measured using the MTT assay and is expressed as OD values at 72h. DATS inhibited the growth of A375 cells but in the presence of haemoglobin (10 µM) its anti-proliferative effect was significantly reversed. Experiments were run in triplicate (\*\*P<0.001 vs CTL; °°° P<0.001 vs DATS).

#### ***4.2 Hydrogen sulfide donors cause cell cycle arrest and induce apoptosis of human melanoma***

In order to clarify whether the antiproliferative effect exhibited by DATS was due to a necrotic or apoptotic process, A375 human melanoma cells were treated with DATS and apoptosis was determined by annexin V/propidium iodide (PI) staining, which detects the externalization of phosphatidylserine (PS). This dual staining distinguishes between unaffected cells (unlabeled; quadrant 3 Figure 13A), early apoptotic cells (annexin V-positive; quadrant 4, Figure 13A), late apoptotic cells (annexin V-positive, PI-positive; quadrant 2, Figure 13A), and necrotic (PI-positive; quadrant 1; Figure 13A). Treatment of A375 cells for 3, 6, 24 and 48 h with DATS (100  $\mu$ M) resulted in a time-dependent induction of apoptosis. In particular, at 48 h almost all cells (93%) exhibited markers of late apoptosis (Figure 13B). This effect was accompanied by a time-dependent cleavage of caspase 3 and of its substrate poly(adenosine diphosphate-ribose) polymerase (PARP) (Figure 13C). In addition, DATS treatment of A375 cells induced time-dependent accumulation of G0/G1-phase populations (Figure 14). As expected, in DATS-treated cells, a reciprocal reduction of cell ratio in S and G2/M phases was also observed (Figure 14). Therefore, by donating hydrogen

sulfide, DATS induces apoptosis and cell cycle arrest of human melanoma cells.

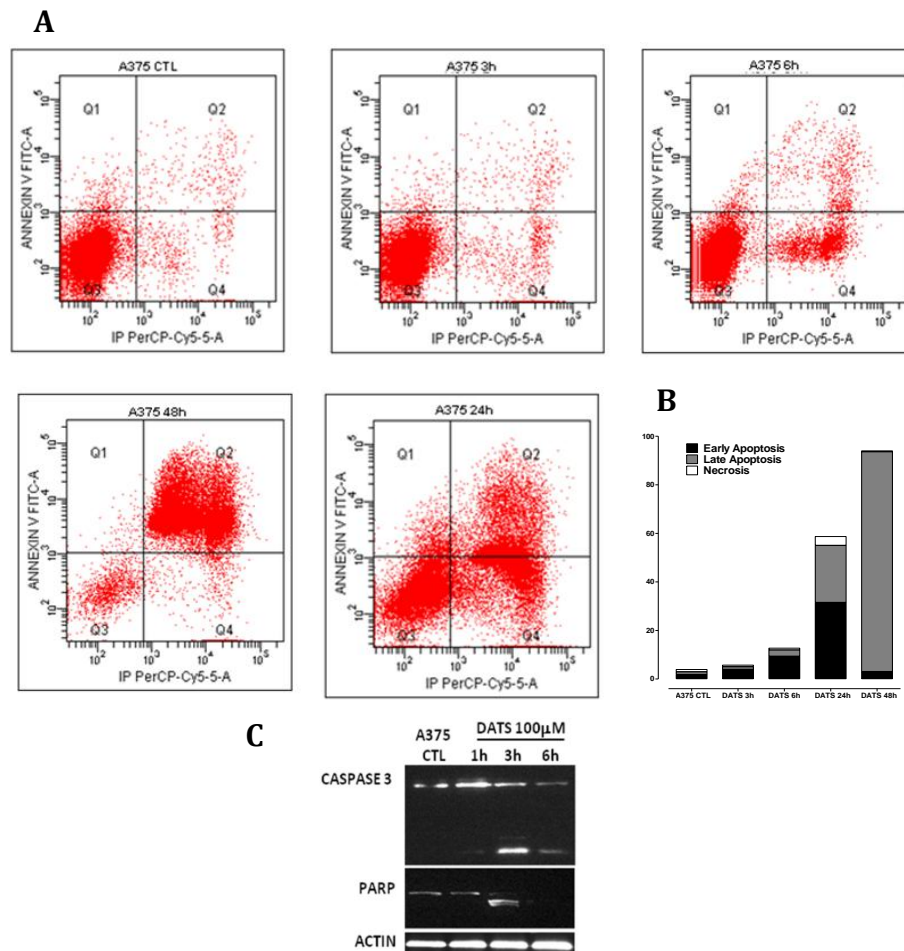


**Figure 13. Induction of apoptosis by the H<sub>2</sub>S-releasing donor DATS.**

**(A)** Cells were treated with DATS (100 μM) at different time points and apoptosis was determined by annexin V/propidium iodide (PI) staining. This dual staining distinguishes between unaffected cells (unlabeled; quadrant 3, Q3), early apoptotic cells (annexin V positive; quadrant 4, Q4), late apoptotic cells (annexin V positive, PI positive; quadrant 2, Q2), and necrotic (PI positive; quadrant 1, Q1). Treatment of A375 cells for 3-6-24-48 h with DATS (100 μM) resulted in a time-dependent induction of apoptosis. **(B)** Quantitative analysis of DATS-induced A375 apoptosis at various time points showing that at 48 h almost all cells (93%) exhibit markers of late apoptosis. **(C)** Western blot analysis of caspase 3 and PARP in A375 whole-cell lysates. A375 cells were incubated with DATS 100 μM for 1-3-6 hours and a time-dependent cleavage of caspase 3 and of its substrate PARP was observed. Actin was detected as loading control.

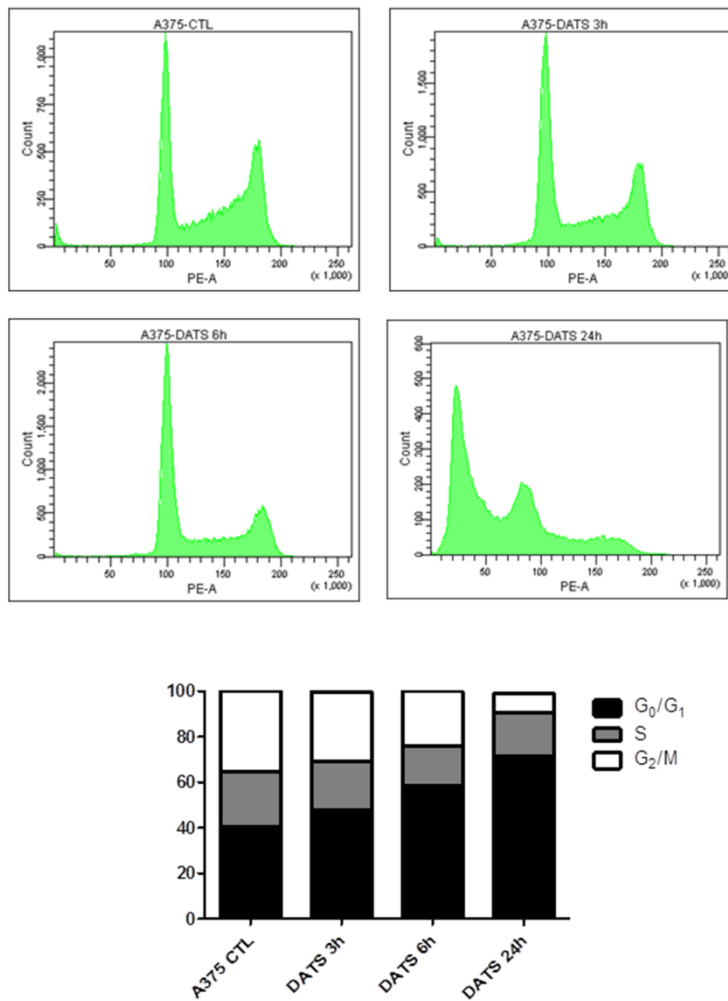


**Figure 14. Inhibition of cell cycle progression of human melanoma cells by DATS.**

DNA histogram shows the accumulation of G0/G1-phase cells induced by DATS in A375 cells and cell cycle arrest by the H<sub>2</sub>S-releasing donor DATS. Quantitative analysis of cell cycle distribution of A375 control-treated or DATS-treated at various time points. DATS treatment of A375 cells induced a time-dependent accumulation of G0/G1-phase populations (—). As expected, in DATS treated cells, a reciprocal reduction of cell ratio in S (grey □) G2/M-phases (□) was also observed.

### **4.3 Hydrogen sulfide donors inhibit NF- $\kappa$ B activation and down-regulate NF- $\kappa$ B-dependent anti-apoptotic genes**

Nuclear factor- $\kappa$ B (NF- $\kappa$ B) proteins are normally sequestered in the cytoplasm in an inactive form closely associated with the inhibitory protein inhibitor of kappa light chain gene enhancer in B cells-alpha ( $I\kappa B\alpha$ ). Several reports have shown that in melanoma the constitutive activation of NF- $\kappa$ B confers tumor survival capacity and avoidance of apoptosis<sup>45</sup>.

Western blot analysis carried out on the cytosolic extracts obtained from A375 cells treated with DATS 100  $\mu$ M for 15, 30 and 60 min showed an inhibition of  $I\kappa B\alpha$  degradation at the earliest time points (Figure 15A). To investigate the effect of hydrogen sulfide on NF- $\kappa$ B activity, A375 cells were treated with DATS (100  $\mu$ M) at different time points (1, 3 and 6 h; Figure 15B). The A375 cell line was found to display a constitutively high NF- $\kappa$ B DNA binding activity, as compared with NHEM, which was reduced in a time-dependent manner by DATS. In fact, treatment with DATS (100  $\mu$ M) for 3 and 6 h caused a significant ( $P < 0.001$ ) inhibition of NF- $\kappa$ B-DNA binding activity by 30 and 76%, respectively (Figure 15C). The major NF- $\kappa$ B band in A375 cells consisted of the p50 and p65 subunits. Following on, we assessed the expression of three anti-apoptotic proteins, X-

chromosome-linked inhibitor of apoptosis protein (XIAP), FLICE-inhibitory protein (c-FLIP) and B cell lymphoma gene-2 (Bcl-2), whose expression is modulated by the transcriptional activity of NF- $\kappa$ B. Western blot experiments showed that DATS markedly decreased the expression of all the anti-apoptotic genes considered (Figure 16), confirming NF- $\kappa$ B involvement.

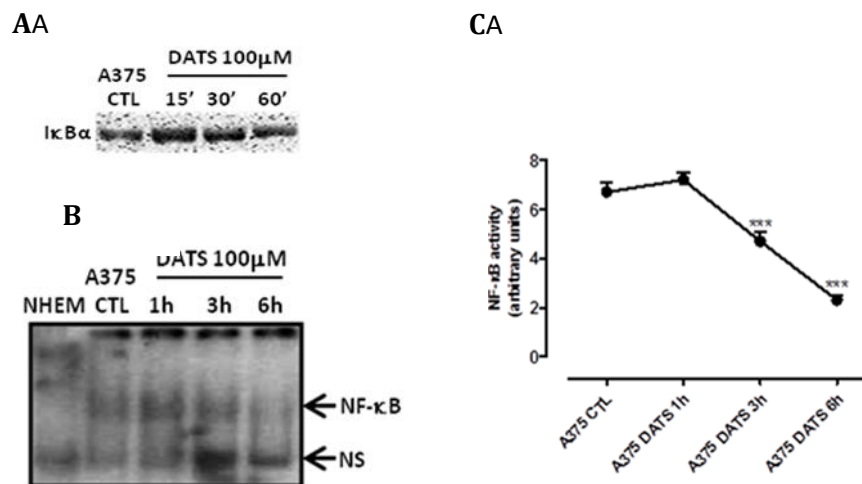


**Figure 15. Melanoma cells constitutively express activated NF- $\kappa$ B to promote anti-apoptotic and pro-survival signaling.**

(A) Western blot analysis carried out on the cytosolic extracts obtained from A375 cells treated with DATS 100  $\mu$ M for 15, 30, and 60 min shows an inhibition of I $\kappa$ B $\alpha$  degradation at the earliest time points. (B) Nuclear extracts from control-treated and DATS-treated A375 cells collected at 1-3-6 h were analyzed by EMSA for NF- $\kappa$ B activation. The A375 cell line displayed a constitutively high NF- $\kappa$ B DNA binding activity, as compared to NHEM, that was reduced in a time-dependent manner by DATS. These data are expressed as arbitrary units and shown in panel C, (\*\*\*) $P < 0.001$  vs CTL).

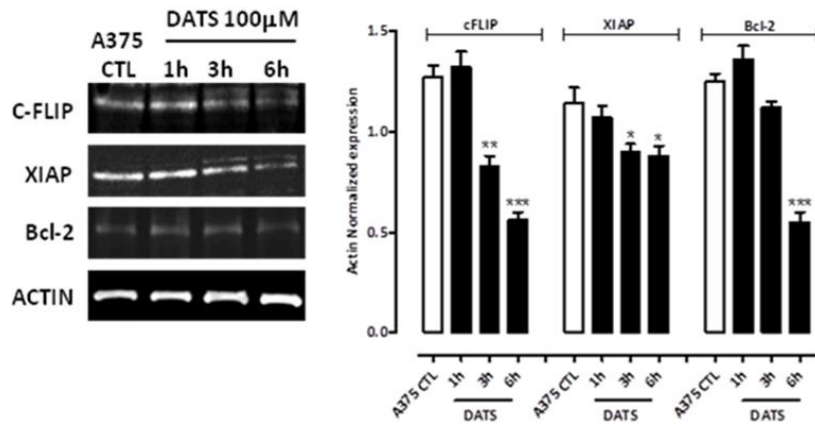


**Figure 16. Hydrogen sulfide donors down-regulate NF-κB-dependent anti-apoptotic genes**

Western blot analysis and relative densitometry of c-FLIP, XIAP and Bcl-2 carried out on A375 cells treated with DATS 100 μM for 1-3-6 h. The hydrogen sulfide donor markedly decreased the expression of all the anti-apoptotic genes analyzed; \*\*\*P<0.001; \*\*P<0.01; \*P<0.05 vs CTL. Actin was detected as a loading control.

#### ***4.4 Expression of CSE, CBS and of 3-MST in human melanoma cell lines***

In order to clarify the involvement of the endogenous pathway of H<sub>2</sub>S in melanoma we performed a quantitative real-time PCR (qPCR) analysis of the expression levels of CSE, CBS and 3-MST genes in NHEM and in a panel of four distinct human melanoma cell lines (A375, Sk-Mel-5, Sk-Mel-28 and PES 43). As shown in Figure 17, the expression of the three genes was always very low in NHEM as opposed to melanoma cell lines, where CSE, CBS and 3-MST were differentially expressed. In particular CSE, but not CBS or 3-MST, was upregulated in all the cell lines considered, although the difference was not statistically significant (Figure 17).

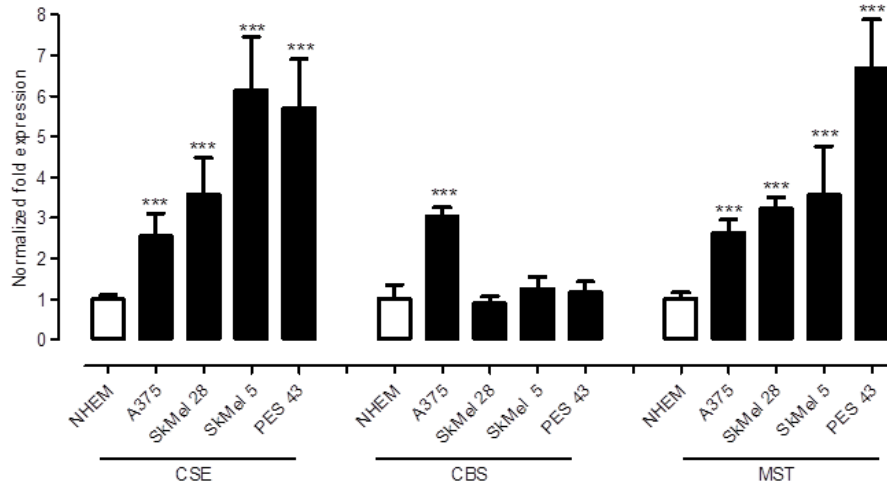


**Figure 17. CSE, CBS and 3-MST qPCR analysis.**

mRNA expression levels of CSE, CBS and 3-MST in NHEM, A375, Sk-Mel-5, Sk-Mel-28 and PES 43 cells evaluated by qPCR analysis. The expression of the three genes was very low in NHEM. In melanoma cell lines CSE, CBS and 3-MST were differentially expressed. The housekeeping gene (ribosomal protein S16) was used as an internal control to normalize the ct values. Each column is the mean  $\pm$ S.E.M. of at least four independent determinations each performed in quadruplicate. \*\*\*P<0.001 vs NHEM

#### **4.5 Overexpression of CSE in A375 cells modifies cell proliferation**

On the basis of the results obtained and to better elucidate the role of CSE in melanoma cells proliferation, we chose, as a tool, the cell line with the lowest CSE expression levels, the A375 melanoma cells. The CSE, CBS and 3-MST genes were transiently overexpressed using an hCSE cDNA/pIRES2-EGFP, an hCBS cDNA/pCMVSPORT6 or a 3-MST/pCI-HA construct. Identical empty vectors lacking a cDNA insert were used as control. Transfection of the cells with CSE cDNA, CBS cDNA, 3-MST cDNA or with the empty vectors did not change the morphological characteristics of the cells. To determine whether the CSE overexpression affected the proliferation of human melanoma cell line, a MTT proliferation assay was carried out. Proliferation of the CSE-overexpressing cells was inhibited by about 30% ( $P < 0.001$ ) as compared with control cells (Figure 18). Treatment with hemoglobin, a H<sub>2</sub>S scavenger, reversed the anti-proliferative effect elicited by CSE overexpression, confirming the specificity of the effect. When A375 CSE-overexpressing cells were grown in the presence of L-cysteine (1 mM) the CSE substrate, the anti-proliferative effect was not significantly increased. CBS overexpression caused only a small inhibition ( $P < 0.05$ ), which was not further increased when the cells were grown in the presence

of L-cysteine. 3-MST overexpression also slightly reduced cell proliferation and this effect was significantly increased ( $P < 0.05$ ) in the presence of the enzyme substrate 3-mercaptopyruvate (3-MP) ( $10 \mu\text{M}$ ) (Figure 18). These data show a major role for CSE in melanoma. We also performed silencing experiments on the A375 cell line. Cells were transiently transfected for 48 h with CSE Pre-designed siRNA, human CBS siRNA SMART pool or human 3-MST siRNA SMART pool. The negative control siRNA was used as internal control. As shown in Figure 19, silencing of the genes did not modify cell proliferation.

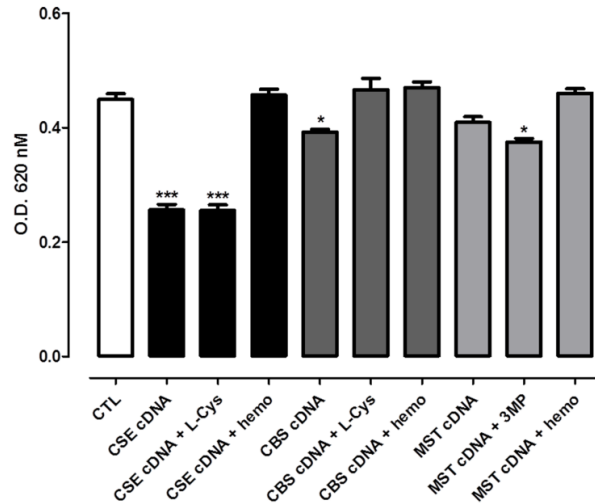


**Figure 18. CSE, CBS and 3-MST genes over-expression in A375 cells.**

CSE over-expression inhibited proliferation of human melanoma cells, as demonstrated by the MTT proliferation assay \*\*\*  $P < 0.001$  vs Control (CTL). CBS over-expression only slightly (10%, \* $P < 0.05$  vs CTL) inhibited proliferation of human melanoma cells that was not further reduced by the addition of L-cysteine (1mM). 3-MST over-expression inhibited cell proliferation of about 7% that following the addition of the enzyme substrate 3-MP (10  $\mu$ M) reached 15% (\* $P < 0.05$  vs CTL). Hemoglobin (10  $\mu$ M) reversed the anti-proliferative effect induced by enzyme over-expression. Each column is the mean  $\pm$ S.E.M. of 6 independent experiments each performed in quadruplicate.

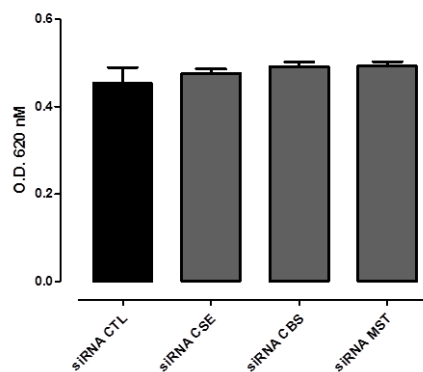


**Figure 19. CSE, CBS and 3-MST silencing in A375 cells.**

CSE, CBS and 3-MST genes silencing did not modify proliferation of human melanoma cells, as demonstrated by the MTT proliferation assay. Each column is the mean  $\pm$ S.E.M. of 3 independent experiments each performed in quadruplicate.

#### ***4.6 Hydrogen sulfide inhibits the growth of melanoma cutaneous in vivo in mice***

To better elucidate the role of H<sub>2</sub>S in melanoma development, we used a well-known murine model of melanoma<sup>376</sup>, which is induced by subcutaneously injecting B16-F10 murine cells in C57BL/6 mice. L-Cysteine (300 and 600 mg/kg), the CSE substrate, was administered orally to mice. At day 14 after tumor implantation, a significantly, dose-dependent, reduction in tumor volume and weight was observed in L-cysteine-treated mice ( $0.240 \pm 0.09$  cm<sup>3</sup> mean tumor volume L-cys 300mg/kg vs control mice  $0.365 \pm 0.04$  cm<sup>3</sup> mean tumor volume,  $P < 0.05$  and  $110 \pm 9$  mg mean tumor weight vs control mice  $221 \pm 30$  mg mean tumor weight  $P < 0.01$ ;  $0.168 \pm 0.03$  cm<sup>3</sup> mean tumor volume L-cys 600mg/kg vs control mice  $0.365 \pm 0.04$  cm<sup>3</sup> mean tumor volume,  $P < 0.001$  and  $65 \pm 2$  mg mean tumor weight vs control mice  $221 \pm 30$  mg mean tumor weight,  $P < 0.001$ ) (Figure 20). To verify the specificity of the effect of L-cysteine we used two selective inhibitors of the enzymes CBS and CSE, DL-propargilglycine (PAG) (CSE inhibitor) and the acid aminoacetic (CHH) (inhibitor of CBS), both at a dose of 10mg/kg. These inhibitors were administered alone or together with L-cysteine (600 mg/Kg).

As shown in Figure 21, the L-cysteine alone reduced by 51% the volume of the tumor mass ( $0.134 \pm 0.03$  cm<sup>3</sup> vs  $0.348 \pm$

0.03 cm<sup>3</sup> control mice, P <0.001) and 57% of the weight (220.3 ± 48.3 mg vs 532.8 ± 53.5 mg control mice, P <0.01). This protective effect was significantly reduced by the PAG (0.320 ± 0.05 cm<sup>3</sup> vs 0.134 ± 0.03 cm<sup>3</sup> L-cysteine alone, P <0.001; 497 ± 93.3 mg vs 220.3 ± 48.3 mg L-cysteine alone, P <0.01). In contrast, CHH did not alter the effect of cysteine (0.211 ± 0.05 cm<sup>3</sup>; 214.7 ± 32 mg). When administered alone both PAG and CHH didn't significantly alter tumor growth (data not shown).

The tumor growth inhibition obtained by the endogenous-CSE-derived hydrogen sulfide was mimicked by the exogenous hydrogen sulfide delivered to mice following administration of DATS. In fact, DATS (50 mg/kg) significantly (P<0.001) inhibited tumor growth by 67% (0.07 ± 0.001 cm<sup>3</sup> mean tumor volume; 88 ± 15,3 mg mean tumor weight) as compared with control mice (0.210 ± 0.004 cm<sup>3</sup> mean tumor volume; 358 ± 37,3 mg mean tumor weight)(Figure 22).

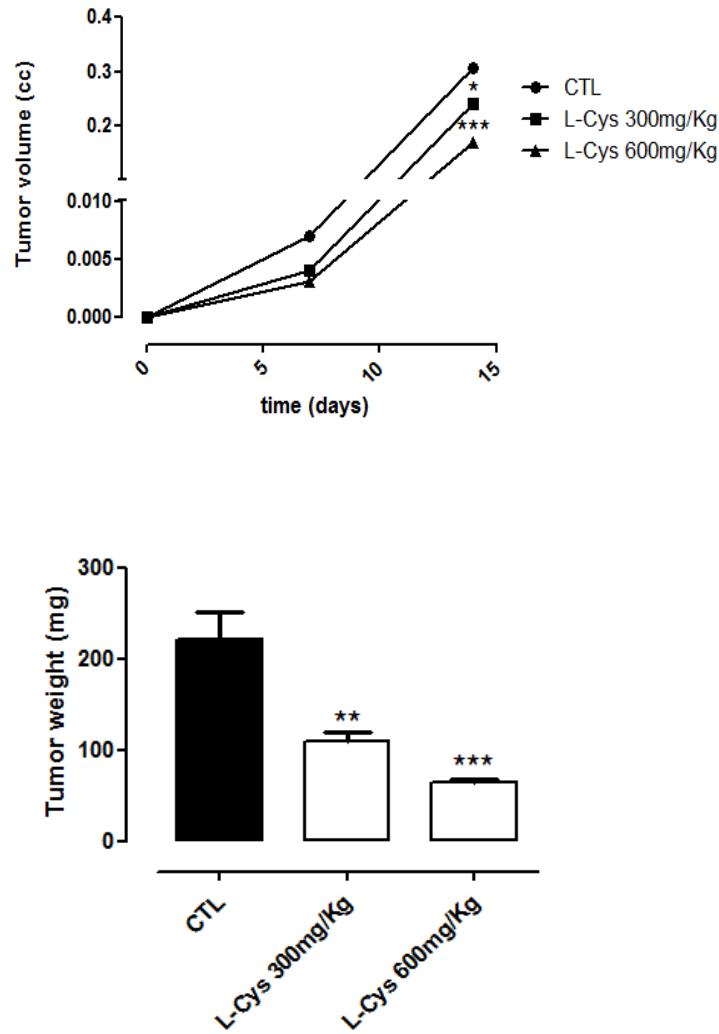


**Figure 20. Hydrogen sulfide inhibits tumor growth *in vivo*.**

L-cysteine (L-cys 300 mg/Kg, ■) and (600 mg/Kg, ▲), were given orally to mice; control mice (●) received vehicle only. Tumor volume was monitored on the indicated days. The average tumor volume with standard error is plotted against the days after tumor implant. L-cysteine significantly reduced tumor volume in dose-dependent manner ( $*P < 0.05$  vs control;  $***P < 0.001$  vs control,  $n=8$ ; day 14). The average tumor weight with standard error shows that L-cysteine significantly reduced tumor weight in dose-dependent manner ( $**P < 0.01$  vs control;  $***P < 0.001$  vs control,  $n=8$ ; day 14).

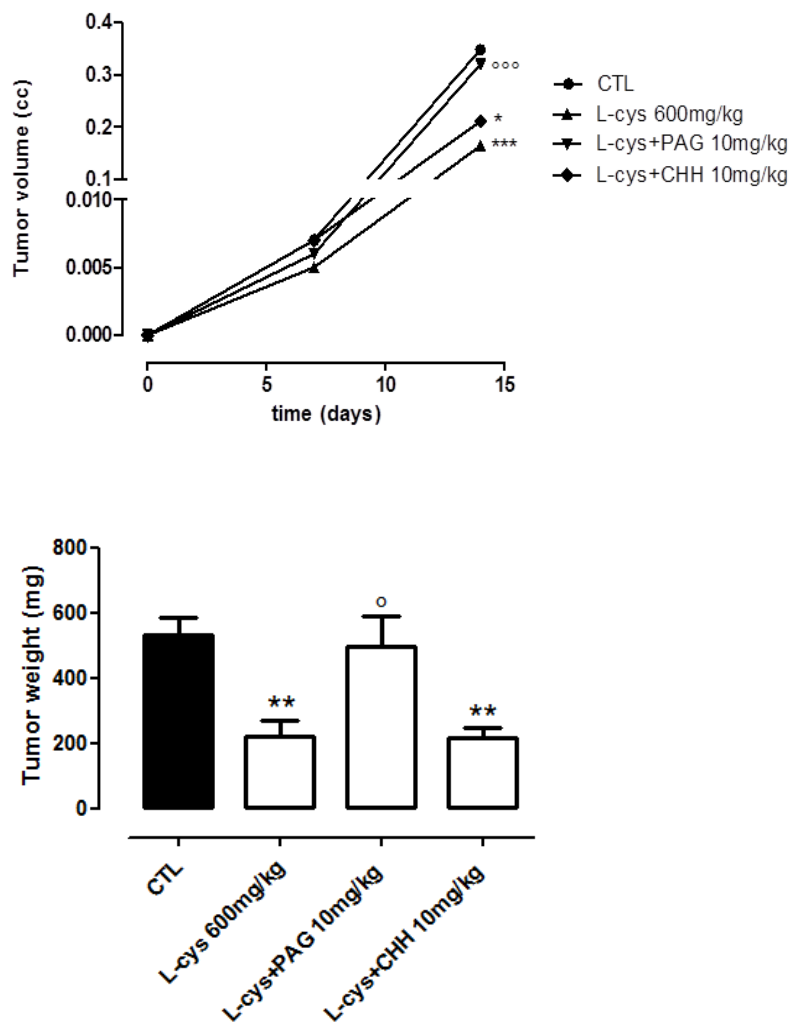


**Figure 21. Hydrogen sulfide inhibits tumor growth *in vivo*.**

L-cysteine (L-cys 600 mg/Kg, ▲), L-cys+PAG (10 mg/Kg) (▼) or L-cys+CHH (10 mg/Kg) (◆) were given orally to mice; control mice (●) received vehicle only. Tumor volume was monitored on the indicated days. The average tumor volume with standard error is plotted against the days after tumor implant. L-cysteine significantly reduced tumor volume ( $***P < 0.001$  vs control, n=8; day 14); the inhibitory effect of L-cysteine was abolished by PAG ( $^{\circ}P < 0.001$  vs L-cys, n=8) but CHH did not alter the effect of cysteine ( $*P < 0.05$  vs control vs control, n=8; day 14). The average tumor weight with standard error shows that L-cysteine significantly reduced tumor weight ( $**P < 0.01$  vs control, n=8; day 14); the inhibitory effect of L-cysteine was abolished by PAG ( $^{\circ}P < 0.05$  vs L-cys, n=8) but not CHH ( $**P < 0.05$  vs control vs control, n=8; day 14). When administered alone both PAG and CHH didn't significantly alter tumor growth (data not shown).

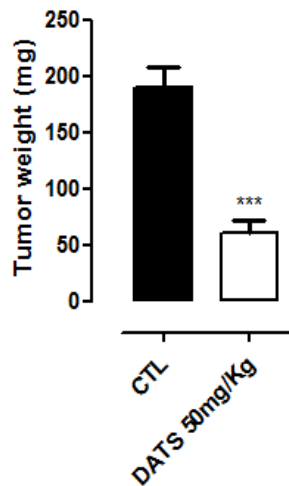
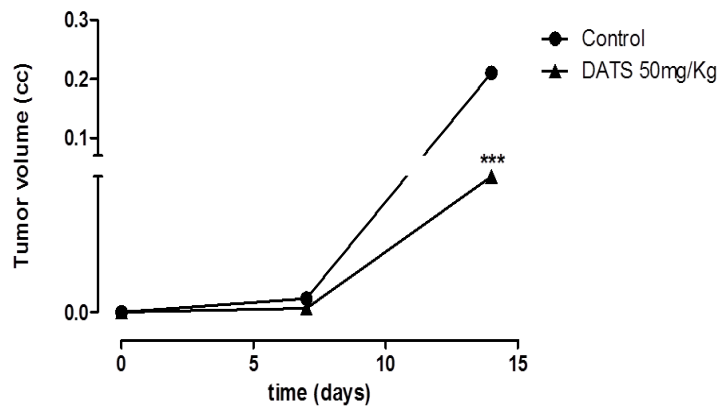


**Figure 22. Hydrogen sulfide inhibits tumor growth *in vivo*.**

The H<sub>2</sub>S-donor DATS (50 mg/Kg, ▲) were given orally to mice; control mice (●) received vehicle only. Tumor volume was monitored on the indicated days. The average tumor volume with standard error is plotted against the days after tumor implant. DATS significantly inhibited tumor volume and tumor weight (\*\*\*)  $P < 0.001$  vs control, n=8; day 14).

#### ***4.7 Effect of hydrogen sulfide donors on MAPK/ERK and PI3/AKT pathways***

Two of the most frequently deregulated pathways in melanoma are mitogen-activated protein kinase (MAPK)/ERK and phosphoinositide 3-kinase (PI3K)/AKT<sup>73</sup>. These two pathways play an important role in melanoma development and progression and are involved in the mechanism of resistance to targeted therapy<sup>146</sup>. Therefore, we wanted to investigate whether H<sub>2</sub>S was able to adjust these two important "pathways". Western blot experiments showed that DATS (100 μM) significantly reduced both the intensity of the band phospho-AKT and phospho-ERK in a time-dependent manner, indicating an inhibition of their activation (Figure 23). Thus, the proapoptotic effects of hydrogen sulfide on human melanoma involve a reduced activation of the AKT/p-AKT and ERK/p-ERK signaling pathways.

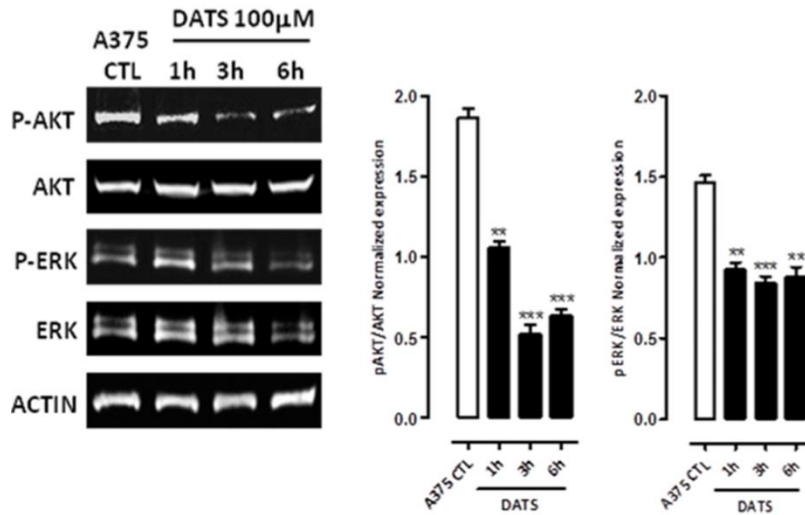


**Figure 23. Hydrogen sulfide donors down-regulate AKT and ERK pathways**

Western blot analysis and relative densitometry of phospho- and total AKT and ERK in A375 cells treated with DATS 100  $\mu$ M for 1-3-6h. Both p-AKT and p-ERK band intensity was time-dependently reduced following treatment with DATS (100  $\mu$ M); \*\*\* $P < 0.001$ ; \*\* $P < 0.01$  vs CTL. Actin was detected as a loading control. Experiments ( $n=3$ ) were run in triplicate.

#### ***4.8 Hydrogen sulfide inhibits A375rVem cell proliferation***

To assess whether H<sub>2</sub>S is efficacy also in conditions of resistance to therapy, we generated vemurafenib-resistant A375 (A375rVem) melanoma cells. A375 cells harbor the BRAF V600E mutation and are sensitive to vemurafenib treatment (100 nM). Drug-resistant A375 cells were obtained through treatment with increasing concentrations of vemurafenib<sup>145</sup> (Figure 24).

Treatment with DATS inhibited significantly the growth of A375rVem cells in a concentration- and time- dependent manner (Figure 25).



#### ***4.9 Hydrogen sulfide inhibits metastatic melanoma in vivo in mice***

To investigate the role of H<sub>2</sub>S in melanoma progression, we performed a murine model of metastatic melanoma which is induced by injecting 5x10<sup>5</sup> cells B16/F-10 into the tail vein of mice C57BL/6. Through the circle cells reach the lungs, where they are visible as metastatic foci rich in melanin<sup>377</sup>. The mice were treated with DATS (50 mg/kg) or with L-cysteine (1000 mg/kg) while control mice received only the vehicle, by orally administration. After 14 days the lungs were removed and was calculated the percentage of metastatic affected area, using the software Image J. Results show that treatment with L-cysteine reduced of about 65% the development of lung metastases compared to control mice (metastatic area: L-cys 4.4% vs control mice 70%). Similar effects are shown by DATS which reduced of about 67% the metastatic area (metastatic area: DATS 3.3% vs 70% control mice) (Figure 26).

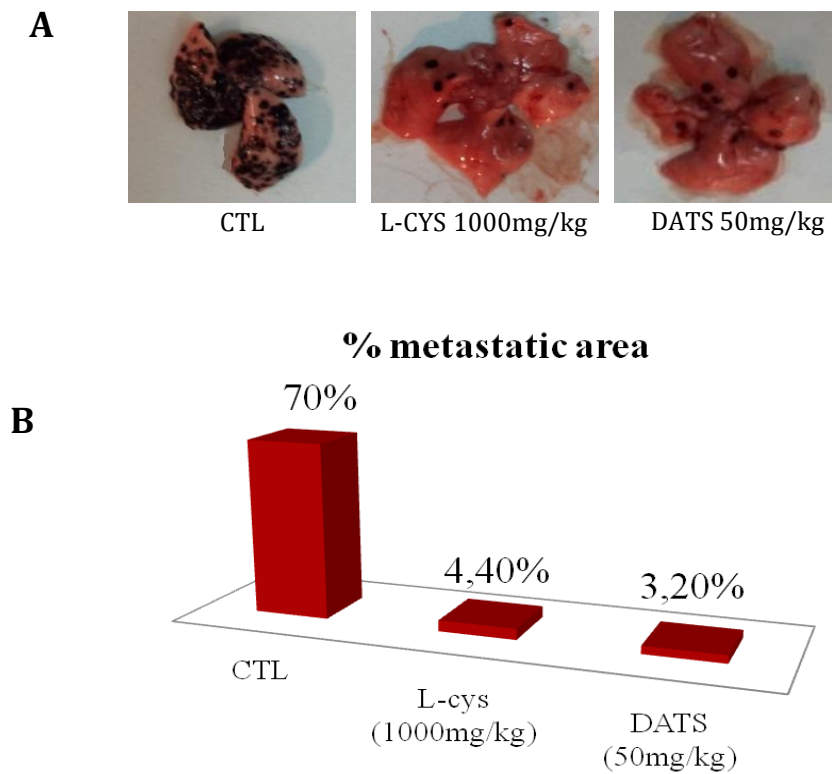


**Figure 26. Hydrogen sulfide reduces lung metastasis growth *in vivo*.**

The H<sub>2</sub>S-donor DATS (50 mg/Kg) and L-cysteine (1000 mg/Kg) were given orally to mice; control mice received vehicle only. L-cysteine reduced of about 65% the metastatic area; DATS reduced of about 67% the metastatic area **(A)** Gross examination of representative lungs **(B)** Graphical representation of the number of lung metastases in treated mice. Image J software was used for quantitative analyses.

#### ***4.10 CSE, CBS and 3-MST expression in human nevi***

Expression of CSE, CBS and 3-MST was evaluated in six compound nevi, four junctional nevi and four dysplastic nevi. As shown in Table 6, all the dysplastic nevi (100%) were positive for CSE, negative for CBS and variable for 3-MST. Representative immunohistochemical-positive expressions of CSE, CBS and 3-MST in nevi and in melanomas, but not in lymph node metastases, are shown in Figure 27.

#### ***4.11 CSE, CBS and 3-MST expression in human primitive melanoma and metastases.***

All specimens of primary melanoma analyzed by immunohistochemistry (n = 4) were positive for CSE expression (Table 7). CBS and 3-MST displayed a variable, but always very low, expression level in primary tumor (pT) (Table 7). A total of 72 melanoma metastases were analyzed. Metastases obtained were either lymph node metastases (n = 14) or tissue metastases (n = 58). Tissue metastases were distributed as follows: skin (22/58), lung (25/58), liver (6/58) and intestinal metastases (5/58). CSE-positive metastases were 39% (28/72); among these positive cases, 93% (26/28) were no lymph node metastases. CBS-positive metastases were 30% (22/72); among these positive cases

91% (20/22) were no lymph node metastases. 3-MST-positive metastases were 28% (20/72) none of which were lymph node metastases.

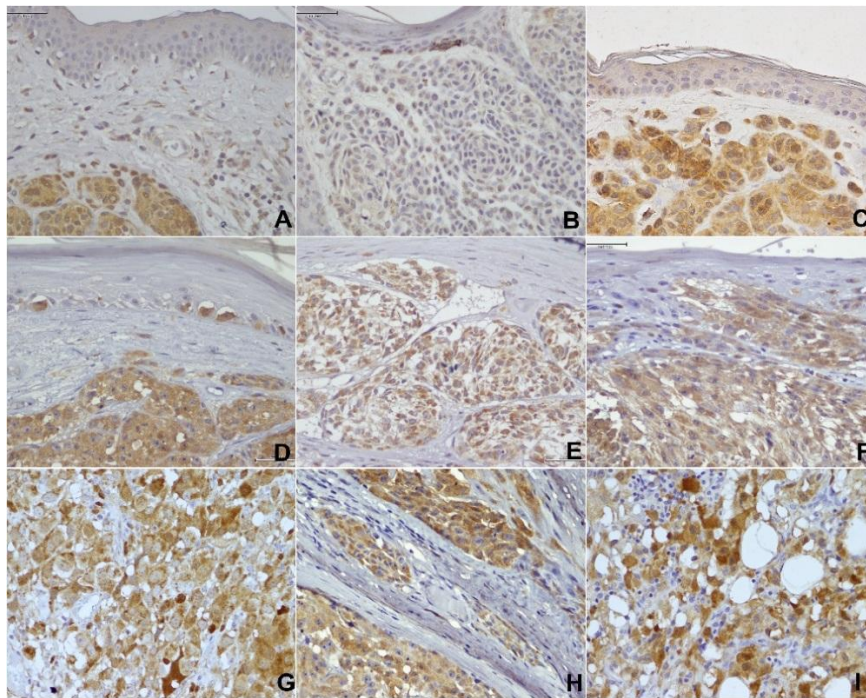


**Figure 27. CSE, CBS and 3-MST immunohistochemical analysis.**

Representative immunohistochemical positive expression of CSE, CBS and 3-MST in nevi (A, B, C; 40X); in melanomas (D, E, F; 40X); in no lymph nodes metastases (G,H, I; 40X).

	CSE		CBS		3-MST	
	(-)	(+)	(-)	(+)	(-)	(+)
<b>Nevi</b>						
Compound	3 (50%)	3 (50%)	3 (50%)	3 (50%)	5 (83%)	1 (17%)
Junction	2 (50%)	2 (50%)	3 (75%)	1 (25%)	3 (75%)	1 (25%)
Dysplastic	0	4 (100%)	4 (100%)	0	1 (25%)	3 (75%)

**Table 6. CSE, CBS and 3-MST immunohistochemical analysis**

Contingency table of CSE, CBS and 3-MST expression in nevi. In rows the frequencies are indicated in absolute values. The percentage is reported in brackets. Abbreviations: “pT” primary tumor; (-) no/low expression; (+) high expression.

pT	CSE		CBS		3-MST	
	(-)	(+)	(-)	(+)	(-)	(+)
1	0	4 (100%)	3 (75%)	1 (25%)	3 (75%)	1 (25%)
2	0	4 (100%)	3 (75%)	1 (25%)	3 (75%)	1 (25%)
3	0	4 (100%)	4 (100%)	0	2 (50%)	2 (50%)
4	0	4 (100%)	3 (75%)	1 (25%)	3 (75%)	1 (25%)
<b>Metastasis sites</b>						
No Lymph Node	32 (55.2%)	26 (44.8%)	38 (65.5%)	20 (34.5%)	38 (65.5%)	20 (34.5%)
Lymph Node	12 (85.7%)	2 (14.3%)	12 (85.7%)	2 (14.3%)	14 (100%)	0

**Table 7. CSE, CBS and 3-MST immunohistochemical analysis**

Contingency table of CSE, CBS and 3-MST expression in primitive melanoma and metastases. All specimens were analyzed by immunohistochemistry. The frequencies are indicated in rows in absolute values. The percentage is reported in brackets. ‘pT’ primary tumor; (-) no/low expression; (+) high expression.

# DISCUSSION

---

Melanoma, the deadliest form of skin cancer, is among the most aggressive and treatment-resistant human cancers. The incidence of malignant melanoma is rising faster, indeed only from 1980 to 2009 the incidence has increased fivefold. Each year, more than 132,000 patients are diagnosed with this type of cancer<sup>378</sup>. It is becoming clear that melanoma constitutes a heterogeneous group of tumors with different patterns of oncogenic mutation, overexpression and genomic amplification. The mutation rate of melanoma is higher than other aggressive tumors, probably due to the involvement of ultraviolet (UV) radiation in the genesis of superficial cutaneous melanoma<sup>53</sup>. The most frequent driver mutations in melanoma involve genes as BRAF, NRAS, KIT, GNAQ, and GNA11. Constitutive upregulation of the MAPK pathway by a BRAFV600 mutation occurs in about 50% of melanomas. This leads to increased oncogenic properties such as tumor cell invasion, metastatic potential, and resistance to apoptosis<sup>73</sup>.

Multiple cellular pathways have been implicated in melanomagenesis, ranging from signal transduction to developmental and transcriptional pathways and cell cycle.

The interactions between the various signalling molecules involved in melanoma progression are best viewed as a series of links between a number of interconnected nodes.

If melanoma is diagnosed at an early stage surgical excision is curative in approximately 99% of patients. However, later stages have poor prognosis due to lack of responsiveness to traditional chemotherapeutics<sup>13</sup>. Over the last 30 years, no drug or combination of drugs have demonstrated significant impact to improve patient survival for long time. From 1995 to 2000, the use of cytokines such as interferon and interleukin became treatment options. In 2011, new drugs were approved by the U.S. Food and Drug Administration, including peginterferon alfa-2 $\beta$  for patients with stage III disease, vemurafenib for patients with metastatic melanoma with the BRAF V600E mutation, the MEK1/2 inhibitor trametinib and the monoclonal antibody ipilimumab, directed to the CTLA-4 T lymphocyte receptor. Other trials for new additional agents and combinations targeting the MAPK, PI3K/AKT/mTOR (PI3K), c-kit, are currently in progress. Individualized targeted therapy has showed response rates, in terms of overall survival, that have never been described in melanoma before. However, early development of resistance is the major drawback of this therapy. It is known that about 50% of patients treated with BRAF or MEK inhibitors have disease progression within 6–

7 months after the initiation of treatment due mostly to reactivation of the MAPK pathway. So, metastatic melanoma is generally still incurable. Therefore, it is critical to identify other important potential targets in melanoma development and progression that are amenable to pharmacological inhibition.

In the last few years, several physiological and pathophysiological roles have been proposed for the gasotransmitter hydrogen sulfide, along with a plethora of cellular and molecular targets<sup>222</sup>. CSE produces H<sub>2</sub>S from L-cysteine alone in the presence of pyridoxal 5'-phosphate, whereas CBS generates H<sub>2</sub>S by condensation of L-cysteine and other thiols, such as L-homocysteine. Sequential reaction by the PLP-dependent enzyme, CAT, and a PLP-independent enzyme, 3-MST, has also been proposed as a potential H<sub>2</sub>S-producing pathway. CAT forms 3-mercaptopyruvate from L-cysteine and  $\alpha$ -ketoglutarate, and 3-MST subsequently catalyzes the formation of H<sub>2</sub>S from 3-mercaptopyruvate in the presence of reducing agents.

A number of studies have investigated the role of H<sub>2</sub>S in inducing cell death and evidence has been presented that this gas can exert both pro- and anti-apoptotic activity in cultured cells<sup>250; 379</sup>. It has been shown previously that CSE is expressed in melanoma cell lines<sup>375</sup> but the role of the hydrogen sulfide pathway has never been investigated.

Conversely, a role for this pathway has been proposed in colon and ovarian cancer, where it is mainly driven by CBS<sup>314-315</sup>.

The aim of my PhD project was to evaluate the role of the metabolic H<sub>2</sub>S pathway in human melanoma.

To address this issue we:

- (iv) evaluated the role of H<sub>2</sub>S on human melanoma cell proliferation and explained its possible mechanism of action;
- (v) evaluated the role of the endogenous pathway of H<sub>2</sub>S in melanoma development and progression;
- (vi) showed the clinical relevance of the H<sub>2</sub>S donors in order to propose them as new therapeutic agents.

Controversy exists on the role of H<sub>2</sub>S on cancer cell proliferation because of the complexity of DNA damage and repair. The activation of the H<sub>2</sub>S pathway has been shown to be able to exert both pro- and anti-apoptotic activity in cultured cells<sup>250; 379</sup>. These studies have been conducted on immortalized cell lines mainly using NaHS as the exogenous source of hydrogen sulfide. The use of NaHS as donor has two main drawbacks: (i) the fast kinetics of hydrogen sulphide release and (ii) the high concentrations used, often in the mM range. These two issues suggest that discrepancies (e.g. pro- and anti-apoptotic effect) may lie in the choice of the hydrogen sulfide donors used. Sulfide salts

such as NaHS and sodium sulfide ( $\text{Na}_2\text{S}$ ) on addition of water generate a burst of hydrogen sulfide within a short period as opposed to the organic donors<sup>352</sup>. Since cell culture takes place over a period of hours or days, it is likely that little, if any, hydrogen sulphide is present in medium within a short time of adding either NaHS or  $\text{Na}_2\text{S}$ . It is therefore necessary to perform repeated challenge or to use high (mM) doses. In a recent comparative study showing differences between fast (NaHS) and slow-release (GYY4137)  $\text{H}_2\text{S}$  donors, it has been demonstrated that only GYY4137 caused a concentration-dependent killing of several human cancer cell lines<sup>352</sup>. Therefore, in our study we used both fast (NaHS) and slow releasers (DATS, GYY4137, thioglycine and L-thiovaline). All the compounds used, except NaHS, although with different  $\text{IC}_{50}$ , inhibited cellular proliferation. The most active among the  $\text{H}_2\text{S}$ -donors tested was DATS and it was selected for the molecular studies since its hydrogen sulfide-delivering property had been well characterized<sup>236</sup>. Cytofluorimetric studies demonstrated that the anti-proliferative effect of DATS was due to its ability to induce apoptosis and cell cycle arrest in G<sub>0</sub>/G<sub>1</sub>-phase. Caspase-3 is the main 'effector' caspase in the apoptotic pathway, which acts through cleavage of its well-known substrate PARP. The finding that DATS induces caspase 3 activation further confirmed that  $\text{H}_2\text{S}$  triggers apoptosis. Many

chemotherapeutic agents cause cell-cycle arrest but not apoptosis and this is one of the mechanisms leading to chemoresistance. In fact, growth arrest allows cells to repair their DNA and limits the efficacy of chemotherapy. Thus, by overriding tumor resistance to apoptosis, agents such as hydrogen sulphide donors are of great potential value. The apoptotic machinery can be controlled, at least in part, by NF- $\kappa$ B, which regulates transcription of the Bcl-2 family members<sup>41</sup>. Constitutive activation of NF- $\kappa$ B has been described in melanoma<sup>42</sup>. The activation of NF- $\kappa$ B promotes the multiple steps in melanoma progression such as transformation, initiation, promotion, angiogenesis, invasion and enhanced metastatic potential of malignant melanoma cells<sup>43</sup>. Moreover, NF- $\kappa$ B activated would be responsible of resistance of cancer cells to chemotherapeutic agents<sup>44</sup>.

Here we show that hydrogen sulphide donors inhibit I $\kappa$ B $\alpha$  degradation and this effect was associated to the inhibition of NF- $\kappa$ B nuclear translocation and activation. The issue of whether exogenous hydrogen sulfide inhibits<sup>233; 358; 380-384</sup> or activates<sup>238</sup> NF- $\kappa$ B signaling pathway has been a matter of debate. Indeed, in the relevant literature diametrically opposite views exist on the roles of this gas in NF- $\kappa$ B activation. However, the different experimental settings (in vitro versus in vivo) coupled to the different stimuli as well as to the protocols used do not allow a clear conclusion to be

drawn. It has been shown that the slow-releasing hydrogen sulfide donor derivatives of diclofenac<sup>234; 295</sup> and aspirin<sup>361</sup> also inhibit NF- $\kappa$ B activation. In addition, it has recently been shown that hydrogen sulfide inhibits NF- $\kappa$ B activation in ox LDL-induced macrophage inflammation through both sulfhydration of free thiol group on cysteine 38 in p65 subunit and inhibition of I $\kappa$ B $\alpha$  degradation<sup>385</sup>. In our study and experimental settings we found that hydrogen sulfide inhibits I $\kappa$ B $\alpha$  degradation, leading to inhibition of NF- $\kappa$ B nuclear translocation.

Thus our results are in line with the inhibitory effect of hydrogen sulfide on NF- $\kappa$ B activation<sup>233; 358; 380-384</sup>. The fact that NF- $\kappa$ B is inhibited by H<sub>2</sub>S is also supported by the finding that treatment with hydrogen sulfide donors greatly decreased the expression of the anti-apoptotic proteins c-FLIP, XIAP and Bcl-2. Indeed, these proteins are known to be transcriptionally regulated by NF- $\kappa$ B<sup>42</sup>.

To evaluate the involvement of the hydrogen sulfide pathway in melanoma, we analysed the expression of the enzymes involved in H<sub>2</sub>S synthesis, CBS, CSE and 3-MST, in several melanoma cell lines, widely used in the relevant literature. All the melanoma cells selected expressed CSE, CBS and 3-MST differently. Whereas CSE expression was higher in all melanoma cells analysed as compared with NHEM, CBS expression was enhanced in A375 cells only, and

3-MST showed a variable pattern of expression among all cell lines.

Thus, to obtain further insights into the role of these enzymes in melanoma we perform a molecular modulation study selecting as a tool the A375 cell line. Overexpression of CSE in A375 inhibited cellular proliferation (50%). Treatment with hemoglobin, a hydrogen sulfide scavenger, reversed the anti-proliferative effect elicited by CSE overexpression, confirming the specificity of the effect. CBS overexpression caused only a small inhibition of cell proliferation (about 10%) that was not further increased by the addition of L-cysteine. The same magnitude of effect, about 8%, was observed following 3-MST overexpression. Addition of 3-MP, the enzyme substrate, increased the anti-proliferative effect up to 15%. Therefore, these results underline the primary role of CSE versus CBS and 3-MST. On the other hand, the silencing of all three enzymes did not modify cellular proliferation, implying that reduction of the basal endogenous level of H<sub>2</sub>S production does not affect cell survival, or a compensatory mechanism may intervene.

To support these results, we developed a translational in vivo pre-clinical approach. For this purpose we used an animal model that recapitulates human cutaneous melanoma progression, the spontaneous C57BL/6-derived B16 melanoma cell line<sup>376</sup> because it is well-established and

is a widely used tumor model. We demonstrated that L-cysteine, the natural substrate of CSE, significantly reduced tumor volume and this effect was completely abolished by PAG, the selective CSE inhibitor, but not CHH, the CBS inhibitor. To further support our in vitro findings we also used DATS in vivo. DATS significantly inhibited tumor volume development proving that the tumor growth inhibition obtained by the endogenous-CSE-derived hydrogen sulfide was mimicked by the exogenous hydrogen sulfide delivered to mice following administration of DATS. To better define the mechanism by which this critical anti-tumor effect is achieved, we investigated on the possible involvement of the MAPK/ERK and the PI3K/AKT pathways. These pathways are the two most frequently deregulated pathways in melanoma and are also involved in primary and secondary resistance to BRAF inhibitors<sup>73; 133; 141; 145</sup>. We have shown that DATS inhibited the phosphorylation-activation of AKT and ERK. Our results are in agreement with other reports showing that exogenous hydrogen sulfide downregulates both AKT and MAPK pathways<sup>381; 383-384</sup>. Starting from evidence that MAPK and PI3K/AKT pathways are involved in melanoma progression (abnormal proliferation, angiogenesis, invasion and metastasis) and resistance to therapy with BRAF inhibitor, we have

investigated the role of H<sub>2</sub>S in these conditions mimicking these clinical situations.

Acquired resistance to vemurafenib is a major factor limiting successful, long term targeted therapy for patient with malignant melanoma<sup>142</sup>. For this purpose we have generated vemurafenib-resistant A375 melanoma cells, harbor the BRAFV600E mutation, and we have demonstrate that DATS is able to inhibit their proliferation. Therefore, DATS overcomes resistance to vemurafenib *in vitro*.

Otherwise, we have performed a murine model of metastatic melanoma demonstrating that both L-cysteine and DATS, significantly, inhibited lung metastasis formation.

Finally to give another clinical relevance to this study and to obtain further insights into the role of the hydrogen sulphide pathway in melanoma we analysed the expression of CSE, CBS and 3-MST in human tissue samples. The immunohistochemical analysis performed on more than 100 human samples demonstrated that CSE expression increased from nevi to primary melanoma, decreased in tissue metastases and was absent in lymph node metastases. Conversely, analysis of CBS expression revealed that this enzyme was absent in dysplastic nevi. Positive CBS expression was found in only 25% of the primary melanomas analyzed. Therefore, as opposed to other types of cancer<sup>314;315</sup> CBS does not appear to play an important

role in human melanoma. 3-MST expression was always extremely variable in the human specimens analyzed (from nevi to metastasis). The finding that CSE expression is higher in primary melanoma than in distant metastatic melanoma suggests the involvement of this pathway in the progression of melanoma. These data support our hypothesis that CSE derived hydrogen sulfide plays a major role in melanoma. Our results are in line with a previous study showing that overexpression of CSE in HEK-293 results in the inhibition of cellular proliferation and DNA synthesis<sup>195</sup>.

Our study demonstrates that in A375 cells, CSE but not CBS overexpression induces spontaneous apoptosis and exogenous hydrogen sulfide induces apoptosis. This apoptotic effect involves: (i) the suppression of pro-survival pathways associated to NF- $\kappa$ B transcription activity as demonstrated by the decreased expression of c-FLIP, XIAP and Bcl-2 and (ii) the inhibition of the activation of AKT and ERK1/2 downstream signalling pathways.

Moreover, hydrogen sulphide inhibiting simultaneously both the MAPK and PI3K/AKT pathways, is effective in the treatment of both cutaneous and metastatic melanoma *in vivo* and in inhibiting growth of vemurafenib melanoma resistant cells.

All these data confirm the involvement of hydrogen sulfide in melanoma progression.

In conclusion we have demonstrated, thanks also to the evidence acquired with human specimens, the involvement of the L-cysteine/CSE/hydrogen sulfide pathway in human melanoma. Our study provides proof-of-principle toward establishing this pathway as a diagnostic tool or a potential therapeutic target in human melanoma.

# REFERENCE

---

1. Koch CM. Melanoma. *Oncol.* 27:99-101 (2004).
2. J. Y. Lin, D. E. Fisher. Melanocyte biology and skin pigmentation. *Nature.* 445: 843–850 (2007).
3. D. Mitra et al. An ultraviolet-radiation-independent pathway to melanoma carcinogenesis in the red hair/fair skin background. *Nature.* 491: 449–453 (2012).
4. Miller AJ and Mihm MC Jr. Melanoma. *N Engl J Med.* 355(1):51-65 (2006).
5. Gilchrist BA, Eller MS, Geller AC, Yaar M. The pathogenesis of melanoma induced by ultraviolet radiation. *N Engl J Med.* 340(17):1341-8 (1999).
6. Pho L, Grossman D and Leachman SA: Melanoma genetics: A review of genetic factors and clinical phenotypes in familial melanoma. *Curr Opin Oncol.* 18(2): 173-179 (2006).
7. Erickson C, Driscoll MS. Melanoma epidemic: facts and controversies. *Clin Dermatol.* 28(3):281–286 (2010).
8. Siegel R., Ma J., Zou Z., Jemal A. CA Cancer. *J. Clin.* 64: 9–29 (2014).
9. Bleyer A, Viny A, Barr R. Cancer in 15- to 29-year-olds by primary site. *Oncologist.* 11(6):590-601 (2006).
10. Beddingfield FC 3rd, Cinar P, Litwack S et al. An analysis of SEER and the California Cancer Registry data on gender and melanoma incidence. *J Invest Dermatol* (2002).
11. Garbe C, Leiter U. Melanoma epidemiology and trends. *Clin Dermatol.* 27(1):3–9 (2009).
12. Clark WH. Tumour progression and the nature of cancer. *Br J Cancer* 64: 631–644 (1991).
13. Balch CM, Soong SJ, Gershenwald JE, et al. Prognostic factors analysis of 17,600 melanoma patients: validation of the American Joint Committee on Cancer melanoma staging system. *J Clin Oncol.* 19:3622-34 (2001).

14. Balch CM, Gershenwald JE, Soong SJ, Thompson JF, Atkins MB, Byrd DR, et al. Final version of 2009 AJCC melanoma staging and classification. *J Clin Oncol.* 27: 6199–6206 (2009).
15. Seger R and Krebs EG. The MAPK signaling cascade. *FASEB J.* 9(9):726-35. (1995).
16. Omholt K, Platz A, Kanter L, Ringborg U, Hansson J. NRAS and BRAF mutations arise early during melanoma pathogenesis and are preserved throughout tumor progression. *Clin Cancer Res.* 9: 6483-6488 (2003).
17. Chen J, Fujii K, Zhang L, Roberts T, Fu H. Raf-1 promotes cell survival by antagonizing apoptosis signal-regulating kinase 1 through a MEK-ERK independent mechanism. *Proc Natl Acad Sci USA.* 98: 7783-7788 (2001).
18. Baumann B, Weber CK, Troppmair J, Whiteside S, Israel A, Rapp UR et al. Raf induces NF-kappaB by membrane shuttle kinase MEKK1, a signaling pathway critical for transformation. *Proc Natl Acad Sci USA.* 97:4615-4620 (2000).
19. Chapman PB, Hauschild A, Robert C, Haanen JB, Ascierto P, Larkin J et al. Improved survival with vemurafenib in melanoma with BRAF V600E mutation. *N Engl J Med.* 364: 2507-2516 (2011).
20. Jakob JA, Bassett Jr RL, Ng CS, Curry JL, Joseph RW, Alvarado GC et al. NRAS mutation status is an independent prognostic factor in metastatic melanoma. *Cancer.* 118(16):4014-23 (2012).
21. Sekulic, P. Haluska Jr., A. J. Miller et al., "Malignant melanoma in the 21st century: the emerging molecular landscape," *Mayo Clinic Proceedings.* 83 (7): 825–846 (2008).
22. Vivanco, C.L. Sawyers, The phosphatidylinositol 3-Kinase AKT pathway in human cancer. *Nat. Rev. Cancer* 2: 489–501(2002).

23. M.A. Davies, The role of the PI3K-AKT pathway in melanoma, *Cancer J.* 18: 142–147(2012).
24. B.D. Manning, L.C. Cantley, AKT/PKB signaling: navigating downstream, *Cell.* 129: 1261–1274(2007).
25. Song G, Ouyang G, Bao S. The activation of Akt/PKB signaling pathway and cell survival. *J Cell Mol Med.* 9(1):59-71 (2005).
26. Liu P, Cheng H, Roberts TM, et al. Targeting the phosphoinositide 3-kinase pathway in cancer. *Nat Rev Drug Discov.* 8:627–44 (2009).
27. DH, et al. mTOR interacts with raptor to form a nutrient-sensitive complex that signals to the cell growth machinery. *Cell.* 110(2):163–175 (2002).
28. Vezina C, Kudelski A, Sehgal SN. Rapamycin (AY-22,989), a new antifungal antibiotic. I. Taxonomy of the producing streptomycete and isolation of the active principle. *J Antibiot (Tokyo).* 28(10):721–726 (1975).
29. N. Hay, N. Sonenberg, Upstream and downstream of mTOR. *Genes Dev.* 18: 1926–1945(2004).
30. Sarbassov DD, et al. Rictor, a novel binding partner of mTOR, defines a rapamycin-insensitive and raptor-independent pathway that regulates the cytoskeleton. *Curr Biol.* 14(14):1296–1302 (2004)
31. D.D. Sarbassov, D.A. Guertin, S.M. Ali, D.M. Sabatini, Phosphorylation and regulation of Akt/PKB by the rictor-mTOR complex. *Science* 307: 1098–1101 (2005).
32. Cantley LC, Neel BG. New insights into tumor suppression: PTEN suppresses tumor formation by restraining the phosphoinositide 3-kinase/AKT pathway. *Proc Natl Acad Sci U S A* 96:4240-5 (1999).
33. Slipicevic, et al., Expression of activated Akt and PTEN in malignant melanomas: relationship with clinical outcome. *Am. J. Clin. Pathol.* 124: 528–536 (2005).

34. M. Karbowniczek, C.S. Spittle, T. Morrison, H. Wu, E.P. Henske, mTOR is activated in the majority of malignant melanomas. *J. Invest. Dermatol.* 128: 980–987 (2008).
35. Stahl JM, Sharma A, Cheung M, et al. Deregulated Akt3 activity promotes development of malignant melanoma. *Cancer Res.* 64:7002-10 (2004).
36. D.L. Dai, M. Martinka, G. Li, Prognostic significance of activated Akt expression in melanoma: a clinicopathologic study of 292 cases. *J. Clin. Oncol. Off. J. Am. Soc. Clin. Oncol.* 23: 1473–1482(2005)
37. Thompson JE and Thompson CB. Putting the rap on Akt. *J Clin Oncol.* 22:4217-4226 (2004).
38. Aggarwal BB, Kunnumakkara AB, Harikumar KB, Gupta SR, Tharakan ST, et al. Signal transducer and activator of transcription-3, inflammation, and cancer: How intimate is the relationship? *Ann. NY Acad. Sci.* 1171:59–76 (2009).
39. Hayden MS and Ghosh S. Signaling to NF- $\kappa$ B. *Genes dev.* 18:2195-224 (2004).
40. Ghosh, S., May, M.J., and Kopp, E.B. NF-kappa B and Rel proteins: evolutionarily conserved mediators of immune responses. *Annu. Rev. Immunol.* 16: 225-60 (1998).
41. Karin, M. & Lin, A. NF- $\kappa$ B at the crossroad of Life and Death. *Nature Immunol.* 3, 221–227 (2002).
42. Gilmore TD et al, Rel/NF-kappaB/IkappaB signal transduction pathway and cancer. *Cancer Treat Res.* 115, 241-65 (2003).
43. McNulty SE, Del Rosario R, Cen D, Meyskens FL Jr, Yang S. Comparative expression of NF $\kappa$ B proteins in melanocytes of normal skin vs benign intradermal naevus and human metastatic melanoma biopsies. *Pigment Cell Res.* 17:173-80 (2004).
44. Katayoun I. Amiri and Ann Richmond. Role of nuclear factor- $\kappa$ B in melanoma. *Cancer Metastasis Rev.* 24(2): 301–313 (2005).

45. Yukiko Ueda and Ann Richmond NF- $\kappa$ B activation in melanoma. *Pigment Cell Res.* 19(2): 112–124 (2006).
46. Liu J, Suresh Kumar KG, Yu D, Molton SA, McMahon M, Herlyn M, Thomas-Tikhonenko A, Fuchs SY. Oncogenic BRAF regulates  $\beta$ -Trcp expression and NF- $\kappa$ B activity in human melanoma cells. *Oncogene.* 26(13):1954-1958 (2007).
47. Madrid LV, Mayo MW, Reuther JY, Baldwin AS Jr. Akt stimulates the transactivation potential of the RelA/p65 Subunit of NF-kappa B through utilization of the Ikappa B kinase and activation of the mitogen-activated protein kinase p38. *J Biol Chem* 276:18934–18940 (2001).
48. Dhawan P, Richmond A: A novel NF-kappa B-inducing kinase-MAPK signaling pathway up-regulates NF-kappa B activity in melanoma cells. *J Biol Chem.* 277:7920-8 (2002).
49. Li X, Stark GR. NFkappaB-dependent signaling pathways. *Exp Hematol.* 30:285–296 (2002).
50. Castelli C, Sensi M, Lupetti R, Mortarini R, Panceri P, Anichini A, Parmiani G. Expression of interleukin 1 alpha, interleukin 6, and tumor necrosis factor alpha genes in human melanoma clones is associated with that of mutated N-RAS oncogene. *Cancer Res.* 54:4785–4790 (1994).
51. Norris JL, Baldwin AS. Oncogenic Ras enhances NF-kappaB transcriptional activity through Raf-dependent and Raf-independent mitogen-activated protein kinase signaling pathways. *J Biol Chem.* 274: 13841–13846 (1999).
52. G. A. Croghan, V. J. Suman, W. J. Maples et al., A study of paclitaxel, carboplatin, and bortezomib in the treatment of metastatic malignant melanoma: a phase 2 consortium study. *Cancer.* 116 (14): 3463–3468 (2010).
53. Garibyan L, Fisher DE. How sunlight causes melanoma. *Curr Oncol Rep.* 12:319–326 (2010).
54. Berger, M.F. et al. Melanoma genome sequencing reveals frequent PREX2 mutations. *Nature* 485: 502–506 (2012).

55. Hodis, E. et al. A landscape of driver mutations in melanoma. *Cell*. 150: 251–263 (2012).
56. R. Roskoski, RAF protein-serine/threonine kinases: structure and regulation. *Biochem. Biophys. Res. Commun.* 399: 313–317 (2010).
57. K.P. Hoeflich, et al., Oncogenic BRAF is required for tumor growth and maintenance in melanoma models. *Cancer Res.* 66: 999–1006 (2006).
58. P.M. Pollock, et al., High frequency of BRAF mutations in nevi. *Nat. Genet.* 33: 19–20.38–40 (2003).
59. H. Davies, et al., Mutations of the BRAF gene in human cancer. *Nature*. 417: 949–954 (2002).
60. Wan PT, Garnett MJ, Roe SM, Lee S, Niculescu-Duvaz D, Good VM, Jones CM, Marshall CJ, Springer CJ, Barford D, Marais R and Cancer Genome P. Mechanism of activation of the RAF-ERK signaling pathway by oncogenic mutations of B-RAF. *Cell*. 116 (6): 855-867 (2004).
61. Albino, A.P. et al. Analysis of ras oncogenes in malignant melanoma and precursor lesions: correlation of point mutations with differentiation phenotype. *Oncogene*. 4: 1363–1374 (1989).
62. Curtin, J.A. et al. Somatic activation of KIT in distinct subtypes of melanoma. *J. Clin. Oncol.* 24: 4340–4346 (2006).
63. Beadling, et al., KIT gene mutations and copy number in melanoma subtypes, *Clin. Cancer Res. Off. J. Am. Assoc. Cancer Res.* 14: 6821–6828 (2008).
64. J.R. Todd, L.L. Scurr, T.M. Becker, R.F. Kefford, H. Rizos, The MAPK pathway functions as a redundant survival signal that reinforces the PI3K cascade in c-Kit mutant melanoma. *Oncogene*. 33: 236–245 (2014).
65. Van Raamsdonk, C.D. et al. Frequent somatic mutations of GNAQ in uveal melanoma and blue naevi. *Nature*. 457: 599–602 (2009).

66. Van Raamsdonk, C.D. et al. Mutations in GNA11 in uveal melanoma. *N. Engl. J. Med.* 363: 2191–2199 (2010).
67. Bartkova, J. et al. The p16–cyclin D/Cdk4–pRb pathway as a functional unit frequently altered in melanoma pathogenesis. *Cancer Res.* 56: 5475–5483 (1996)
68. Dahl, C. et al. Mutual exclusivity analysis of genetic and epigenetic drivers in melanoma identifies a link between p14 ARF and RARbeta signaling. *Mol. Cancer Res.* 11: 1166–1178 (2013).
69. Chin L, Garraway LA, Fisher DE. Malignant melanoma: genetics and therapeutics in the genomic era. *Genes Dev.* 20:2149–2182 (2006).
70. Meyle, K.D. and Guldberg, P. Genetic risk factors for melanoma. *Hum. Genet.* 126: 499–510 (2009).
71. Nathanson KL, Martin AM, Wubbenhorst B, Greshock J, Letrero R, D’Andrea K, O’Day S, Infante JR, Falchook GS, Arkenau HT, Millward M, Brown MP, Pavlick A, Davies MA, Ma B, Gagnon R, et al. Tumor genetic analyses of patients with metastatic melanoma treated with the BRAF inhibitor Dabrafenib (GSK2118436). *Clinical cancer research : an official journal of the American Association for Cancer Research.* (2013).
72. Michaloglou, C. et al. BRAFE600-associated senescence-like cell cycle arrest of human naevi. *Nature.* 436: 720–724 (2005).
73. Hodis E, Watson IR, Kryukov GV, Arold ST, Imielinski M, Theurillat JP, Nickerson E, Auclair D, Li L, Place C, Dicara D, Ramos AH, Lawrence MS, Cibulskis K, Sivachenko A, Voet D, et al. A landscape of driver mutations in melanoma. *Cell.* 150(2): 251-263 92012).
74. Hussussian CJ, Struewing JP, Goldstein AM, Higgins PA, Ally DS, Sheahan MD, Clark WH, Jr., Tucker MA and Dracopoli NC. Germline p16 mutations in familial melanoma. *Nature genetics.* 8(1): 15-21 (1994).

75. Polsky D, Bastian BC, Hazan C, Melzer K, Pack J, Houghton A, Busam K, Cordon-Cardo C and Osman I. HDM2 protein overexpression, but not gene amplification, is related to tumorigenesis of cutaneous melanoma. *Cancer research*. 61(20): 7642-7646 (2001).
76. Gembarska A, Luciani F, Fedele C, Russell EA, Dewaele M, Villar S, Zwolinska A, Haupt S, de Lange J, Yip D, Goydos J, Haigh JJ, Haupt Y, Larue L, Jochemsen A, Shi H, et al. MDM4 is a key therapeutic target in cutaneous melanoma. *Nature medicine*. (2012).
77. Matin RN, Chikh A, Law Pak Chong S, Mesher D, Graf M, Sanza P, Senatore V, Scatolini M, Moretti F, Leigh IM, Proby CM, Costanzo A, Chiorino G, Cerio R, Harwood CA and Bergamaschi D. p63 is an alternative p53 repressor in melanoma that confers chemoresistance and a poor prognosis. *The Journal of experimental medicine*. (2013).
78. Bergamaschi D, Samuels Y, Sullivan A, Zvelebil M, Breysens H, Bisso A, Del Sal G, Syed N, Smith P, Gasco M, Crook T and Lu X. iASPP preferentially binds p53 proline-rich region and modulates apoptotic function of codon 72-polymorphic p53. *Nature genetics*. 38(10): 1133-1141 (2006).
79. Muthusamy V, Hobbs C, Nogueira C, Cordon-Cardo C, McKee PH, Chin L and Bosenberg MW. Amplification of CDK4 and MDM2 in malignant melanoma. *Genes, chromosomes & cancer*. 45(5): 447-454 (2006).
80. Zuo L, Weger J, Yang Q, Goldstein AM, Tucker MA, Walker GJ, Hayward N and Dracopoli NC. Germline mutations in the p16INK4a binding domain of CDK4 in familial melanoma. *Nature genetics*. 12(1): 97-99 (1996).
81. Tsao H, Zhang X, Benoit E and Haluska FG. Identification of PTEN/MMAC1 alterations in uncultured melanomas and melanoma cell lines. *Oncogene*. 16(26): 3397-3402 (1998).
82. Cao J, Wan L, Hacker E, Dai X, Lenna S, Jimenez-Cervantes C, Wang Y, Leslie NR, Xu GX, Widlund HR, Ryu B, Alani RM,

- Dutton-Regester K, Goding CR, Hayward NK, Wei W, et al. MC1R Is a Potent Regulator of PTEN after UV Exposure in Melanocytes. *Molecular cell*. 51(4): 409-422 (2013).
83. Omholt, K. et al. Mutations of PIK3CA are rare in cutaneous melanoma. *Melanoma Res*. 16: 197–200 (2006).
84. Stahl JM, Sharma A, Cheung M, Zimmerman M, Cheng JQ, Bosenberg MW, Kester M, Sandirasegarane L and Robertson GP. Deregulated Akt3 activity promotes development of malignant melanoma. *Cancer research*. 64(19): 7002-7010 (2014).
85. Shull AY, Latham-Schwark A, Ramasamy P, Leskoske K, Oroian D, Birtwistle MR and Buckhaults PJ. Novel somatic mutations to PI3K pathway genes in metastatic melanoma. *PloS one*. 7(8): e43369 (2012).
86. Scortegagna M, Ruller C, Feng Y, Lazova R, Kluger H, Li JL, De SK, Rickert R, Pellicchia M, Bosenberg M and Ronai ZA. Genetic inactivation or pharmacological inhibition of Pdk1 delays development and inhibits metastasis of Braf::Pten melanoma. *Oncogene*. (2013)
87. Nikolaev SI, Rimoldi D, Iseli C, Valsesia A, Robyr D, Gehrig C, Harshman K, Guipponi M, Bukach O, Zoete V, Michielin O, Muehlethaler K, Speiser D, Beckmann JS, Xenarios I, Halazonetis TD, et al. Exome sequencing identifies recurrent somatic MAP2K1 and MAP2K2 mutations in melanoma. *Nature genetics*. 44(2): 133- 139 (2012).
88. Garraway LA, Widlund HR, Rubin MA, Getz G, Berger AJ, Ramaswamy S, Beroukhim R, Milner DA, Granter SR, Du J, et al. Integrative genomic analyses identify MITF as a lineage survival oncogene amplified in malignant melanoma. *Nature*. 436: 117–122 (2005).
89. Yokoyama S, Woods SL, Boyle GM, Aoude LG, MacGregor S, Zismann V, Gartside M, Cust AE, Haq R, Harland M, Taylor JC, Duffy DL, Holohan K, Dutton-Regester K, Palmer JM, Bonazzi V, et al. A novel recurrent mutation in MITF predisposes to

- familial and sporadic melanoma. *Nature*. 480(7375): 99-103 (2011).
90. Bertolotto et al., *Nature*. 480(7375): 94-8 (2011).
91. Balch CM, Gershenwald JE, Soong SJ, Thompson JF, Atkins MB, Byrd DR, Buzaid AC, Cochran AJ, Coit DG, Ding S, Eggermont AM, Flaherty KT, Gimotty PA, Kirkwood JM, McMasters KM, Mihm MC Jr, Morton DL, Ross MI, Sober AJ, Sondak VK. Final version of 2009 AJCC melanoma staging and classification. *J Clin Oncol*. 27(36): 6199-206 (2009).
92. Wong J, Skinner K, Kim K, Foshag L, Morton D. The role of surgery in the treatment of recurrent melanoma. *Surgery*. 113: 389-394 (1993).
93. Sosman JA, Moon J, Tuthill RJ, Warneke JA, Vetto JT, Redman BG, et al. A phase 2 trial of complete resection for stage IV melanoma: results of Southwest Oncology Group Clinical Trial S9430. *Cancer*. 117: 4740-4706 (2011)
94. Pirard D, Heenen M, Melot C, Vereecken P. Interferon alpha as adjuvant postsurgical treatment of melanoma: a meta-analysis. *Dermatology*. 208: 43-48 (2004).
95. Delaney G, Barton M, Jacob S. Estimation of an optimal radiotherapy utilization rate for melanoma: a review of the evidence. *Cancer*. 100: 1293-1301 (2004).
96. O'Day S, Boasberg P. Management of metastatic melanoma 2005. *Surg Oncol Clin N Am*. 15:419-37 (2006).
97. Lee B, Mukhi N, Liu D. Current management and novel agents for malignant melanoma. *J Hematol Oncol*. 5:3. (2012).
98. Ives NJ, Stowe RL, Lorigan P, Wheatley K. Chemotherapy compared with biochemotherapy for the treatment of metastatic melanoma: a meta-analysis of 18 trials involving 2,621 patients. *J Clin Oncol*. 25: 5426-5434 (2007).
99. M. H. Greene, T. I. Young, W. H. Clark Jr. *Lancet* 317: 1196-99 (1981).

100. Morton DL, Eilber FR, Holmes EC, et al. BCG immunotherapy of malignant melanoma: summary of a seven-year experience. *Ann Surg.* 180(4): 635–643 (1974).
101. Dranoff G. GM-CSF-secreting melanoma vaccines. *Oncogene.* 22(20): 3188–3192 (2003).
102. von Wussow P, Block B, Hartmann F, Deicher H. Intralesional interferon-alpha therapy in advanced malignant melanoma. *Cancer.* 61(6): 1071–1074 (1988).
103. Blanchard T, Srivastava PK, Duan F. Vaccines against advanced melanoma. *Clin Dermatol.* 31(2): 179–190 (2013).
104. D. Wolchok et al., Nivolumab plus ipilimumab in advanced melanoma. *N. Engl. J. Med.* 369: 122–133 (2013).
105. Yamamoto T, Ueta E, Osaki T. Apoptosis induction by interleukin-2-activated cytotoxic lymphocytes in a squamous cell carcinoma cell line and Daudi cells – involvement of reactive oxygen species-dependent cytochrome c and reactive oxygen species-independent apoptosis-inducing factors. *Immunology* .110: 217–224 (2003).
106. Atkins MB, Lotze MT, Dutcher JP, Fisher RI, Weiss G, Margolin K, et al. High-dose recombinant interleukin 2 therapy for patients with metastatic melanoma: analysis of 270 patients treated between 1985 and 1993. *J Clin Oncol.* 17: 2105–2116 (1999).
107. Temple-Oberle CF, Byers BA, Hurdle V, Fyfe A, McKinnon JG. Intra-lesional interleukin-2 therapy for in transit melanoma. *J Surg Oncol.* 109(4):327–331 (2014).
108. Barth RJJ, Mule JJ, Spiess PJ, et al. Unique murine tumor-associated antigens identified by tumor infiltrating lymphocytes. *J Immunol.* 144: 1531–1537 (1990).
109. Rosenberg SA, Spiess P, Lafreniere R. A new approach to the adoptive immunotherapy of cancer with tumor-infiltrating lymphocytes. *Science.* 233: 1318–1321 (1986).

110. Rosenberg S, Yang J, Sherry R, Kammula U, Hughes M, Phan G, et al. Durable complete responses in heavily pretreated patients with metastatic melanoma using T cell transfer immunotherapy. *Clin Cancer Res.* 17: 4550–4557 (2011).
111. A. H. Sharpe. Mechanisms of costimulation. *Immunol. Rev.* 229: 5–11 (2009).
112. Chambers CA, Kuhns MS, Egen JG, Allison JP. CTLA-4-mediated inhibition in regulation of T cell responses: mechanisms and manipulation in tumor immunotherapy. *Annu Rev Immunol.* 19: 565–594 (2001).
113. Peggs KS, Quezada SA, Korman AJ, Allison JP. Principles and use of anti-CTLA4 antibody in human cancer immunotherapy. *Curr Opin Immunol.* 18: 206–213 (2006).
114. Camacho LH, Antonia S, Sosman J, Kirkwood JM, Gajewski TF, Redman B, et al. Phase I/II trial of tremelimumab in patients with metastatic melanoma. *J Clin Oncol.* 27: 1075–1081 (2009).
115. Ribas A, Kefford R, Marshall MA, Punt CJ, Haanen JB, Marmol M, et al. Phase III randomized clinical trial comparing tremelimumab with standard-of-care chemotherapy in patients with advanced melanoma. *J Clin Oncol.* 31: 616–622 (2013).
116. Hodi FS, O'Day SJ, McDermott DF, Weber RW, Sosman JA, Haanen JB, et al. Improved survival with ipilimumab in patients with metastatic melanoma. *N Engl J Med.* 363:711–23 (2010).
117. Robert C, Thomas L, Bondarenko I, O'Day S, Weber J, Garbe C, et al. Ipilimumab plus dacarbazine for previously untreated metastatic melanoma. *N Engl J Med.* 364: 2517–2526 (2011).
118. Sapoznik S, Hammer O, Ortenberg R, Besser MJ, Ben-Moshe T, Schachter J and Markel G. Novel antimelanoma immunotherapies: disarming tumor escape mechanisms. *Clinical & developmental immunology.* 2012:818214 (2012).

119. Iwai Y, Ishida M, Tanaka Y, Okazaki T, Honjo T and Minato N. Involvement of PD-L1 on tumor cells in the escape from host immune system and tumor immunotherapy by PD-L1 blockade. *Proceedings of the National Academy of Sciences of the United States of America*. 99(19):12293-12297. (2002)
120. Topalian SL, Hodi FS, Brahmer JR, et al. Safety, activity, and immune correlates of anti-PD-1 antibody in cancer. *N Engl J Med*. 366(26): 2443–2454 (2012).
121. Hamid et al., Safety and tumor responses with lambrolizumab (anti-PD-1) in melanoma. *N. Engl. J. Med*. 369, 134–144 (2013).
122. Iwai Y, Ishida M, Tanaka Y, Okazaki T, Honjo T, Minato N. Involvement of PD-L1 on tumor cells in the escape from host immune system and tumor immunotherapy by PD-L1 blockade. *Proc Natl Acad Sci U S A*. 99(19):11293–12297 (2002)
123. Sznol M. et al., Survival and longterm follow-up and response in patients (pts) with advanced melanoma (MEL) in a phase I trial of nivolumab (anti-PD-1); BMS-936558: ONO-4538). *J Clin Oncol* 31: abstr. 9006, ASCO meeting abstract, (2013).
124. Robert C, Ribas A, Wolchok JD, Hodi FS, Hamid O, Kefford R, et al. Anti-programmed-death-receptor-1 treatment with pembrolizumab in ipilimumab-refractory advanced melanoma: a randomised dose-comparison cohort of a phase 1 trial. *Lancet*. 384: 1109–1117 (2014).
125. Brahmer JR, Tykodi SS, Chow LQ, Hwu WJ, Topalian SL, Hwu P, et al. Safety and activity of anti-PD-L1 antibody in patients with advanced cancer. *N Engl J Med*. 366:2455-2465 (2012).
126. Hamid O, Sosman JA, Lawrence DP, et al. Clinical activity, safety, and biomarkers of MPDL3280A, an engineered PD-L1 antibody in patients with locally advanced or metastatic melanoma (mM). *J Clin Oncol*. (2013).
127. Wolchok JD, Kluger H, Callahan MK, Postow MA, Rizvi NA, Lesokhin AM, Segal NH, Ariyan CE, Gordon RA, Reed K, Burke

- MM, Caldwell A, Kronenberg SA, Agunwamba BU, Zhang X, Lowy I, et al. Nivolumab plus Ipilimumab in Advanced Melanoma. *The New England journal of medicine*. (2013).
128. Wilhelm, S. M., Carter, C., Tang, L., Wilkie, D., McNabola, A., et al. BAY 43-9006 exhibits broad spectrum oral antitumor activity and targets the RAF/MEK/ERK pathway and receptor tyrosine kinases involved in tumor progression and angiogenesis. *Cancer Res*. 64, 7099–7109 (2004).
129. Eisen T, Ahmad T, Flaherty KT, et al. Sorafenib in advanced melanoma: a phase II randomised discontinuation trial analysis. *Br J Cancer*. 95(5):581–586 (2006).
130. Bollag, G., Hirth, P., Tsai, J., Zhang, J., Ibrahim, P. N., et al. Clinical efficacy of a RAF inhibitor needs broad target blockade in BRAF-mutant melanoma. *Nature*. 467, 596–599 (2010).
131. Tsai J, Lee JT, Wang W, Zhang J, Cho H, Mamo S, Bremer R, Gillette S, Kong J, Haass NK, Sproesser K, Li L, Smalley KS, Fong D, Zhu YL, Marimuthu A, Nguyen H, Lam B, Liu J, Cheung I, Rice J, Suzuki Y, Luu C, Settachatgul C, Shellooe R, Cantwell J, Kim SH, Schlessinger J, Zhang KY, West BL, Powell B, Habets G, Zhang C, Ibrahim PN, Hirth P, Artis DR, Herlyn M and Bollag G: Discovery of a selective inhibitor of oncogenic B-Raf kinase with potent antimelanoma activity. *Proc Natl Acad Sci USA* 105(8): 3041-3046 (2008).
132. Chapman PB, Hauschild A, Robert C, Haanen JB, Ascierto P, Larkin J, Dummer R, Garbe C, Testori A, Maio M, Hogg D, Lorigan P, Lebbe C, Jouary T, Schadendorf D, Ribas A, O'Day SJ, Sosman JA, Kirkwood JM, Eggermont AM, Dreno B, Nolop K, Li J, Nelson B, Hou J, Lee RJ, Flaherty KT, McArthur GA, BRIM-3 Study Group. Improved survival with vemurafenib in melanoma with BRAF V600E mutation. *N Engl J Med*. 364(26): 2507-2516 (2011).
133. Poulikakos PI, Zhang C, Bollaq G, Shokat KM, Rosen N. RAF inhibitors transactivate RAF dimers and ERK signalling in

- cells with wild-type BRAF. *Nature*. 464(7287):427–430 (2010).
134. Sosman JA, Kim KB, Schuchter L, et al. Survival in BRAF V600-mutated advanced melanoma treated with vemurafenib. *N Engl J Med*. 366(8):707–714 (2012).
  135. Hauschild A, Grob JJ, Demidov LV, et al. Dabrafenib in BRAF-mutated metastatic melanoma: a multicentre, open-label, phase 3 randomised controlled trial. *Lancet*. 380(9839):358–365 (2012).
  136. Dummer R, Robert C, Nyakas M, et al. Initial results from a phase I, open-label, dose escalation study of the oral BRAF inhibitor LGX818 in patients with BRAF V600 mutant advanced or metastatic melanoma. *J Clin Oncol*. 31(Suppl 15;abstract 9028) (2013).
  137. Le K, Blomain E, Rodeck U and Aplin AE. Selective RAF inhibitor impairs ERK1/2 phosphorylation and growth in mutant NRAS, vemurafenib-resistant melanoma cells. *Pigment cell & melanoma research*. (2013).
  138. Flaherty, K. T., Puzanov, I., Kim, K. B., Ribas, A., McArthur, G. A., et al. Inhibition of mutated, activated BRAF in metastatic melanoma. *N. Engl. J. Med*. 363, 809–819 (2010).
  139. Whittaker SR, Theurillat JP, Van Allen E, et al. A genome-scale RNA interference screen implicates NF1 loss in resistance to RAF inhibition. *Cancer Discov*. 3: 350–62 (2013).
  140. Van Allen EM, Wagle N, Sucker A, et al. The genetic landscape of clinical resistance to RAF inhibition in metastatic melanoma. *Cancer Discov*. 4: 94–109 (2014).
  141. Shi H, Hugo W, Kong X, et al. Acquired resistance and clonal evolution in melanoma during BRAF inhibitor therapy. *Cancer Discov*. 4: 80–93 (2014).
  142. Chan M, Haydu L, Menzies AM, et al. Clinical characteristics and survival of BRAF-mutant metastatic melanoma patients treated with BRAF inhibitor dabrafenib or vemurafenib

- beyond disease progression. *Proc Am Soc Clin Oncol.* 31 (suppl): abstr 9062 (2013).
143. Azer MWF, Menzies AM, Haydu LE, Kefford RF, Long GV. Patterns of response and progression in patients with BRAF-mutant melanoma metastatic to the brain who were treated with dabrafenib. *Cancer.* 120: 530–36 (2014).
  144. 24. Sullivan RJ, Flaherty KT. Resistance to BRAF-targeted therapy in melanoma. *Eur J Cancer.* 49(6):1297-304 (2013).
  145. Nazarian, R., Shi, H., Wang, Q., Kong, X., Koya, R. C., et al. Melanomas acquire resistance to B-RAF(V600E) inhibition by RTK or N-RAS upregulation. *Nature.* 468, 973–977(2010).
  146. Flaherty KT, Infante JR, Daud A, et al. Combined BRAF and MEK inhibition in melanoma with BRAF V600 mutations. *N Engl J Med.* 367(18):1694-703 (2012).
  147. Muling Mao, Feng Tian, John M. Mariadason, et al. Resistance to BRAF Inhibition in BRAF-Mutant Colon Cancer Can Be Overcome with PI3K Inhibition or Demethylating Agents. *Clin Cancer Res.*19:657-667 (2013).
  148. Das Thakur M, Salangsang F, Landman AS, et al. Modelling vemurafenib resistance in melanoma reveals a strategy to forestall drug resistance. *Nature.* 494(7436):251–255 (2013).
  149. E.M. Wallace, J.P. Lyssikatos, T. Yeh, J.D. Winkler, K. Koch, Progress towards therapeutic small molecule MEK inhibitors for use in cancer therapy. *Curr.Top. Med. Chem.* 5 215–229 (2005).
  150. Neuzillet C, Tijeras-Raballand A, de ML, Cros J, Faivre S and Raymond E: MEK in cancer and cancer therapy. *Pharmacol Ther.* 141(2): 160-171, (2014).
  151. Wright CJ, McCormack PL. Trametinib: first global approval. *Drugs.* 73(11):1245-54 (2013).

152. Flaherty KT, Robert C, Hersey P, et al., for the METRIC Study Group. Improved survival with MEK inhibition in BRAF-mutated melanoma. *N Engl J Med.* 367(2):107-14 (2012).
153. Adjei AA, Cohen RB, Franklin W, et al. Phase I pharmacokinetic and pharmacodynamic study of the oral, small-molecule mitogen-activated protein kinase kinase 1/2 inhibitor AZD6244 (ARRY-142886) in patients with advanced cancers. *J Clin Oncol.* 26(13): 2139–2146 (2008).
154. Ascierto PA, Berking C, Agarwala, et al. Efficacy and safety of the oral MEK162 in patients with locally advanced and unresectable or metastatic cutaneous melanoma harboring BRAFV600 or NRAS mutations. *J Clin Oncol.* 30(Suppl;abstract 8511) (2012).
155. Paraiso KH, Fedorenko IV, Cantini LP, et al. Recovery of phospho-ERK activity allows melanoma cells to escape from BRAF inhibitor therapy. *Br J Cancer.* 102: 1724–30 (2010).
156. Daud A, Weber J, Sosman J, et al. Overall survival update for BR113220 Part C, a Phase II three-arm randomized study of dabrafenib alone (D) vs. a combination of dabrafenib and trametinib (D+T) in pts with BRAF V600 mutation-positive metastatic melanoma. *Society for Melanoma Research International Congress; Philadelphia, PA, USA; (2013).*
157. A. Ribas, et al., Combination of vemurafenib and cobimetinib in patients with advanced BRAF(V600)-mutated melanoma: a phase 1b study. *Lancet Oncol.* 15: 954–965(2014).
158. Kefford R, Miller WH, Tan DS-W, et al. Preliminary results from a phase Ib/II, open-label, dose-escalation study of the oral BRAF inhibitor LGX818 in combination with the oral MEK1/2 inhibitor MEK162 in BRAF V600-dependent advanced solid tumors. *Proc Am Soc Clin Oncol.* 31 (suppl): abstr 9029 (2013).
159. Bozic I, Reiter JG, Allen B, et al. Evolutionary dynamics of cancer in response to targeted combination therapy. *eLife.* 2: e00747 (2013).

160. Carlino MS, Todd JR, Gowrishankar K, et al. Differential sensitivity of melanoma with acquired BRAF inhibitor resistance to MEK and ERK inhibition. *Pigment Cell Melanoma Res.* 26: 992 (2013).
161. Morris EJ, Jha S, Restaino CR, et al. Discovery of a novel ERK inhibitor with activity in models of acquired resistance to BRAF and MEK inhibitors. *Cancer Discov.* 3: 742–50 (2013).
162. Woodman SE, Davies MA. Targeting KIT in melanoma: a paradigm of molecular medicine and targeted therapeutics. *Biochem Pharmacol.* 80(5): 568–574 (2010).
163. Minor DR, Kashani-Sabet M, Garrido M, O'Day SJ, Hamid O, Bastian BC. Sunitinib therapy for melanoma patients with KIT mutations. *Clin Cancer Res.* 18(5): 1457–1463 (2012).
164. Hodi FS, Corless CL, Giobbie-Hurder A, et al. Imatinib for melanomas harboring mutationally activated or amplified KIT arising on mucosal, acral, and chronically sun-damaged skin. *J Clin Oncol.* 31(26): 3182–3190 (2013).
165. Eggermont AM, Robert C. New drugs in melanoma: it's a whole new world. *Eur J Cancer.* 47: 2150-7 (2011).
166. Jakob JA, Bassett RL Jr, Ng CS, et al. NRAS mutation status is an independent prognostic factor in metastatic melanoma. *Cancer.* 118(16): 4014–4023 (2012).
167. Ascierto PA, Schadendorf D, Berking C, Agarwala SS, van Herpen CM, Queirolo P, Blank CU, Hauschild A, Beck JT, St-Pierre A, Niazi F, Wandel S, Peters M, Zubel A and Dummer R:MEK162 for patients with advanced melanoma harbouring NRAS or Val600 BRAF mutations: a non-randomised, open-label phase II study. *Lancet Oncol* 14(3): 249-256, (2013).
168. Stahl JM, Sharma A, Cheung M, Zimmerman M, Cheng JQ, Bosenberg MW, Kester M, Sandirasegarane L and Robertson GP: Deregulated AKT3 activity promotes development of malignant melanoma. *Cancer Res* 64(19): 7002-7010, (2004).

169. Zhou XP, Gimm O, Hampel H, Niemann T, Walker MJ and Eng C: Epigenetic PTEN silencing in malignant melanomas without PTEN mutation. *Am J Pathol* 157(4): 1123-1128, (2000).
170. P. Liu, H. Cheng, T.M. Roberts, J.J. Zhao, Targeting the phosphoinositide 3-kinase pathway in cancer. *Nat. Rev. Drug Discov.* 8: 627–644(2009).
171. B. Markman, R. Dienstmann, J. Taberero, Targeting the PI3K/Akt/mTOR pathway–beyond rapalogs. *Oncotarget* 1: 530–543 (2010).
172. E.K. Rowinsky, Targeting the molecular target of rapamycin (mTOR). *Curr. Opin. Oncol.* 16: 564–575 (2004).
173. K. Margolin, et al., CCI-779 in metastatic melanoma: a phase II trial of the California Cancer Consortium. *Cancer.* 104: 1045–1048 (2005).
174. K.A. Margolin, et al., Randomized phase II trial of sorafenib with temsirolimus or tipifarnib in untreated metastatic melanoma (S0438). *Clin. Cancer Res. Off. J. Am. Assoc. Cancer Res.* 18: 1129–1137.118–120 (2012).
175. A. Carracedo, et al., Inhibition of mTORC1 leads to MAPK pathway activation through a PI3K-dependent feedback loop in human cancer. *J. Clin. Invest.* 118: 3065–3074 (2008).
176. Curtin JA, Fridlyand J, Kageshita T, et al. Distinct sets of genetic alterations in melanoma. *N Engl J Med.* 353: 2135–47 (2005).
177. Filmus J, Robles AI, Shi W, Wong MJ, Colombo LL, Conti CJ. Induction of cyclin D1 overexpression by activated ras. *Oncogene.* 9: 3627–33 (1994).
178. Prickett TD, Agrawal NS, Wei X, Yates KE, Lin JC, Wunderlich JR, Cronin JC, Cruz P, Rosenberg SA and Samuels Y: Analysis of the tyrosine kinome in melanoma reveals recurrent mutations in ERBB4. *Nat Genet.* 41(10): 1127-1132 (2009).
179. Wang R. Toxic gas livesafer. *Sci Am* 302: 66–71 (2010).

180. Wang CL, Maratukulam PD, Lum AM, Clark DS, Keasling JD. Metabolic engineering of an aerobic sulfate reduction pathway and its application to precipitation of cadmium on the cell surface. *Appl Environ Microbiol.* 66: 4497–4502 (2000).
181. Aiking H, Kok K, Van Heerikhuizen H, Vantriet J. Adaptation to cadmium by *Klebsiella aerogenes* growing in continuous culture proceeds mainly via formation of cadmium sulfide. *Appl Environ Microbiol.* 44: 938–944 (1982).
182. Leustek T, Martin MN, Bick J, Davies JP. Pathways and regulation of sulfur metabolism revealed through molecular genetic studies. *Annu Rev Plant Physiol Plant Mol Biol.* 51: 141–166 (2000).
183. Ellis, A. J.; Giggenbach, W. Hydrogen sulfide ionization and sulfur hydrolysis in high temperature solution. *Geochim. Cosmochim. Acta.* 35 (3): 247–260. (1971)
184. Giggenbach, W. Optical spectra of highly alkaline sulfide solutions and the second dissociation constant of hydrogen sulfide. *Inorg. Chem.* 10 (7): 1333–1338 (1971).
185. Myers, R. J. The new low value for the second dissociation constant for H<sub>2</sub>S: its history, its best value, and its impact on the teaching of sulfide equilibria. *J. Chem. Educ.* 63: 687–690 (1986).
186. Breyse PA. Hydrogen sulfide fatality in a poultry feather fertilizer plant. *Am Ind Hyg Assoc J.* 22: 220–222 (1961).
187. Snyder JW, Safir EF, Summerville GP, Middleberg RA. Occupational fatality and persistent neurological sequelae after mass exposure to hydrogen sulfide. *Am J Emerg Med* 13: 199–203 (1995).
188. Zenz C, Dickerson OB, Horvath EP. *Occupational Medicine* (3rd ed.). St. Louis, MO: Mosby, p. 886.) (1994).
189. Evans, C. The toxicity of hydrogen sulphide and other sulphides. *Q. J. Exp. Physiol.* 52:231-48 (1967).

190. Reiffenstein R. J., Hulbert W. C., Roth S.H. Toxicology of Hydrogen Sulfide. *Annu. Rev. Pharmacol. Toxicol.* 32: 109-134 (1992).
191. Stipanuk MH, Ueki I. Dealing with methionine/homocysteine sulfur: cysteine metabolism to taurine and inorganic sulfur. *J. Inherit. Metab. Dis.* (2010).
192. Kamoun P. Endogenous production of hydrogen sulfide in mammals. *Amino Acids.* 26:243–254 (2004).
193. K. Abe, H. Kimura, The possible role of hydrogen sulfide as an endogenous neuromodulator. *J. Neurosci.* 16: 1066–1071(1996).
194. Zhao, W.; Zhang, J.; Lu, Y.; Wang, R. The vasorelaxant effect of H<sub>2</sub>S as a novel endogenous gaseous K<sub>ATP</sub> channel opener. *EMBO J.* 20: 6008–6016 (2001).
195. Yang G, Sun X, Wang R. Hydrogen sulfide-induced apoptosis of human aorta smooth muscle cells via the activation of mitogenactivated protein kinases and caspase-3. *FASEB J.* 18: 1782–1784 (2004).
196. Nagahara N, Ito T, Kitamura H, Nishino T. Tissue and subcellular distribution of mercaptopyruvate sulfurtransferase in the rat: confocal laser fluorescence and immunoelectron microscopic studies combined with biochemical analysis. *Histochem Cell Biol.* 110: 243–250 (1998).
197. Schicho R, Krueger D, Zellef F, et al. Hydrogen sulfide is a novel prosecretory neuromodulator in the guinea-pig and human colon. *Gastroenterology.* 131:1542–1552 (2006).
198. Chen, X., Jhee, K. H. & Kruger, W. D. Production of the neuromodulator H<sub>2</sub>S by cystathionine β-synthase via the condensation of cysteine and homocysteine. *J. Biol. Chem.* 279: 52082–52086 (2004).
199. Beard, R. S. Jr & Bearden, S. E. Vascular complications of cystathionine β-synthase deficiency: future directions for

- homocysteine-to-hydrogen sulphide research. *Am. J. Physiol. Heart Circ. Physiol.* 300: H13–H26 (2011).
200. Sen, U., Mishra, P. K., Tyagi, N. & Tyagi, S. C. Homocysteine to hydrogen sulfide or hypertension. *Cell Biochem. Biophys.* 57: 49–58 (2010).
201. Yamanishi M, Kabil O, Sen S, Banerjee R. Structural insights into pathogenic mutations in heme-dependent cystathionine-beta-synthase. *J Inorg Biochem.* 100: 1988–1995 (2006).
202. Kery, V.; Bukovska, G.; Kraus, J. P. Transsulfuration depends on heme in addition to pyridoxal 50-phosphate. Cystathionine beta-synthase is a heme protein. *J. Biol. Chem.* 269: 25283–25288 (1994).
203. Puranik, M. et al. Dynamics of carbon monoxide binding to cystathionine  $\beta$ -synthase. *J. Biol. Chem.* 281: 13433–13438 (2006).
204. Singh, S., Padovani, D., Leslie, R. A., Chiku, T. & Banerjee, R. Relative contributions of cystathionine  $\beta$ -synthase and  $\gamma$ -cystathionase to H<sub>2</sub>S biogenesis via alternative transsulfuration reactions. *J. Biol. Chem.* 284: 22457–22466 (2009).
205. Stipanuk, M. H. & Beck, P. W. Characterization of the enzymic capacity for cysteine desulphhydration in liver and kidney of the rat. *Biochem. J.* 206: 267–277 (1982).
206. Yang, G. et al. H<sub>2</sub>S as a physiologic vasorelaxant: hypertension in mice with deletion of cystathionine  $\gamma$ -lyase. *Science.* 322: 587–590 (2008).
207. Renga B. Hydrogen sulfide generation in mammals: the molecular biology of cystathionine- $\beta$ -synthase (CBS) and cystathionine- $\gamma$ -lyase (CSE). *Inflamm Allergy Drug Targets.* 10: 85–91 (2011).
208. Levonen AL, Lapatto R, Saksela M, Raivio KO. Human cystathionine- $\gamma$ -lyase: developmental and in vitro expression of two isoforms. *Biochem J.* 347: 291–295 (2000).

209. Ishii. I. et al. Murine cystathionine  $\gamma$ -lyase: complete cDNA and genomic sequences, promoter activity, tissue distribution and developmental expression. *Biochem. J.* 381: 113–123 (2004).
210. Sun, Q.; Collins, R.; Huang, S.; Holmberg-Schiavone, L.; Anand, G. S.; Tan, C. H.; van-den-Berg, S.; Deng, L. W.; Moore, P. K.; Karlberg, T.; Sivaraman, J. Structural basis for the inhibition mechanism of human cystathionine gamma-lyase, an enzyme responsible for the production of H<sub>2</sub>S. *J. Biol. Chem.* 284 (5): 3076–3085 (2009).
211. N. Shibuya, M. Tanaka, M. Yoshida, Y. Ogasawara, T. Togawa, K. Ishii, H. Kimura, 3-Mercaptopyruvate sulfurtransferase produces hydrogen sulphide and bound sulfane sulfur in the brain. *Antioxid. Redox Signal.* 11: 703–714 (2009).
212. D.G. Searcy, S.H. Lee, Sulfur reduction by human erythrocytes. *J. Exp. Zool.* 282: 310–322 (1998).
213. Beerens H, Remond C. Sulfate-reducing anaerobic bacteria in human feces. [Am J Clin Nutr.](#) 30(11): 1770-6 (1977).
214. Belardinelli, M. C.; Chabli, A.; Chadeaux-Vekemans, B.; Kamoun, P. Urinary sulfur compounds in Down syndrome. *Clin. Chem.* 47: 1500–1501 (2001).
215. Lagoutte E, Mimoun S, Andriamihaja M, Chaumontet C, Blachier F, Bouillaud F. Oxidation of hydrogen sulfide remains a priority in mammalian cells and causes reverse electron transfer in colonocytes. *Biochim Biophys Acta.* 1797: 1500–11 (2010).
216. Levitt, M. D.; Furne, J.; Springfield, J.; Suarez, F.; DeMaster, E. Detoxification of hydrogen sulfide and methanethiol in the cecal mucosa. *J. Clin. Invest.* 104: 1107–1114 (1999).
217. Picton, R.; Eggo, M. C.; Merrill, G. A.; Langman, M. J.; Singh, S. Mucosal protection against sulfide: importance of the enzyme rhodanese. *Gut.* 50: 201–205 (2002).
218. Kurzban, G. P.; Chu, L.; Ebersole, J. L.; Holt, S. C. Sulfhemoglobin formation in human erythrocytes by

- cystalytin, an L-cysteine desulphydrase from *Treponema denticola*. *Oral Microbiol. Immunol.* 14: 153–164 (1999).
219. Yang G, Cao K, Wang R. Cystathionine- $\gamma$ -lyase overexpression inhibits cell proliferation via a H<sub>2</sub>S-dependent modulation of ERK1/2 phosphorylation and p21Cip/WAK-1. *J Biol Chem.* 279: 49199–49205 (2004).
220. Smith RP, Abbanat RA. Protective effect of oxidized glutathione in acute sulfide poisoning. *Toxicol Appl Pharmacol.* 9: 209–217 (1966).
221. Ogasawara Y, Isoda S, Tanabe S. Tissue and subcellular distribution of bound and acid-labile sulfur, the enzymic capacity for sulfide production in the rat. *Biol Pharm Bull.* 17: 1535–1542 (1994).
222. Lowicka E, Beltowski J. Hydrogen sulfide (H<sub>2</sub>S): the third gas of interest for pharmacologists. *Pharmacol Rep.* 59: 4–24 (2007).
223. Czyzewski, B. K. & Wang, D. N. Identification and characterization of a bacterial hydrosulphide ion channel. *Nature.* 483: 494–497 (2012).
224. Bindu D. Paul and Solomon H. Snyder. Signalling through protein sulfhydration and beyond. *Nat Rev Mol Cell Biol.* 13(8): 499-507 (2012).
225. Mustafa AK, Gadalla MM, Sen N, Kim S, Mu W, Gazi SK, Barrow RK, Yang G, Wang R, Solomon H. H<sub>2</sub>S signals through protein S-sulfhydration. *Sci Signal.* 2: ra72 (2009).
226. Telezhkin V, Brazier SP, Cayzac S, Müller CT, Riccardi D, Kemp PJ. Hydrogen sulfide inhibits human BKCa channels. *Adv. Exp. Med. Biol.* 648: 65–72 (2009).
227. Sitdikova GF, Weiger TM, Hermann A. Hydrogen sulfide increases calcium-activated potassium (BK) channel activity of rat pituitary tumor cells. *Pflug. Arch.* 459: 389–97 (2010).
228. Sun YG, Cao YX, Wang WW, Ma SF, Yao T, Zhu YC. Hydrogen sulphide is an inhibitor of L-type calcium channels and

- mechanical contraction in rat cardiomyocytes. *Cardiovasc. Res.* 79: 632–41(2008).
229. Matsunami M, Tarui T, Mitani K, Nagasawa K, Fukushima O, et al. Luminal hydrogen sulfide plays a pronociceptive role in mouse colon. *Gut.* 58: 751–61 (2009).
230. Malekova L, Krizanova O, Ondrias K. H<sub>2</sub>S and HS<sup>-</sup> donor NaHS inhibits intracellular chloride channels. *Gen. Physiol. Biophys.* 28: 190–94 (2009).
231. Streng T, Axelsson HE, Hedlund P, Andersson DA, Jordt SE, et al. Distribution and function of the hydrogen sulfide-sensitive TRPA1 ion channel in rat urinary bladder. *Eur. Urol.* 53: 391–99 (2008).
232. Trevisani M, Patacchini R, Nicoletti P, Gatti R, Gazzieri D, et al. Hydrogen sulfide causes vanilloid receptor 1-mediated neurogenic inflammation in the airways. *Br. J. Pharmacol.* 145:1123–31 (2005).
233. OhGS, Pae HO, Lee BS, Kim BN, Kim JM, et al. Hydrogen sulfide inhibits nitric oxide production and nuclear factor- $\kappa$ B via heme oxygenase-1 expression in RAW264.7 macrophages stimulated with lipopolysaccharide. *Free Radic. Biol. Med.* 41: 106–19 (2006).
234. Li L, Rossoni G, Sparatore A, Lee LC, Del Soldato P, Moore PK. Anti-inflammatory and gastrointestinal effects of a novel diclofenac derivative. *Free Radic. Biol. Med.* 42: 706–19 (2007).
235. Li L, Whiteman M, Guan YY, Neo KL, Cheng Y, et al. Characterization of a novel, water-soluble hydrogen sulfide-releasing molecule (GYY4137): new insights into the biology of hydrogen sulfide. *Circulation.* 117: 2351–60 (2008).
236. Benavides GA, Squadrito GL, Mills RW, Patel HD, Isbell TS, et al. Hydrogen sulfide mediates the vasoactivity of garlic. *Proc. Natl. Acad. Sci. USA* 104: 17977–82 (2007).
237. Zhi L, Ang AD, Zhang H, Moore PK, Bhatia M. Hydrogen sulfide induces the synthesis of proinflammatory cytokines

- in human monocyte cell line U937 via the ERK-NF- $\kappa$ B pathway. *J. Leukoc. Biol.* 81: 1322–32 (2007).
238. Sen, N., Paul, B.D., Gadalla, M.M., Mustafa, A.K., Sen, T., Xu, R., Kim, S., and Snyder, S.H. Hydrogen sulfide-linked sulphydration of NF- $\kappa$ B mediates its anti-apoptotic actions. *Mol. Cell.* 45: 13–24 (2012).
239. Li L, Salto-Tellez M, Tan C-H, Whiteman M, Moore PK. GYY4137, a novel hydrogen sulfide-releasing molecule, protects against endotoxic shock in the rat. *Free Radic. Biol. Med.* 47: 103–13 (2009).
240. Calvert JW, Jha S, Gundewar S, Elrod JW, Ramachandran A, et al. Hydrogen sulfide mediates cardioprotection through Nrf2 signaling. *Circ. Res.* 105: 365–74 (2009).
241. Budde MW, Roth MB. Hydrogen sulfide increases hypoxia-inducible factor-1 activity independently of von Hippel-Lindau tumor suppressor-1 in *C. elegans*. *Mol. Biol. Cell.* 21: 212–17 (2010).
242. Yang G, Sun X, Wang R. Hydrogen sulfide-induced apoptosis of human aorta smooth muscle cells via the activation of mitogenactivated protein kinases and caspase-3. *FASEB J.* 18: 1782–1784 (2004).
243. Yang G, Yang W, Wu L, Wang R. H<sub>2</sub>S, endoplasmic reticulum stress and apoptosis of insulin-secreting beta cells. *J Biol Chem.* 282: 16567–16576 (2007).
244. Hu LF, Lu M, Wu ZY, Wong PT, Bian JS. Hydrogen sulfide inhibits rotenone-induced apoptosis via preservation of mitochondrial function. *Mol Pharmacol.* 75: 27–34 (2009).
245. Jeong SO, Pae HO, Oh GS, Jeong GS, Lee BS, et al. Hydrogen sulfide potentiates interleukin-1 $\beta$ -induced nitric oxide production via enhancement of extracellular signal-regulated kinase activation in rat vascular smooth muscle cells. *Biochem. Biophys. Res. Commun.* 345: 938–44 (2006).

246. Cai WJ, Wang MJ, Ju LH, Wang C, Zhu YC. Hydrogen sulfide induces human colon cancer cell proliferation: role of Akt, ERK and p21. *Cell Biol. Int.* 34(6): 565–72 (2010).
247. Papapetropoulos A, Pyriochou A, Altaany Z, Yang G, Maraziotia A, Zhouc Z, Jeschke MG, Branski LK, Herndon DN, Wang R, Szabo C. Hydrogen sulfide is an endogenous stimulator of angiogenesis. *Proc Natl Acad Sci USA.* 106: 21972–21977 (2009).
248. Deplancke B, Gaskins HR. Hydrogen sulfide induces serum-independent cell cycle entry in nontransformed rat intestinal epithelial cells. *FASEB J.* 17: 1310–1312 (2003).
249. Rinaldi L, Gobbi G, Pambianco M, Micheloni C, Mirandola P, Vitale M. Hydrogen sulfide prevents apoptosis of human PMN via inhibition of p38 and caspase 3. *Lab Invest.* 86: 391–397 (2006).
250. Hu LF, Wong PT, Moore PK, Bian JS. Hydrogen sulfide attenuates lipopolysaccharide-induced inflammation by inhibition of p38 mitogen-activated protein kinase in microglia. *J Neurochem.* 100: 1121–1128 (2007).
251. Yong QC, Lee SW, Foo CS, Neo KL, Chen X, Bian JS. 2008. Endogenous hydrogen sulphide mediates the cardioprotection induced by ischemic postconditioning. *Am. J. Physiol. Heart Circ. Physiol.* 295: H1330–40 (2008).
252. Takeuchi H, Setoguchi T, Machigashira M, Kanbara K, Izumi Y. Hydrogen sulphide inhibits cell proliferation and induces cell cycle arrest via an elevated p21Cip1 level in Ca9–22 cells. *J Periodont Res.* 43: 90–95 (2008).
253. Yang G, Wu L, Bryan S, Khaper N, Mani S, Wang R. Cystathionine gamma-lyase deficiency and overproliferation of smooth muscle cells. *Cardiovasc Res.* 86: 487–495 (2010).
254. Deplancke B, Gaskins HR. Hydrogen sulfide induces serum-independent cell cycle entry in nontransformed rat intestinal epithelial cells. *FASEB J.* 17: 1310–1312 (2003).

255. Kimura, Y. & Kimura, H. Hydrogen sulfide protects neurons from oxidative stress. *FASEB J.* 18: 1165–1167 (2004).
256. Shao JL, Wan XH, Chen Y, Bi C, Chen HM, Zhong Y, Heng XH, Qian JQ. H<sub>2</sub>S protects hippocampal neurons from anoxia-reoxygenation through cAMP-mediated PI3K/Akt/p70S6K cell-survival signaling pathways. *J Mol Neurosci.* 43: 453–460 (2011).
257. Lu M, Liu YH, Goh HS, Wang JJ, Yong QC, Wang R, Bian JS. Hydrogen sulfide inhibits plasma renin activity. *J Am Soc Nephrol.* 21: 993–1002 (2010).
258. Bucci M, Papapetropoulos A, Vellecco V, Zhou Z, Pyriochou A, Roussos C, Roviezzo F, Brancaleone V, Cirino G. Hydrogen sulfide is an endogenous inhibitor of phosphodiesterase activity. *Arterioscler Thromb Vasc Biol.* 30: 1998–2004 (2010).
259. Whiteman M, Halliwell B. Protection against peroxynitrite-dependent tyrosine nitration and  $\alpha$ 1-antiproteinase inactivation by ascorbic acid: a comparison with other biological antioxidants. *Free Radic Res.* 25: 275–283 (1996).
260. Wang R. Is H<sub>2</sub>S a stinky remedy for atherosclerosis? *Arterioscler Thromb Vasc Biol.* 29: 156–157 (2009).
261. Yan SK, Chang T, Wang H, Wu L, Wang R, Meng QH. Effects of hydrogen sulfide on homocysteine-induced oxidative stress in vascular smooth muscle cells. *Biochem Biophys Res Commun.* 351: 485–491 (2006).
262. Jeney V, Komódi E, Nagy E, Zarjou A, Vercellotti GM, Eaton JW, Balla G, Balla J. Suppression of hemin-mediated oxidation of low-density lipoprotein and subsequent endothelial reactions by hydrogen sulfide (H<sub>2</sub>S). *Free Radic Biol Med.* 46: 616–623 (2009).
263. Pietri, R., Roman-Morales, E. & Lopez-Garriga, J. Hydrogen sulfide and hemeproteins: knowledge and mysteries. *Antioxid. Redox Signal.* 15: 393–404 (2011).

264. Mancardi D, Penna C, Merlino A, et al. Physiological and pharmacological features of the novel gasotransmitter hydrogen sulfide. *Biochem Biophys Acta*. 864–872 (2009).
265. Whiteman M, Armstrong JS, Chu SH, et al. The novel neuromodulator hydrogen sulfide: and endogenous peroxy-nitrite ‘scavenger’? *J Neurochem*. 90: 765–768 (2004).
266. Whiteman M, Cheung NS, Zhu YZ, et al. Hydrogen sulfide: a novel inhibitor of hypochlorous acid-mediated oxidative damage in the brain? *Biochem Biophys Res Commun*. 326: 794–798 (2005).
267. Sivarajah A, Collino M, Yasin M, Benetti E, Gallicchio M, Mazzon E, Cuzzocrea S, Fantozzi R, Thiernemann C. Antiapoptotic and anti-inflammatory effects of hydrogen sulfide in a rat model of regional myocardial I/R. *Shock*. 31: 267–274 (2009).
268. Geng B, Chang L, Pan C, Qi Y, Zhao J, Pang Y, Du J, Tang C. Endogenous hydrogen sulfide regulation of myocardial injury induced by isoproterenol. *Biochem Biophys Res Commun*. 318: 756–763 (2004).
269. Cheng Y, Ndisang JF, Tang G, Cao K, Wang R. Hydrogen sulfide-induced relaxation of resistance mesenteric artery beds of rats. *Am J Physiol Heart Circ Physiol*. 287: H2316–H2323 (2004).
270. Zanardo RC, Brancaleone V, Distrutti E, Fiorucci S, Cirino G, Wallace JL. Hydrogen sulfide is an endogenous modulator of leukocyte-mediated inflammation. *FASEB J*. 20: 2118–2120 (2006).
271. Wu SY, Pan CS, Geng B, Zhao J, Yu F, Pang YZ, Tang CS, Qi YF. Hydrogen sulphide ameliorates vascular calcification induced by vitamin D3 plus nicotine in rats. *Acta Pharmacol Sin*. 27: 299–306 (2006).
272. Ekundi-Valentim E, Santos KT, Camargo EA, Denadai-Souza A, Teixeira SA, Zanoni CI, Grant AD, Wallace J, Muscará MN,

- Costa SK. Differing effects of exogenous and endogenous hydrogen sulphide in carrageenan-induced knee joint synovitis in the rat. *Br J Pharmacol.* 159: 1463–1474 (2010).
273. Wang Y, Zhao X, Jin H, Wei H, Li W, Bu D. Role of hydrogen sulfide in the development of atherosclerotic lesions in apolipoprotein E knockout mice. *Arterioscler Thromb Vasc Biol.* 29: 173–179 (2009).
274. Elkayam A, Mirelman D, Peleg E, Wilchek M, Miron T, Rabinkov A, Sadetzki S, Rosenthal T. The effect of allicin and enalapril in fructose induced hyper-insulinemic hyper-lipidemic hypertensive rats. *J Hypertens.* 14: 377–381 (2001).
275. L.W. DeBoer, J.D. Folts, Garlic extract prevents acute platelet thrombus formation in stenosed canine coronary arteries. *Am. Heart J.* 117: 973–975 (1989).
276. Zagli G, Patacchini R, Trevisani M, Abbate R, Cinotti S, et al. Hydrogen sulfide inhibits human platelet aggregation. *Eur. J. Pharmacol.* 559:65–68 (2007).
277. H. Kiesewetter, F. Jung, G. Pindur, E.M. Jung, C. Mrowietz, E. Wenzel, Effect of garlic on thrombocyte aggregation, microcirculation, and other risk factors. *Int. J. Clin. Pharmacol. Ther. Toxicol.* 29: 151–155 (1991).
278. Coletta C., Papapetropoulos A., Erdelyi K., Olah G., Modis K., Panopoulos P., Asimakopoulou A., Gero D., Sharina I., Martin E., Szabo C. Hydrogen sulfide and nitric oxide are mutually dependent in the regulation of angiogenesis and endothelium-dependent vasorelaxation. *Proc. Natl. Acad. Sci. USA* 109: 9161–9166 (2012).
279. Kimura, H. Hydrogen sulfide induces cyclic AMP and modulate the NMDA receptor. *Biochem. Biophys. Res. Commun.* 267 (1): 129–133 (2000).
280. Garcia-Bereguian MA, Samhan-Arias AK, Martin-Romero FJ, Gutierrez-Merino C. Hydrogen sulfide raises cytosolic

- calcium in neurons through activation of L-type Ca<sup>2+</sup> channels. *Antioxid Redox Signal*. 10: 31–42 (2008).
281. Cheung NS, Peng ZF, Chen MF, Moore PK, Whiteman M. Hydrogen sulfide induced neuronal death occurs via glutamate receptor and is associated with calpain activation and lysosomal rupture in mouse primary cortical neurons. *Neuropharmacology*. 53: 505–514 (2007).
282. Qu, K.; Chen, C. P.; Halliwell, B.; Moore, P. K.; Wong, P. T. Hydrogen sulfide is a mediator of cerebral ischemic damage. *Stroke*. 37: 889–893 (2006).
283. Beyer, K.; Lao, J. I.; Carrato, C.; Rodriguez-Vila, A.; Latorre, P.; Matar o, M.; Llopis, M. A.; Mate, J. L.; Ariza, A. Cystathionine beta synthase as a risk factor for Alzheimer disease. *Curr. Alzheimer Res*. 1: 127–133 (2004).
284. Qu, K.; Lee, S. W.; Bian, J. S.; Low, C. M.; Wong, P. T. H. Hydrogen sulfide: neurochemistry and neurobiology. *Neurochem. Int*. 52: 155–165 (2008).
285. Han Y, Qin J, Chang X, Yang Z, Tang X, Du J. Hydrogen sulfide may improve the hippocampal damage induced by recurrent febrile seizures in rats. *Biochem Biophys Res Commun*. 327: 431–436 (2005).
286. Kawabata A, Ishiki T, Nagasawa K, Yoshida S, Maeda Y, Takahashi T, Sekiguchi F, Wada T, Ichida S, Nishikawa H. Hydrogen sulfide as a novel nociceptive messenger. *Pain*. 132: 74–81 (2007).
287. Nagai Y, Tsugane M, Oka J, Kimura H. Hydrogen sulfide induces calcium waves in astrocytes. *FASEB J*. 18: 557–559 (2004).
288. Warenycia MW, Smith KA, Blashko CS, Kombian SB, Reiffenstein RJ. Monoamine oxidase inhibition as a sequel of hydrogen sulfide intoxication: increases in brain catecholamine and 5-hydroxytryptamine levels. *Arch Toxicol*. 63: 131–136 (1989).

289. Valitutti S, Castellino F, Musiani P. Effect of sulfurous (thermal) water on T lymphocyte proliferative response. *Ann Allergy*. 65: 463–468 (1990).
290. Mariggio MA, Minunno V, Riccardi S, Santacroce R, De Rinaldis P, Fumarulo R. Sulfide enhancement of PMN apoptosis. *Immunopharmacol Immunotoxicol*. 20: 399–408 (1988).
291. N. Dufton, J. Natividad, E.F. Verdu, J.L.Wallace, Hydrogen sulfide and resolution of acute inflammation: a comparative study utilizing a novel fluorescent probe. *Scientific Rep*. 2: 499 (2012).
292. Oh GS, Pae HO, Lee BS, Kim BN, Kim JM, Kim HR, Jeon SB, Jeon WK, Chae HJ, Chung HT. Hydrogen sulfide inhibits nitric oxide production and nuclear factor-kappaB via heme oxygenase-1 expression in RAW2647 macrophages stimulated with lipopolysaccharide. *Free Radical Biol Med*. 41: 106–119 (2006).
293. Sen N., Paul B.D., Gadalla M.M., Mustafa A.K., Sen T., Xu R., et al. Hydrogen sulfide-linked sulfhydration of NFkB mediates its antiapoptotic actions. *Mol. Cell*. 45: 13–24 (2012).
294. Esechie A, Kiss L, Olah G, Horvath EM, Hawkins H, Szabó C, Traber DL. Protective effect of hydrogen sulfide in a murine model of acute lung injury induced by combined burn and smoke inhalation. *Clin Sci*. 115: 91–97 (2008).
295. Wallace, J.L., Caliendo, G., Santagada, V., Cirino, G., Fiorucci, S. Gastrointestinal safety and anti-inflammatory effects of a hydrogen sulfide-releasing diclofenac derivative in the rat. *Gastroenterology*. 132: 261–271 (2007).
296. S.A. Mard, H. Askari, N. Neisi, A. Veisi, Antisecretory effect of hydrogen sulphide on gastric acid secretion and the involvement of nitric oxide. *BioMed Res. Int*. 2014: 480921 (2014).
297. J.L. Wallace, G. Cirino, V. Santagada, G. Caliendo, Hydrogen sulfide derivatives of nonsteroidal anti-inflammatory drugs.

- United States Patent Application* No.WO/2008/009127 (2008).
298. Bhatia M, Sidhapuriwala J, Moochhala SM, Moore PK. Hydrogen sulfide is a mediator of carrageenan-induced hindpaw oedema in the rat. *Br J Pharmacol.* 145: 141–144 (2005).
  299. Bhatia M, Wong FL, Fu D, Lau HY, Moochhala SM, Moore PK. Role of hydrogen sulphide in acute pancreatitis and associated lung injury. *FASEB J.* 19: 623–625 (2005).
  300. Li L, Bhatia M, Zhu YZ, Zhu YC, Ramnath RD, Wang ZJ, Anuar FB, Whiteman M, Salto-Tellez M, Moore PK. Hydrogen sulfide is a novel mediator of lipopolysaccharide-induced inflammation in the mouse. *FASEB J.* 19: 1196–1198 (2005).
  301. Zhang H, Zhi L, Moore PK, Bhatia M. Role of hydrogen sulfide in cecal ligation and puncture-induced sepsis in the mouse. *Am J Physiol Lung Cell Mol Physiol.* 290: L1193–L1201 (2006).
  302. Gardiner SM, Kemp PA, March JE, Bennett T. Regional haemodynamic responses to infusion of lipopolysaccharide in conscious rats: effects of pre- or post-treatment with glibenclamide. *Br J Pharmacol.* 128: 1772–1778 (1999).
  303. Zhang H, Bhatia M. Hydrogen sulfide: a novel mediator of leukocyte activation. *Immunopharmacol Immunotoxicol.* 1: 1–15 (2008).
  304. Whiteman M, Li L, Rose P, Tan CH, Parkinson DB, Moore PK. The effect of hydrogen sulfide donors on lipopolysaccharide-induced formation of inflammatory mediators in macrophages. *Antioxid Redox Signal.* 12: 1147–1154 (2010).
  305. Baskar, R., Sparatore, A., Del Soldato, P., Moore, P.K. Effect of S-diclofenac, a novel hydrogen sulfide releasing derivative inhibits rat vascular smooth muscle cell proliferation. *Eur. J. Pharmacol.* 594: 1–8 (2008).

306. Baskar, R., Li, L., Moore, P.K. Hydrogen sulfide-induces DNA damage and changes in apoptotic gene expression in human lung fibroblast cells. *FASEB J.* 21: 247–255 (2007).
307. Baskar, R., Moore, P.K. Nuclear accumulation and up regulation of p53 and its associated proteins after H<sub>2</sub>S treatment in human lung fibroblasts. *J. Cell. Mol. Med.* 12: 2297–2300 (2008).
308. Wang R. Signaling pathways for the vascular effects of hydrogen sulfide. *Curr Opin Nephrol Hypertens.* 20: 107–112 (2011).
309. Zhang LM, Jiang CX, Liu DW. Hydrogen sulfide attenuates neuronal injury induced by vascular dementia via inhibiting apoptosis in rats. *Neurochem Res.* 34: 1984–1992 (2009).
310. Yin WL, He JQ, Hu B, Jiang ZS, Tang XQ. Hydrogen sulfide inhibits MPP(+)-induced apoptosis in PC12 cells. *Life Sci.* 85: 269–275 (2009).
311. Cao, Q., Zhang, L., Yang, G., Xu, C., Wang, R. Butyrate-stimulated H<sub>2</sub>S production in colon cancer cells. *Antioxi. Redox. Signal.* 12: 1101–1109 (2010).
312. Cai WJ, Wang MJ, Ju LH, Wang C, Zhu YC. Hydrogen sulfide induces human colon cancer cell proliferation: role of Akt, ERK and p21. *Cell Biol Int.* 34: 565–572 (2010).
313. Gemici B., Elsheikh W., Feitosa K.B., Costa S.K.P., Muscara M.N., Wallace J.L. H<sub>2</sub>S-releasing drugs: Anti-inflammatory, cytoprotective and chemopreventative potential. *Nitric Oxide.* 14: S1089-8603 (2014).
314. Bhattacharyya, S., Saha, S., Giri, K., Lanza, I. R., Nair, K. S., Jennings, N. B., Rodriguez-Aguayo, C., Lopez-Berestein, G., Basal, E., Weaver, A. L. et al. Cystathionine Beta-Synthase (CBS) Contributes to Advanced Ovarian Cancer Progression and Drug Resistance. *PLoS One.* 8, e79167 (2013).
315. Szabo, C., Coletta, C., Chao, C., Modis, K., Szczesny, B., Papapetropoulos, A. and Hellmich, M. R. Tumor-derived

- hydrogen sulfide, produced by cystathionine-beta-synthase, stimulates bioenergetics, cell proliferation, and angiogenesis in colon cancer. *Proc Natl Acad Sci U S A* 110: 12474-12479 (2013).
316. Sanokawa-Akakura R, Ostrakhovitch EA, Akakura S, Goodwin S, Tabibzadeh S. . A H<sub>2</sub>S-Nampt dependent energetic circuit is critical to survival and cytoprotection from damage in cancer cells. *PLoS One*. 9(9):e108537 (2014).
317. Distrutti E, Sediari L, Mencarelli A, Renga B, Orlandi S, et al. Evidence that hydrogen sulfide exerts antinociceptive effects in the gastrointestinal tract by activating KATP channels. *J. Pharmacol. Exp. Ther.* 316: 325–35 (2006).
318. Monjok EM, Kulkarni KH, Kouamou G, McKoy M, Opere CA, et al. Inhibitory action of hydrogen sulfide on muscarinic receptor-induced contraction of isolated porcine irides. *Exp. Eye Res.* 87: 612–16 (2008).
319. Kubo S, Doe I, Kurokawa Y, Kawabata A. Hydrogen sulfide causes relaxation in mouse bronchial smooth muscle. *J. Pharmacol. Sci.* 104: 392–96 (2007).
320. Yang, W., Yang, G., Jia, X., Wu, L. & Wang, R. Activation of KATP channels by H<sub>2</sub>S in rat insulin-secreting cells and the underlying mechanisms. *J. Physiol.* 569: 519–531 (2005).
321. Chen YH, Yao WZ, Ding YL, Geng B, Lu M, Tang CS. Effect of theophylline on endogenous hydrogen sulfide production in patients with COPD. *Pulm Pharmacol Ther.* 21: 40–46 (2008).
322. Li SB, Tong XS, Wang XX, Jin XH, Ye H. Regulative mechanism of budesonide on endogenous hydrogen sulfide, cystathionine-gamma-lyase and cystathionine-beta-synthase system in asthmatic rats. *Zhongguo Dang Dai Er Ke Za Zhi.* 12: 654–657 (2010).
323. Wang PP, Zhang G, Wondium T, Ross B, Wang R. Hydrogen sulfide and asthma. *Exp Physiol.* 96: 847–852 (2011).
324. Chen YH, Wu R, Geng B, Qi YF, Wang PP, Yao WZ, Tang CS. Endogenous hydrogen sulfide reduces airway inflammation

- and remodeling in a rat model of asthma. *Cytokine*. 45: 117–123 (2009).
325. DeLeon ER, Stoy GF, Olson KR. Passive loss of hydrogen sulfide in biological experiments. *Anal Biochem*. 421: 203–7 (2012).
326. Beauchamp RO Jr, Bus JS, Popp JA, Boreiko CJ, Andjelkovich DA. A critical review of the literature on hydrogen sulfide toxicity. *Crit Rev Toxicol*. 13: 25–97 (1984).
327. Toombs CF, Insko MA, Wintner EA, Deckwerth TL, Usansky H, Jamil K, et al. Detection of exhaled hydrogen sulphide gas in healthy human volunteers during intravenous administration of sodium sulphide. *Br J Clin Pharmacol*. 69:626–36 (2010).
328. Banerjee S.K., Maulik S.K. Effect of garlic on cardiovascular disorders: a review. *Nutr J*. 1:4 (2002).
329. Corzo-Martínez M, Nieves C, Villamiel M. Biological properties of onions and garlic. *Trends Food Sci Technol*. 18: 609–625 (2007).
330. Steinmetz, K.A. & J.D. Potter. Vegetables, fruit, and cancer prevention: a review. *J. Am. Diet. Assoc*. 96: 1027–1039 (1996).
331. Block, E. The chemistry of garlic and onions. *Sci. Am*. 252: 114–119 (1985).
332. Munchberg U, Anwar A, Mecklenburg S, Jacob C. Polysulfides as biologically active ingredients of garlic. *Org Biomol Chem*. 5: 1505–1518 (2007).
333. Steudel R, Albertsen A. Sulphur compounds CLVII. Determination of cysteine-Ssulphonate by ion pair chromatography and its formation by autoxidation of cysteine persulphide. *J Chromatogr*. 606: 260–263 (1992).
334. Insko MA, Deckwerth TL, Hill P, Toombs CF, Szabo C. Detection of exhaled hydrogen sulphide gas in rats exposed to intravenous sodium sulphide. *Br J Pharmacol*. 157:944–51 (2009).

335. Chuah SC, Moore PK, Zhu YZ. S-allylcysteine mediates cardioprotection in an acute myocardial infarction rat model via a hydrogen sulfide-mediated pathway. *Am J Physiol Heart Circ Physiol.* 293: H2693–H2701 (2007).
336. Elkayam A, Mirelman D, Peleg E, Wilchek M, Miron T, Rabinkov A, Sadetzki S, Rosenthal T. The effect of allicin and enalapril in fructose induced hyper-insulinemic hyper-lipidemic hypertensive rats. *J Hypertens.* 14: 377–381 (2001).
337. Gupta VB, Indi SS, Rao KS. Garlic extract exhibits anti-amyloidogenic activity on amyloid-beta fibrillogenesis: relevance to Alzheimer's disease. *Phytother Res.* 23: 111–115 (2009).
338. Sendl A, Elbl G, Steinke B, Redl K, Breu W, Wagner H. Comparative pharmacological investigations of *Allium ursinum* and *Allium sativum*. *Planta Med.* 58: 1–7 (1993).
339. Vazquez-Prieto MA, Gonzalez RE, Renna NF, Galamarini CR, Miatello RM. Aqueous garlic extracts prevent oxidative stress and vascular remodeling in an experimental model of metabolic syndrome. *J Agric Food Chem.* 58: 6630–6635 (2010).
340. Pedraza-Chaverri J, Tapia E, Medina-Campos O, de los Angeles N, Granados M, Franco M. Garlic prevents hypertension induced by chronic inhibition of nitric oxide synthesis. *Life Sci.* 62: 71–77 (1998).
341. Wu L, Noyan Ashraf MH, Facci M, Wang R, Paterson PG, Ferrie A, Juurlink BH. Dietary approach to attenuate oxidative stress, hypertension, and inflammation in the cardiovascular system. *Proc Natl Acad Sci USA* 101: 7094–7099 (2004).
342. Ye L, Dinkova-Kostova AT, Wade KL, Zhang Y, Shapiro TA, Talalay P. Quantitative determination of dithiocarbamates in human plasma, serum, erythrocytes and urine: pharmacokinetics of broccoli sprout isothiocyanates in humans. *Clin Chim Acta.* 316: 43–53 (2002).

343. Jackson SJ, Singletary KW, Venema RC. Sulforaphane suppresses angiogenesis and disrupts endothelial mitotic progression and microtubule polymerization. *Vascul Pharmacol.* 46: 77–84 (2007).
344. Zhu H, Jia Z, Strobl JS, Ehrich M, Misra HP, Li Y. Potent induction of total cellular and mitochondrial antioxidants and phase 2 enzymes by cruciferous sulforaphane in rat aortic smooth muscle cells: cytoprotection against oxidative and electrophilic stress. *Cardiovasc Toxicol.* 8: 115–25 (2008).
345. Calabrese V, Cornelius C, Dinkova-Kostova AT, Calabrese EJ, Mattson MP. Cellular stress responses, the hormesis paradigm, and vitagenes: novel targets for therapeutic intervention in neurodegenerative disorders. *Antioxid Redox Signal.* 13: 1763–811 (2010).
346. Pei Y, Wu B, Cao Q, Wu L, Yang G. H<sub>2</sub>S mediates the anti-survival role of sulforaphane on human prostate cancer cells. *Toxicol Appl Pharmacol.* 257: 420–428 (2011).
347. Voon YY, Hamid NSA, Rusul G, Osman A, Quek SY. Volatile flavour compounds and sensory properties of minimally processed durian (*Durio zibethinus* cv. D24) fruit during storage at 4°C. *Postharvest Biol Technol.* 46: 76–85 (2007).
348. Leontowicz H, Leontowicz M, Haruenkit R, Poovarodom S, Jastrzebski Z, Drzewiecki J, Ayala ALM, Jesion I, Trakhtenberg S, Gorinstein S. Durian (*Durio zibethinus* Murr.) cultivars as nutritional supplementation to rat's diets. *J Food Chem Toxicol.* 486: 581–589 (2008).
349. Chau WS, Chung HY. Volatile compounds in thousand-year-old eggs. Technical Poster 88A-10, Session-Food Chemistry: Flavor. Proc IFT Annual Meeting New Orleans (2001).
350. Geypens B, Claus D, Evenepoel P, Hiele M, Maes B, Peeters M, Rutgeerts P, Ghosset Y. Influence of dietary protein supplements on the formation of bacterial metabolites in the colon. *Gut.* 41: 70–76 (1997).

351. Khosrow Kashfi and Kenneth R. Olson. Biology and therapeutic potential of hydrogen sulfide and hydrogen sulfide-releasing chimeras. *Biochem Pharmacol.* 85(5): 689–703 (2013).
352. Lee ZW, Zhou J, Chen CS, Zhao Y, Tan CH, Li L, et al. The slow-releasing hydrogen sulphide donor, GYY4137, exhibits novel anti-cancer effects in vitro and in vivo. *PLoS One.* 6: e21077 (2011).
353. Yu F, Zhao J, Tang CS, Geng B. Effect of synthesized GYY4137, a slowly releasing hydrogen sulfide donor, on cell viability and distribution of hydrogen sulfide in mice. *Beijing Da Xue Xue Bao.* 42: 493–7 (2010).
354. Wang Q, Wang XL, Liu HR, Rose P, Zhu YZ. Protective effects of cysteine analogues on acute myocardial ischemia: novel modulators of endogenous H<sub>2</sub>S production. *Antioxid Redox Signal.* 12: 1155–65 (2010).
355. Chuah SC, Moore PK, Zhu YZ. S-allylcysteine mediates cardioprotection in an acute myocardial infarction rat model via a hydrogen sulfide-mediated pathway. *Am J Physiol Heart Circ Physiol.* 293: H2693–701 (2007).
356. Gong QH, Wang Q, Pan LL, Liu XH, Xin H, Zhu YZ. S-propargyl-cysteine, a novel hydrogen sulfide-modulated agent, attenuates lipopolysaccharide-induced spatial learning and memory impairment: involvement of TNF signaling and NF-kappaB pathway in rats. *Brain Behav Immun.* 25: 110–9 (2011).
357. Ma K, Liu Y, Zhu Q, Liu CH, Duan JL, Tan BK, et al. H<sub>2</sub>S donor, S-propargyl-cysteine, increases CSE in SGC-7901 and cancer-induced mice: evidence for a novel anti-cancer effect of endogenous H<sub>2</sub>S? *PLoS One.* 6: e20525 (2011).
358. Pan LL, Liu XH, Gong QH, Zhu YZ. S-Propargyl-cysteine (SPRC) attenuated lipopolysaccharide induced inflammatory response in H9c2 cells involved in a hydrogen sulfide-dependent mechanism. *Amino Acids.* 41: 205–15 (2011).

359. Liu C, Gu X, Zhu YZ. Synthesis and biological evaluation of novel leonurine-SPRC conjugate as cardioprotective agents. *Bioorg Med Chem Lett.* 20: 6942–6 (2010).
360. Steegborn C, Clausen T, Sondermann P, Jacob U, Worbs M, Marinkovic S, Rand H, Wahl MC. Kinetics and inhibition of recombinant human cystathionine  $\gamma$ -lyase: toward the rational control of transsulfuration. *J Biol Chem.* 274: 12675–12684 (1999).
361. Rossoni G, Manfredi B, Tazzari V, Sparatore A, Trivulzio S, Del Soldato P, Ferruccio B. Activity of a new hydrogen sulfide-releasing aspirin (ACS14) on pathological cardiovascular alterations induced by glutathione depletion in rats. *Eur J Pharmacol.* 648: 139–145 (2010).
362. Rossoni G, Sparatore A, Tazzari V, Manfredi B, Del Soldato P, Berti F. The hydrogen sulfide-releasing derivative of diclofenac protects against ischemia-reperfusion injury in the isolated rabbit heart. *Br J Pharmacol.* 153: 100–109 (2008).
363. Shukla N, Rossoni G, Hotston M, Sparatore A, Del Soldato P, Tazzari V, Persad R, Angelini GD, Jeremy JY. Effect of hydrogen sulfide-donating sildenafil (ACS6) on erectile function and oxidative stress in rabbit isolated corpus cavernosum and in hypertensive rats. *BJU Int.* 103: 1522–1529 (2009).
364. Lee M, Tazzari V, Giustarini D, Rossi R, Sparatore A, Del Soldato P, McGeer E, McGeer PL. Effects of hydrogen sulfide-releasing L-DOPA derivatives on glial activation: potential for treating Parkinson disease. *J Biol Chem.* 285: 17318–17328 (2010).
365. Osborne NN, Ji D, Abdul Majid AS, Fawcett RJ, Sparatore A, Del Soldato P ACS67, a hydrogen sulfide-releasing derivative of latanoprost acid, attenuates retinal ischemia and oxidative stress to RGC-5 cells in culture. *Invest Ophthalmol Vis Sci.* 51: 284–294 (2010).

366. Perrino E, Cappelletti G, Tazzari V, Giavini E, Del Soldato P, Sparatore A. New sulfurated derivatives of valproic acid with enhanced histone deacetylase inhibitory activity. *Bioorgan Med Chem Lett.* 18: 1893–1897 (2009).
367. d'Emmanuele de Villa Bianca, R.; Sorrentino, R.; Maffia, P.; Mirone, V.; Imbimbo, C.; Fusco, F.; De Palma, R.; Ignarro; Cirino, G. Hydrogen sulfide as a mediator of human corpus cavernosum smooth-muscle relaxation. *Proc. Natl. Acad. Sci. U.S.A.* 106 (11): 4513–4518 (2009).
368. Fiorucci, S.; Antonelli, E.; Distrutti, E.; Rizzo, G.; Mencarelli, A.; Orlandi, S.; Zanardo, R.; Renga, B.; Di Sante, M.; Morelli, A.; Cirino, G.; Wallace, J. L. Inhibition of hydrogen sulfide generation contributes to gastric injury caused by anti-inflammatory nonsteroidal drugs. *Gastroenterology.* 129: 1210–1224 (2005).
369. Sidhapuriwala J, Li L, Sparatore A, Bhatia M, Moore PK. Effect of S-diclofenac, a novel hydrogen sulfide releasing derivative, on carrageenan-induced hindpaw oedema formation in the rat. *Eur J Pharmacol.* 569: 149–154 (2007).
370. Bhatia M, Sidhapuriwala JN, Sparatore A, Moore PK. Treatment with H<sub>2</sub>S-releasing diclofenac protects mice against acute pancreatitis-associated lung injury. *Shock.* 29: 84–88 (2008).
371. Fiorucci, S.; Orlandi, S.; Mencarelli, A.; Caliendo, G.; Santagada, V.; Distrutti, E.; Santucci, L.; Cirino, G.; Wallace, J. L. Enhanced activity of a hydrogen sulfide releasing derivative of mesalamine (ATB-429) in a mouse model of colitis. *Br. J. Pharmacol.* 150: 996–1002 (2007).
372. Distrutti, E.; Sediari, L.; Mencarelli, A.; Renga, B.; Orlandi, S.; Russo, G.; Caliendo, G.; Santagada, V.; Cirino, G.; Wallace, J. L.; Fiorucci, S. 5-Amino-2-hydroxybenzoic acid 4-(5-thioxo-5H-[1,2]dithiol-3yl)-phenyl ester (ATB-429), a hydrogen sulfidereleasing derivative of mesalamine, exerts antinociceptive effects in a model of postinflammatory

- hypersensitivity. *J. Pharmacol. Exp. Ther.* 319 (1): 447–458 (2006).
373. Wallace; Caliendo,G.; Santagada, V.; Cirino,G. Markedly reduced toxicity of a hydrogen sulphide-releasing derivative of naproxen (ATB-346). *Br. J. Pharmacol.* 159 (6): 1236–1246 (2010).
374. Elsheikh W, Blackler RW, Flannigan KL, Wallace JL. Enhanced chemopreventive effects of a hydrogen sulfide-releasing anti-inflammatory drug (ATB-346) in experimental colorectal cancer. *Nitric Oxide.* 41: 131-7 (2014).
375. Jurkowska, H., Placha, W., Nagahara, N., and Wrobel, M. The expression and activity of cystathionine-gamma-lyase and 3-mercaptopyruvate sulfurtransferase in human neoplastic cell lines. *Amino Acids.* 41: 151–158 (2011).
376. Berkelhammer, J., Oxenhandler, R.W., Hook, R.R. Jr, and Hennessy, J.M. Development of a new melanoma model in C57BL/6 mice. *Cancer Res.* 42: 3157–3163 (1982).
377. Isaiah J. Fidler. Biological Behavior of Malignant Melanoma Cells Correlated to their survival in vivo. *Cancer Research.* 35: 218-224 (1975).
378. Naser N. Cutaneous melanoma - a 30-year-long epidemiological study conducted in a city in southern Brazil, from 1980-2009. *An Bras Dermatol.* 86:932-41 (2011).
379. Taniguchi, S., Kang, L., Kimura, T., and Niki, I. Hydrogen sulphide protects mouse pancreatic beta-cells from cell death induced by oxidative stress, but not by endoplasmic reticulum stress. *Br. J. Pharmacol.* 162: 1171–1178 (2011).
380. Fan, H., Guo, Y., Liang, X., Yuan, Y., Qi, X., Wang, M., Ma, J., and Zhou, H. Hydrogen sulfide protects against amyloid betapeptide induced neuronal injury via attenuating inflammatory responses in a rat model. *J. Biomed. Res.* 27: 296–304 (2013).
381. Guo, R., Wu, K., Chen, J., Mo, L., Hua, X., Zheng, D., Chen, P., Chen, G., Xu, W., and Feng, J. Exogenous hydrogen sulphide

- protects against doxorubicin-induced inflammation and cytotoxicity by inhibiting p38MAPK/NF $\kappa$ B pathway in H9c2 cardiac cells. *Cell. Physiol. Biochem.* 32: 1668–1680 (2013).
382. Li, L., Fox, B., Keeble, J., Salto-Tellez, M., Winyard, P.G., Wood, M.E., Moore, P.K., and Whiteman, M. The complex effects of the slow-releasing hydrogen sulfide donor GYY4137 in a model of acute joint inflammation and in human cartilage cells. *J. Cell Mol. Med.* 17: 365–376 (2013).
383. Shankar, S., Chen, Q., Ganapathy, S., Singh, K.P., and Srivastava, R.K. Diallyl trisulfide increases the effectiveness of TRAIL and inhibits prostate cancer growth in an orthotopic model: molecular mechanisms. *Mol. Cancer Ther.* 7: 2328–2338 (2008).
384. Tripatara, P., Patel, N.S., Collino, M. et al. Generation of endogenous hydrogen sulfide by cystathionine gamma-lyase limits renal ischemia/reperfusion injury and dysfunction. *Lab. Invest.* 88: 1038–1048 (2008).
385. Du, J., Huang, Y., Yan, H. et al. Hydrogen sulfide suppresses oxidized low-density lipoprotein (ox-LDL)-stimulated monocyte chemoattractant protein 1 generation from macrophages via the nuclear factor  $\kappa$ B (NF- $\kappa$ B) pathway. *J. Biol. Chem.* 289: 9741–9753 (2014).